Inertia Effect of the Heart as a Contributing Factor in Aortic Injuries in Near-Side Impacts

by

Cristina G. Echemendia Fuentes
B.S. in Mechanical Engineering, 1997, ITESM-CEM
M.S. in Engineering Management, August 2006, George Washington University

School of Engineering and Applied Science at
The George Washington University

December 19th, 2008

Thesis directed by

Kennerly Digges, PhD
Research Professor of Engineering and Applied Science

The School of Engineering and Applied Science of The George Washington University certifies that Cristina G. Echemendia Fuentes has passed the Final Examination for the degree of Master of Science as of December 19th, 2008. This is the final and approved form of the thesis.

Inertia Effect of the Heart as a factor in aortic injuries in Near-Side Vehicle-to-Vehicle Crashes

Cristina G. Echemendia Fuentes

Research Committee:

Azim Eskandarian

Kennerly Digges

Steve Kan

Pedro Silva

Majid Manzari

Abstract

There are more than 42,000 fatalities and 2.9 million people injured per year due to motor-vehicle accidents in the United States and an additional cost to society estimated at $230.6 billion per year, according to the National Highway Traffic Safety Administration (NHTSA 2005). Motor vehicle crashes remain a leading cause of death among the younger population between the ages of 4 -34 and among the top ten causes of death for all age groups (NHTSA, 2006) and they deserve further study to prevent accidents and reduce their effects.

Side-impact crashes are the most harmful type of planar crashes. Although their frequency is about 28% of all crash types, they account for 30% of the serious injuries. One of the reasons for the higher injury potential of side-impact crashes is the reduced crush space between the passenger and the striking vehicle. Also, the fleet in the United States has shifted to a larger proportion of pickups and SUVs, whose size and weight make passenger cars more vulnerable than ever.

As will be discussed further in Chapter 3, blunt trauma aortic injuries are one of the leading causes of fatalities in side-impact crashes. The aorta is the main blood vessel of the human body and it supplies blood to all of the body's vital organs. The blunt trauma that occurs in side-impacts can cause partial or total rupture of the aorta, resulting in excessive blood loss and, potentially, death.

Previous studies (Steps 2004) (Bertrand, et al., 2008) have established crash factors that could be used to predict aortic injury using real-world cases. These crash factors include age, restraints, delta-v, intrusion, crush, direction of force, and crash type. Other studies have attempted to establish the injury mechanisms for aortic injury, but to this date there is no general consensus on the evaluation criteria and the attempts to try to better understand these injury mechanisms are ongoing.

This study attempts to further investigate the proposed injury mechanisms for aortic injury such as Viscous Criterion, Chest Compression and the inertial effect of the heart in the thoracic cavity. Criteria that use Chest Compression and compression velocity have been researched by impacting the chest of cadavers with a cylindrical impactor (Hardy, et al., 2008). However, this type of testing is unable to evaluate how the inertial effect of the heart may contribute to loading the aorta. The reason was that the cadavers were not subjected to crash forces that simulated a side-impact. These studies demonstrated that the aorta is very weak in resisting tension loading that may be caused by the motion of the heart relative to the aortic arch. Other studies, with cadavers subjected to side-impact conditions, suggested that aortic injury was influenced by the magnitude of the upward acceleration acting parallel to the spine (Cavanaugh, et al., 2005). This type of acceleration would cause the heart to move upward and load the aorta in tension. One purpose of this study is to further evaluate the forces that act on the aorta, including those produced by the heart as a consequence of upward acceleration.

Several scenarios were modeled using LS-DYNA and MADYMO to reproduce currently available tests. These tests include the NCAP, NCAP Y-Damage and IIHS Side-impact test. The NCAP Y-Damage test was proposed by Steps as the test condition that most closely mimics the crash environment that produced the aortic injuries observed in low severity crashes (Steps, 2004). The NCAP and IIHS tests are routinely conducted to provide consumer information on crash safety. These scenarios were varied by adding airbags. The purpose of the air bag simulations was to determine the degree to which these safety systems reduced the risk of aortic injury. Sled tests were also modeled with and without a six inch pelvic offset in order to reproduce Cavanaugh's cadaver sled tests (Cavanaugh, et al., 2005).

The modeling of these scenarios will be helpful to better understand the factors that contribute to the injury mechanism. Several injury parameters proposed by previous research studies (Cavanaugh, Koh, et al. 2005), such as Chest Compression, Viscous Criterion, Spinal

Accelerations, etc. are analyzed. The effect of Spinal Acceleration is studied by adding a spring mass model within the Human Facet MADYMO Model, and exposing the resulting model to the selected crash environments. The inertia of the heart causing the aorta to stretch in the longitudinal direction is proposed as a possible injury mechanism.

Results conclude that the inertia effect is a possible factor in the injury mechanisms of aortic rupture. This stretching of the aorta as the result of inertia effect of the heart is present in the side-impact environments that were simulated. The aortic stretch is more severe in the higher severity cases and the Y-Damage pattern of the vehicle-to-vehicle simulations. It was also more severe in the pelvic offset sled tests, conforming to the previous cadaver research results from Cavanaugh.

Acknowledgements

This thesis represents a milestone in my career as a mechanical engineer; it is the result of many experiences from undergrad, to my first job, to the GWU NCAC and the culmination of a learning process that has just begun. For these I am grateful.

First and foremost I want to thank my advisor and professor Kennerly Digges. He helped me come up with my thesis topic and guided me through the many months of development. He gave me the technical and moral support that I needed and the encouragement to continue and refine the final work of which I'm proud.

Steve Kan, Director of the NCAC, thank you for the opportunity to join the Transportation Safety program as a full-time student and for the support to complete my research.

Thanks to Richard Morgan, Research Scientist of the NCAC, who has been a solid advisor on all technical matters. I attribute a lot of the reading I have done to you, thank you for your support and confidence.

My work would not be complete without simulations and for that I thank Roel Van de Valde, who taught me MADYMO. A short time learning has resulted in a comprehensive study thanks to you.

I thank the Committee Members for the time they took to review my work and their valuable comments to make my work better.

I thank my Lee, my loving husband. He has helped me gain confidence, has taught me commitment, and has demonstrated what unconditional support is. In good times and bad… thank you for making it all good.

Mami, Dora Hilda, who showed me how to love learning. The many hours we spent together growing up by her side doing homework while she was writing her own thesis, were an inspiration. I have learned strength, discipline, and dedication from her.

My sister, Ana, who has been a role model throughout my life, has always been there to support me and give me precious advice. This endeavor would have been impossible without her.

I would also like to thank my father Gustavo without your support I would have never had such good education.

I want to recognize Judy Shem who has made life easier for me through the past two years. All fellowship graduates have her to thank on a daily basis.

Table of Contents

List of Figures

List of Tables

1 Introduction

Among the most serious types of crashes, side-impact is only second to frontal impact, resulting in one of the highest injury and fatality rates in the United States. About 28 percent of all injury severity crashes are the result of side-impact crashes and 30 percent of Abbreviated Injury Scale (AIS) 3+ severity crashes are side-impact crashes as well. This type of crash can be categorized further as “near” and “far” side-impacts. Near-side-Impacts usually have several AIS3+ head and chest injuries.

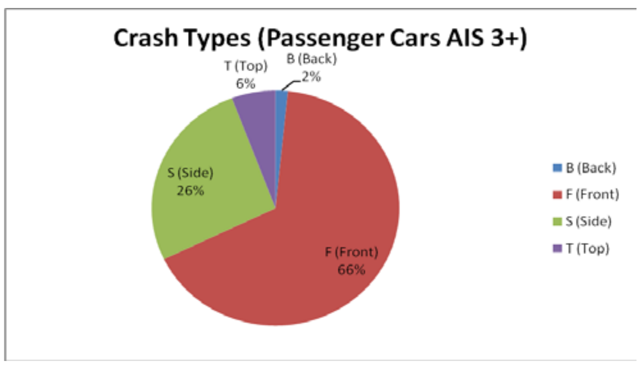

Figure 1 - Crash Types – AIS3 +

Head injuries are very common in near-side-impact crashes and occur due to the contact of the head with the A or B pillar, the fender/hood of the striking vehicle or the fixed object it is striking. Chest injuries are also very common and generally occur as a result of the contact of the arm/chest with the door and door handles of the vehicles. In the case of a vehicle-to-vehicle side-impact, the struck vehicle has a lower stiffness on the side of the vehicles than any frontal part of another vehicle. Therefore, a large amount of intrusion is usually present in these type of accidents. The rate of intrusion is also an important factor when evaluating the severity of a crash.

Blunt trauma aortic injury is one of the leading causes of death in high-speed blunt trauma, which occurs in side-impact crashes. The aorta is the main blood vessel of the human body and it supplies blood to all of the body's vital organs. Blunt trauma can cause partial or total rupture of the aorta resulting in excessive blood loss and possible death.

To study the biomechanics of a specific event we need to do research in injury mechanisms, mechanical responses, injury tolerances and simulations of human impact. Cadaver testing, although not perfect, is an important way of obtaining data to study the first three areas mentioned. In this thesis, Cavanaugh's cadaver sled tests (Cavanaugh, et al., 2005) were used as reference to study aortic injury.

Research on real-world crashes is also important to understand the injury mechanisms. By examining the National Automotive Sampling System (NASS) database we can obtain some insight on possible injury mechanisms. It is important to understand how an injury occurs in order to find a way to prevent it. Real-world analysis helps understand the frequency, severity and impact on the injured population and the cost to society.

Crash test dummies are helpful in evaluating the safety of a vehicle. The dummies measure the mechanical responses in an event and help us make an assessment on the possible injuries that a human could have in a similar event. In this thesis, we examine the mechanical responses of MADYMO's Human Facet Model in different vehicle-to-vehicle environments, as well as, sled testing, to study aortic injury.

Vehicle Standards and Consumer Information initiatives tests use several injury criteria for the head, thorax, pelvis, femur, etc. However, there are still no universal injury criterion for the thorax and abdomen when exposed to side-impacts. The existing injury criteria are used to analyze skeletal fractures but are not sufficient to analyze internal organ injuries. For these reasons, there have been several cadaver sled tests which have helped in the research and development of other injury criteria. These tests include analysis on the impact forces and film analysis and will be discussed in a later section of the thesis.

1.1 Approach

The goal of this thesis is to apply crash data analysis and modeling of a human subjected to a side crash in order to better understand aortic injury mechanisms. The research will apply regression analysis to crash data in an attempt to determine factors that may influence the incidence of aortic injuries. It will conduct in-depth studies of individual cases with aortic injury to further examine the crash factors. It will apply MADYMO modeling to determine the degree to which NCAP and IIHS consumer information crash tests produce environments that are like those that cause aortic injury. In order to determine the crash environment for these test conditions, Finite Element Method (FEM) models will be used. The study will investigate the degree to which side air bags are likely to mitigate aortic injuries. It will simulate Cavanaugh's cadaver sled tests that produced aortic injuries to study how variations in test conditions may influence the risk of aortic injury.

Finally, the thesis will explore the inertial effect of the heart as a factor of the injury mechanisms of aortic rupture using multidisciplinary methods and previous research studies to reproduce environments conducive to aortic injury. This approach consists of examining previous studies and real-world crashes, to model vehicle-to-vehicle and sled test crash environments, to analyze the response of the Human Facet Model and to incorporate a spring mass model to these computer modeled environments to explore the inertia effect of the heart in the z (upward) direction.

1.1.1 Examine Previous Research Studies

Existing studies are explored to better understand the current side-impact injury criteria. These studies generally involve cadaver testing and they explore the injuries that result from a side-impact. The cadavers in these types of studies are equipped with instrumentation that takes several measurements and the cadavers are also examined after the impact to evaluate its injuries. The most common injuries are skeletal, but these studies, also, analyze the damage done to internal organs and soft tissue. The literature only contains one set of cadavers with aortic injuries produced by side-impact crash tests (Cavanaugh, et al., 2005). This result is remarkable in view of the more than 50 tests reported in the literature. Most of these cadaver studies were unsuccessful in producing aortic injuries until a more recent study where the cadavers were inverted (Hardy, et al., 2008). When the cadavers were impacted by a cylindrical impactor aortic tears consistently occurred. The results from these studies are reviewed in this thesis to further study the injury criteria, to compare data and to evaluate important predictors of aortic injury.

1.1.2 Analysis of Real-world Accident Data

Real-world crashes selected from NHTSA's NASS database were reviewed to better understand the environments that are more conducive to aortic injuries. These crashes were categorized in low and high-severity crashes. The focus of this thesis is on low-severity cases because the chance of survivability is higher. Several variables are selected and analyzed to establish if there is a correlation between each variable and aortic injury. Once some of these variables are identified as possible predictors of aortic injury a logistic regression was performed on the data set to see if the variable is statistically significant

1.1.3 Computer Modeling of NCAP test with Taurus 2001

Computer modeling is an important tool used to recreate several vehicle-to-vehicle impacts and to explore the effects of the crash on the occupant. Some vehicle-to-vehicle tests were recreated using a Finite Element Model of the 2001 Taurus, and a Finite Element Model of NHTSA's deformable barrier or the IIHS deformable barrier. TNO's Human Facet Model was used in the MADYMO model. The MADYMO Human Facet Model was subjected to a crash pulse and door intrusion as predicted by the FEM simulation. The responses of the Human Facet Model were then analyzed and compared to each other to see the differences between the different crash environments. These tests were performed with and without a side airbag to examine the behavior of the Human Facet Model in an environment with and without a countermeasure.

1.1.4 Computer Modeling of Cadaver Sled Tests

Cadaver sled tests like those conducted by Cavanaugh were modeled to study the response of the Human Facet Model in a sled test environment with and without a six inch pelvic offset. Similar to the vehicle-to-vehicle crash modeling, the purpose of the cadaver sled test is to better understand the interaction and response of the Human Facet Model in a specific environment.

1.1.5 Spring-Mass Model to study inertia effect on Z (upward) direction

A spring-mass model was incorporated in the Human Facet Model in both vehicle-to-vehicle and sled test modeling scenarios. The characteristics of the spring were assigned to coincide with the characteristics of the aortic tissue testing. Also, joints and attachments were created to represent the heart-aorta-spine structure in the thoracic cavity. This model will help us study the inertia effect of the heart in the z-direction that could cause longitudinal stretching of the aorta when exposed to the mentioned crash scenarios. This inertia effect is the isolated response of the inertia of the heart, not taking into consideration the interaction due to Chest Compression.

1.2 Vehicle Standards in the US

In this section, I will explore different standards. The National Highway Traffic Safety Administration (NHTSA) issues the Federal Motor Vehicle Safety Standards (FMVSS) and Regulations. Vehicle manufacturers must conform to these standards and regulations in order to sell their motor vehicles in the United States. These safety standards are the minimum safety performance requirements and are created to protect the general public from unreasonable risk of crashes involving motor vehicles.

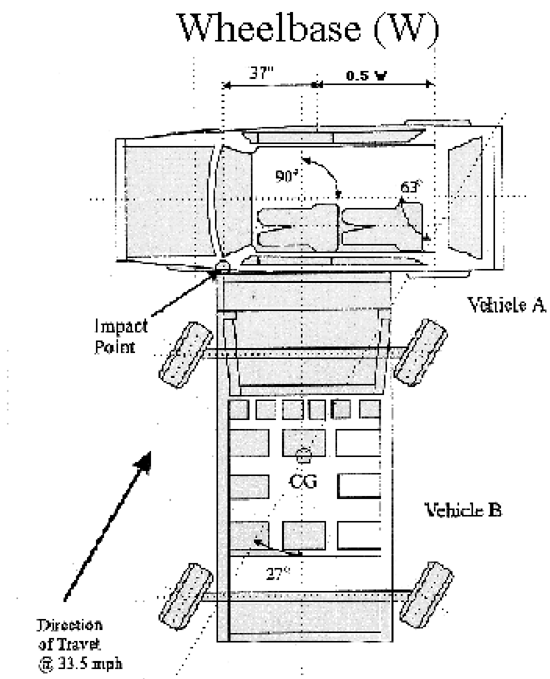

Figure 2 - FMVSS 214 Diagram (Buzztrader.com and CyberWebInc 2007)

The NHTSA has several safety standards for components, fire, occupant protection, etc. The FMVSS-214 is the standard involving side-impact protection. This standard specifies the minimum necessary requirements a passenger car needs to protect occupants in side-impact crashes. This test consists of a side-impact of a moving deformable barrier against the vehicle being tested. The barrier velocity and track is at 63 degrees vehicle centerline, but the barrier face is at 90 degrees upon impact. The speed of the moving deformable barrier for the FMVSS 214 is 54km/h (33.5mph).

1.3 Consumer Information

There are other major initiatives that assess the vehicle occupant protection performance for consumer information. The new car assessment program (NCAP) and the Insurance Institute of Highway Safety (IIHS) are two of the testing agencies and they determine occupant safety of new vehicle models by measuring the responses of dummies in a crash test. These tests usually vary the configuration of the FMVSS tests and have improved the crashworthiness of today's passenger vehicles.

The NCAP test for side-impact was added to the program in 1996 for testing lateral impact protection. The configuration of this test is similar to NHTSA's FMVSS 214 but at a higher speed of 61.9kph (38.5mph). These tests have the following star ratings:

5 stars	Less than 6% chance of serious injury
4 stars	6-10% chance of serious injury
3 stars	11-20% chance of serious injury
2 stars	21-25% chance of serious injury
1 star	More than 25% chance of serious injury

The IIHS also has a different configuration. It consists of a side-impact at 90 degrees, with a heavier and taller moving deformable barrier and a speed of 50km/h (31mph). The IIHS tests evaluate injury measures, head protection and structural integrity. The results of these tests are also published to inform the consumer. The injury ratings used by the IIHS are good, acceptable, marginal and poor.

1.4 Side-Impact Protection

Preventing injuries in side-impact is a challenging problem. There is very limited available crush distance and space in the door to implement countermeasures. Side-impact protection consists of vehicle side stiffness, interior geometry, airbags and padding.

One of the methods car manufacturers use to protect passengers is the use of side-impact bars to change and improve side stiffness. The side-impact bars are usually located inside the doors of the vehicle. These bars help lessen the amount of intrusion the vehicle has in the event of an accident.

Another method is the side airbag which was introduced in the mid 1990s. Side airbags are devices that help protect the occupant's head and/or chest in the event of side-impact. There are three types of side airbags: Chest, Head and Head/Chest combination. These airbags are mounted in the side of the seat, in the door or in the roof rail and they protect the chest and/or head of the occupants. Some side airbag varieties may also prevent total or partial ejections in the event of a rollover after a side crash.

The side airbags inflate in a fraction of a second and reduce the injury severity by preventing the occupant's head or chest strike against a hard surface. The vehicle is equipped with sensors that determine the severity of the crash and will deploy the airbag when necessary. Generally, side airbags stay inflated for several seconds after the initial impact in case there is a rollover. By covering the windows they may prevent ejections.

In the past NHTSA established side occupant protection performance but did not require vehicles to be equipped with any particular technology, such as side airbags. In 2003 automakers made a voluntary agreement to have airbags in at least half of their vehicles by 2007. Following that, NHTSA enacted a new mandate in 2007 where all car manufacturers must phase in additional side-impact protection as a standard feature for their cars, trucks and SUVs. This new mandate will take effect in September 1, 2009 and every car manufacturer must comply within four years.

2 Background on Aortic Injuries

Motor vehicle collisions are responsible for most cases of aortic injury in the United States (Burkhart, et al., 2001). Other mechanisms contributing to aortic injury cases include pedestrian incidents or falls. Aortic injury is the second most common cause of death in blunt trauma cases. Most of the patients that sustain an aortic injury die at the scene but the ones that survive the event have a good expectation of survival if the injury is detected in a timely manner. Severe collisions are almost always accompanied by multiple injuries which make treatment and diagnosis difficult, increasing the threat to life.

2.1 Injury Mechanisms

Previous research studies have been performed to establish the mechanical parameters implicated in causing a specific injury. The injury mechanism is established by finding a consistent result in a specific hypothesis. The thorax cavity holds some of the most important organs in the human body. The rib cage and the thoracic spine are the structures that protect those organs.

The human body may be exposed to high forces in a car crash. These forces can be high enough to cause fractures of the ribs and sternum, lung contusions, lung punctures, as well as torn blood vessels. The rate of loading is an important factor in these injuries. When slow loading occurs, the injuries are mostly caused by the compression and crushing of the rib cage (see Figure 3). In fast loading cases, the transmission of a pressure wave causes the injuries. At intermediate speeds, a combination of forces from compression and viscous response are present (see Figure 3).

In automotive crashes rib compression may induce shear and tensile loading. Aortic tears are present in front and lateral impacts. Studies have shown that the risk of sustaining an aortic tear in near and far side-impacts (2.4% incidence) is twice as high as for frontal impacts(1.1 % incidence) (Bertrand, et al., 2008). To study these injury mechanisms it is necessary to obtain mechanical response data. This can be done by using human cadavers which have a closer response to live humans than dummies. These tests allow us to obtain response data from the head, neck, chest, abdomen and lower extremities. The response data can be analyzed to establish the tolerances of the human body.

Other studies have examined the effect of potential injury due to inertia (see Figure 3) suggesting that rapid deceleration results in aortic injury. These studies have not been conclusive as most of them require the presence of Chest Compression to obtain an aortic injury (Foreman, et al., 2008). Most of these cadaver studies have been unsuccessful in consistently reproducing aortic injury until a recent study done with inverted cadavers where the position of the heart more closely resembles that of a living person (Hardy, et al., 2008).

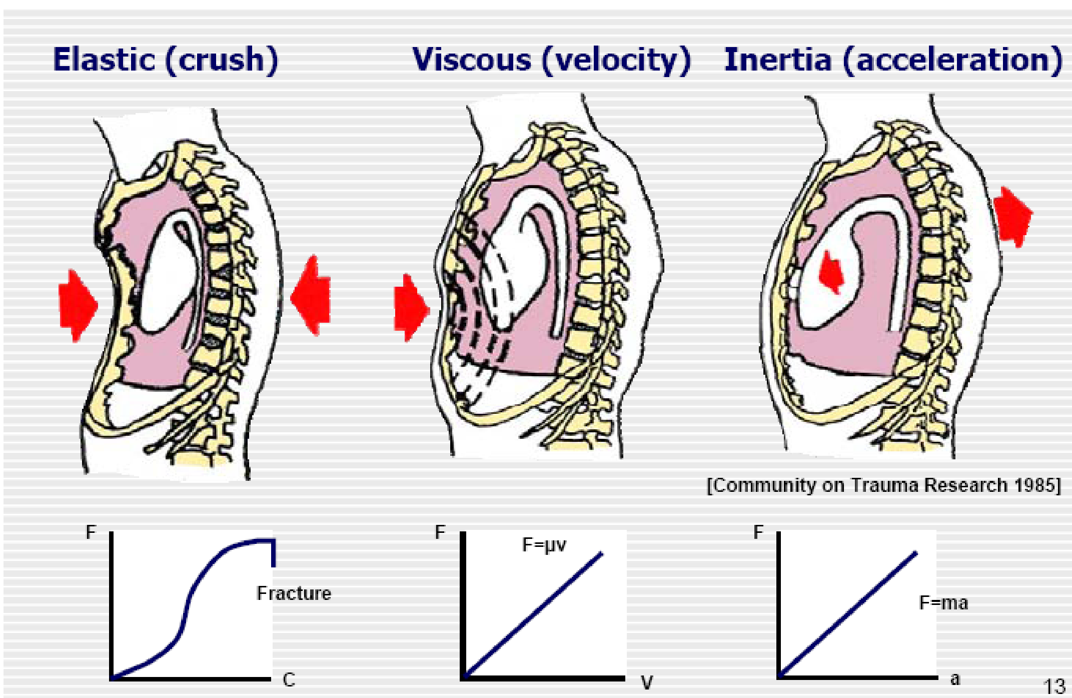

Figure 3 - Mechanisms of injury

Another proposed injury mechanism is the aortic pressure influence. However, studies have concluded that a transverse rupture of the aorta due to pressure alone is unlikely (Hardy, et al., 2006). According to Hardy, the internal pressure may contribute in keeping the aorta tense affecting its position and orientation but only other factors such as Chest Compression can contribute to an aortic tear.

Although cadavers are the most biofidelic subjects, they have several disadvantages. Cadavers have poor repeatability because of age, sex, weight and height variations. Test cadavers are generally from older subjects who present a higher accumulation of plaque in the arteries; studies have found that hardened arteries have a greater risk of damage to the aorta (Hardy, et al., 2008). The following three post-mortem changes in the body are also present. First, the physical properties of tissue change after death. Second, there is lack of muscle tone in the cadaver which may change the posture of the subject. Third the response to acceleration and the location of the internal organs change due to gravity (Hardy, et al., 2008). There are also a series of ethical issues that prevent this practice from being more popular. Dummies on the other hand present no ethical or repeatability problems but their biofidelity is not very precise.

2.2 Anatomy of the aorta

The aorta is a tubular structure and is the major artery in the human body. The aorta originates at the left ventricle of the heart known as the aortic root and ends at the point where it branches into the common iliac arteries. The aorta is divided into three main sections: the ascending aorta, the arch and the descending aorta. The ascending aorta is the section that starts at the heart and ends at the arch of the aorta. The arch of the aorta arches from the ascending aorta to the descending aorta and has three branches commonly called the superior vasculature. The region between the left subclavian artery and the descending aorta is generally known as peri-isthmic region (see Figure 4). The descending aorta originates at the fourth thoracic vertebra and ends near the twelfth thoracic vertebra. It is firmly tethered to the thoracic spine (see Figure 5) by reflection of the pleura, the intercostals arteries and the paravertebral fascia (Hardy, et al., 2008). The ascending aorta and the aortic arch are relatively free to move. The top half of the descending aorta (above the diaphragm) is called the thoracic aorta and the bottom half (below the diaphragm) is called the abdominal aorta.

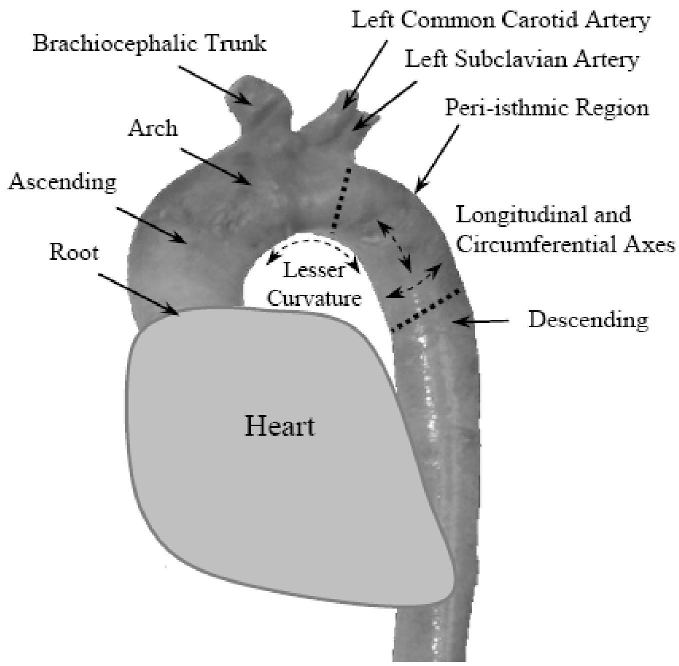

Figure 4- Anatomy of aorta (Hardy, et al., 2008)

Figure 5 – Aorta-Spine Attachment (Steps, 2004)

The aorta is a structure with tubular shape and it has a longitudinal axis and a circumferential axis. Its wall is constructed with three layers also called tunics. The inner layer is called intima, the middle layer is called media and the outer layer adventitia. The inner most layer is the intima as it has direct contact with the blood flow. It is mainly made up by endothelial cells. The middle layer is the media and it is the thickest layer. It consists of smooth muscle cells, elastic connective tissue and a network of binding collagen fibers. The outermost layer is the adventitia and it is the furthest layer from the blood flow. It is composed by connective elastic, collagen fibers and smooth muscle tissue.

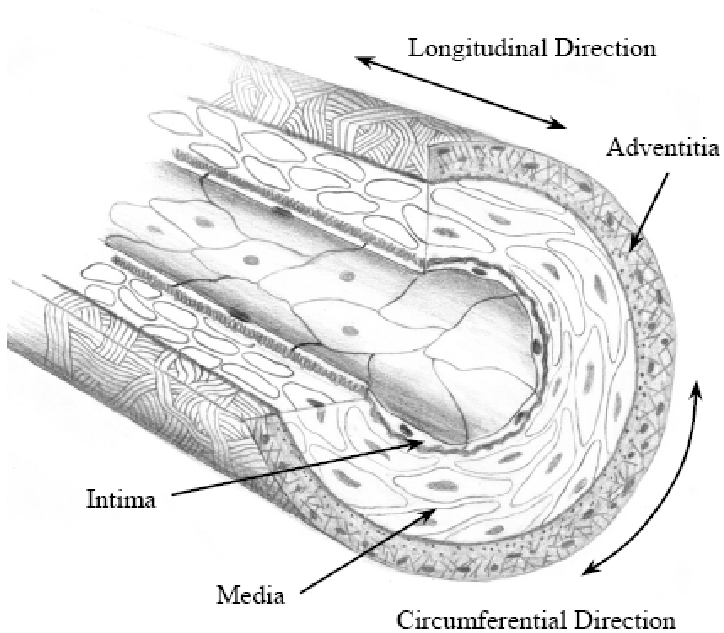

Figure 6 – Wall structure of aorta (Hardy, et al., 2008)

According to Viano's studies on fatal injuries in motor vehicle accidents, aortic injuries appear primarily in the peri-isthums region, the descending aorta (Viano 1983) and the aortic root. Katyal showed that 94 percent of traumatic aorta injuries were present in the peri-isthmic region (Katyal, et al. 1997) in patients from motor vehicle accidents. Wayne State University developed a finite element model of the thorax including skeletal structure and detailed internal organs including the aorta. These simulations showed that the peri-isthmus region has the highest principal stresses in all impact angles tested. Figure 7 shows the peak stress distribution for three tests performed at different angles.

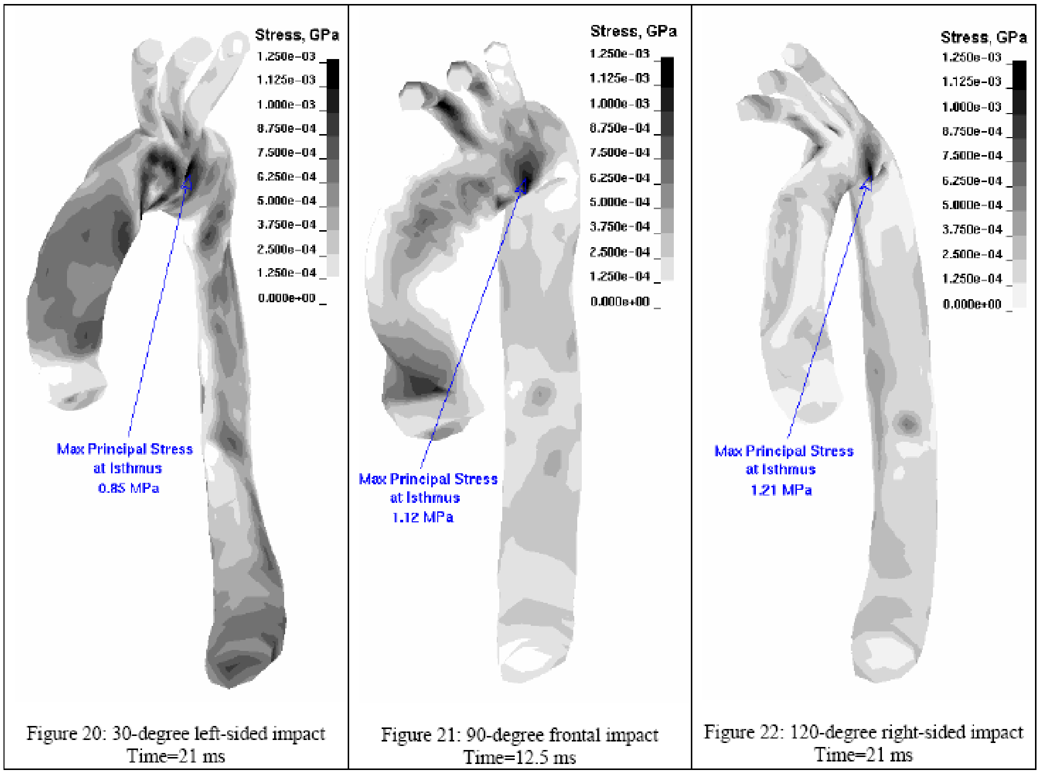

Figure 7 - Maximum principal stresses at the isthmus of the aorta for three impact angles. (Shah, et al., 2001)

2.3 Previous Studies

The study of biomechanics is essential in mitigating motor vehicle fatalities and injuries. Biomechanics is a branch of science that studies the application of mechanical principles to living organisms. Experiments done on biological material, such as animals and cadavers help us to understand and determine the injury mechanisms of a certain event. This branch also helps us to develop injury criteria and establish tolerances in the human body.

There are several proposed injury parameters for aortic injury but we still need to better understand the mechanisms that produce this type of injury. There have been very few cadaver studies that have been able to produce aortic tears from side crash tests. These studies have not been able to provide sufficient information on the motion of the organs inside the chest and the deformation of the aorta during an impact. The position and orientation of the heart on a cadaver is different than the ones in a living human. The loss of muscle tone, changes in mechanical properties of the tissue post-mortem and gravity help change the position and orientation of the heart in the cadaver. This configuration does not generate the longitudinal tension in the peri-isthums region required to produce an aortic tear.

Viano has done extensive cadaver testing in frontal and side-impacts. Forty four blunt lateral impacts were applied to fourteen unembalmed human cadavers. A 23.4 Kg pendulum with a 150 mm diameter struck the cadavers at the chest and abdomen of the cadavers at 4.5, 6.7 or 9.4 m/s. The development the response corridor was the main objective of the study. Autopsies were performed and no aortic injuries were present in any of the test subjects.

The Viscous Criterion and tolerance levels used in this thesis were taken from Viano's studies. The Viscous Criterion is any biomechanical index of injury potential for soft tissue defined by rate sensitive torso compression (Viano and Lau 1986). The Viscous response (VC) is "a time function formed by the product of the velocity of deformation, V(t), and the instantaneous compression C(t)". The Viscous tolerance is defined as the "risk of soft tissue injury associated with a specific impact-induced viscous response, VC. The maximum risk occurs at the peak Viscous response, [VC]max." (Viano and Lau 1986)

$$\mathbf{V(t) = d\,[D(t)]\,/\,dt} \qquad \textbf{Equation 1}$$

V(t) = Velocity of deformation (units m/s)

D(t) = Instantaneous deformation along the direction of the applied impact to the torso.

C(t) = Compression - D(t) / Initial Torso Thickness (dimensionless)

C(t) is a dimensionless number and is usually presented as a percentage and VC's dimensions are the same as the velocity of deformation (m/s). Figure 8 shows instantaneous deformation D(t) and initial torso thickness "D". The compression C(t) is obtained by dividing the instantaneous deformation by the initial torso thickness "D". The derivative of the instantaneous deformation D(t) signal is shown as the velocity of deformation V(t). The product of the Velocity of deformation V(t) and the Compression C(t) is shown as the Viscous Criterion "VC" vs. time graphic in the figure below. The maximum value of this signal is the Peak value of the Viscous Criterion [VC]Max.

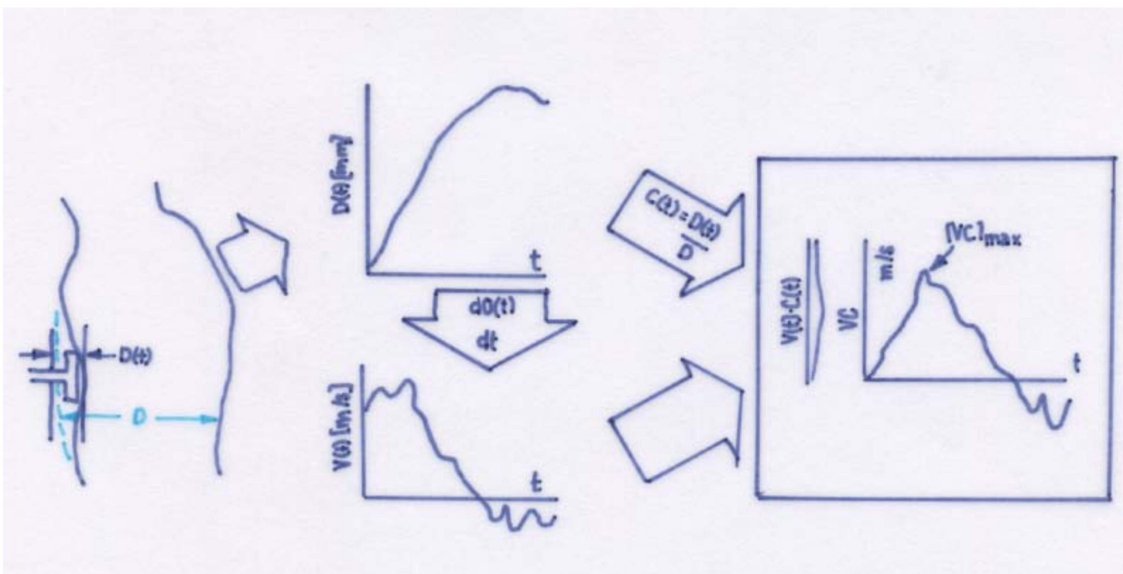

Figure 8. Viscous Criterion defined by the instantaneous deformation. (Viano and Lau 1986)

For lateral impacts, the initial Torso Thickness is half of the width of the body (laterally) where as in frontal impacts it is the width of the body from front to back as shown in Figure 8. The tolerances of the VC and CMax for frontal and lateral impact based on 25 percent probability of injury are shown below.

Table 1 – [VC]Max and CMax Tolerance Levels for Frontal and Side-Impacts based on 25% Probability Injury

Parameter	Frontal Impact (Viano, et al., 1986)	Lateral Impact (Viano, 1989)
Chest [VC]Max	1.0m/s (AIS≥4)	1.47m/s (AIS≥4)
Abdominal[VC]Max	1.2m/s (AIS≥5)	1.98m/s (AIS≥4)
Chest CMax	32%	38.4%
Abdominal CMax	**n/a**	**43.7%**

Cavanaugh attempted to study aortic injuries in a series of horizontally accelerated sled test at speeds between 6.7 to 10.5 m/s. Seventeen cadavers were used in this study and only five of them presented aortic tears. The cadavers presented extensive damage and only some of the aortic tears were clinically relevant. When soft padding was used in some of the tests it diminished the extensive damage to the cadavers and no aortic tears were produced. Cavanaugh then examined the potential injury parameters and using logistic regression analysis identified the combination of [VC]max and T12Z was the best predictor of aortic injury (Cavanaugh, et al., 2005). This study also identified the combination of Upper Sternum Acceleration with Average Spine Acceleration (ASA) and the combination of CMax and T12Z as good predictors of aortic injury (Cavanaugh, et al., 2005). Looking at single injury parameters, Chest Compression (CMax%) and ASA resulted as the good predictors of aortic tears (Cavanaugh, et al., 2005). The logistic regression (linear combination analysis) of these parameters and the logit plot of probabilities are shown below:

Table 2 – Logistic Regression –Linear Combination Analysis (Cavanaugh, et al., 2005)

Combination	K1	K2	K3	Chi-Square	P-Value
K1*T12Z+K2*CMax+K3	0.0236	0.3666	-20.9704	8.438	0.0037
K1*T12Z+K2*[VC]Max+K3	0.0294	4.6622	-10.4518	9.760	0.0018

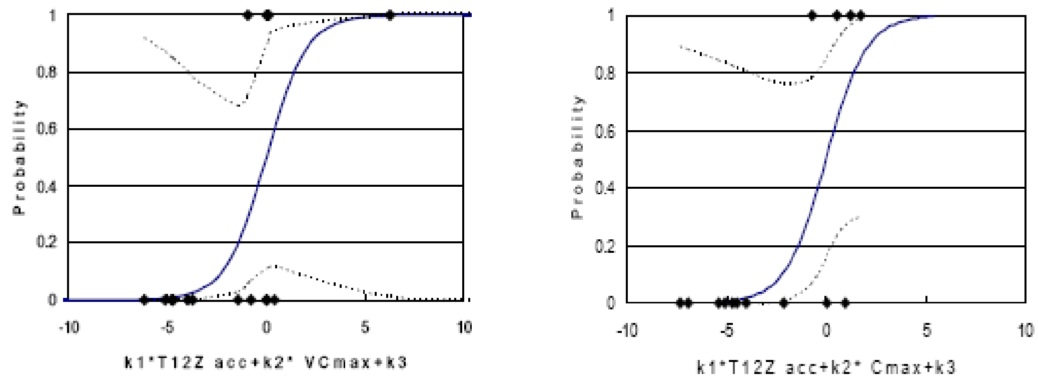

Figure 9 – Logist plot of probability of AIS4 or higher to the aorta vs. combination of T12Z acceleration and [VC]Max (left) and CMax (right) (Cavanaugh, Koh, et al. 2005)

To better understand the mechanisms of injury for aortic ruptures Shah (2007) studied the mechanical properties of the aorta. A high-speed biaxial (longitudinal and circumferential) tissue testing machine was used to stretch a tissue sample. Samples from the ascending aorta, peri-isthmus region or descending aorta were used. The tests were performed at a nominal speed of 1m/s and 5 m/s. Figure 10 shows the stress-strain response for the peri-isthmus region according to Shah's studies.

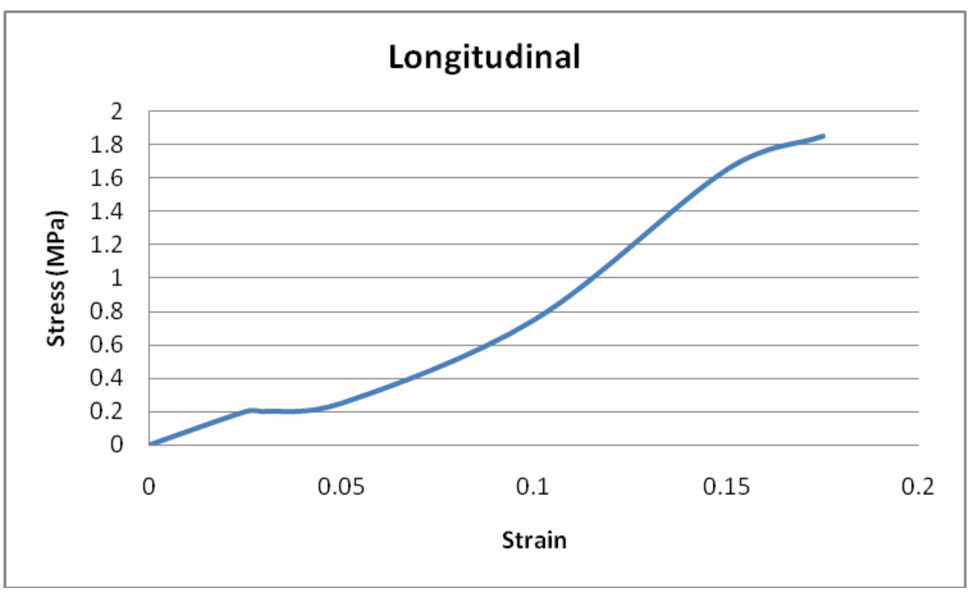

Figure 10 – Longitudinal stress-strain response for the peri-sithmus region of the aorta (Shah 2007)

A recent study (Hardy, et al., 2008) successfully developed a method that can consistently produce clinically relevant aortic tears in cadavers. This method consisted of techniques that would allow the cadaver be tested in a variety of loading conditions and to investigate further the potential mechanisms of injury to the aorta. These techniques allowed the examination of the deformation patterns and strain sustained by the peri-isthums region of the aorta when subjected to an impact. The initial position and orientation of the heart were controlled by having an inverted and angled cadaver such that the organs assume the position of a living human. Eight unembalmed cadavers were tested with different loading conditions. Seven of the eight cadavers sustained aortic injury.

Steps (Steps, 2004) studies confirmed age, delta v and intrusion as predictors of aortic injury and that other injuries in the thorax such as rib fracture are common but not necessary to be present in cases with aortic injuries. She identified that crashes that included damage in the front 2/3 of the vehicle including distributed damage along the side of the vehicle are more likely to present an aortic injury and that it is a statistically significant predictor of aortic injury. Computer modeling was also done in this study where a Y-Damage and a SINCAP test were reproduced. The Y-Damage test resulted in higher z-Spinal Acceleration and Chest Compression.

Studies by Bertrand (Bertrand, et al., 2008) on real-world motor vehicle accidents have focused on identifying the most relevant risk factor of aortic injury and the car crash conditions that are more conducive to this type of injury. Several risk factors such as ETS (equivalent test speed), age, intrusion and seatbelt use have been identified as the main variables influencing aortic injuries. Also, the high frequency of rib fractures present in patients with aortic injuries suggests that the presence of Chest Compression is needed for an aortic injury to occur.

Newman and Rastogi (Newman, et al., 1984) studies observed that in twelve recoded cases of aortic rupture in vehicle accidents, the impact was not completely longitudinal but a lateral component was present. Steps (Steps, 2004) also confirms this finding when comparing a side-impact NCAP test and a Y-Damage test where she found that in the Y-Damage test the lateral loading to the occupant is reduced while the longitudinal loading increases in the thorax (Steps, 2004). Cavanaugh found that the peak acceleration injury predictor was the upper sternum (x direction) acceleration. These studies confirm that lateral and longitudinal components are an important contributing factor in aortic injuries.

2.4 Aortic Injury Detection

Patients with aortic injuries fall into three major categories: Aortic transection, Aortic Hemorrhage and Contained Aortic Injury (Trauma.org, 1989). Aortic transection consists of a total or partial rupture of the aorta. Patients that suffer an aortic transection are generally dead at the scene because of the rapid blood loss. Aortic Hemorrhage occurs when only a small rupture is present, limiting the amount of blood loss. The Contained Aortic injury, also known as an aneurysm, only presents partial tears in the layers of the aortic wall causing it to bulge up because of blood pressure. There is no immediate blood loss but if the condition remains undetected and untreated it could be fatal as it can rupture at any time.

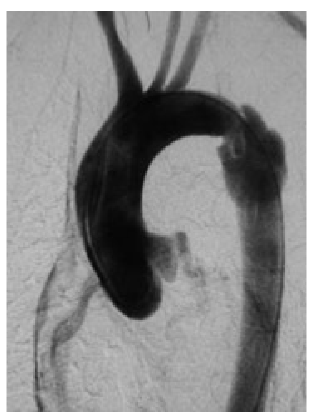

Figure 11 – Angiography of Contained Descending Aorta Injury : Aneurysm showing a bulged up area where blood is being accumulated. (Trauma.org, 1989)

Although the mortality rate is also very high for patients with Aortic Hemorrhage and Contained Aortic Injury, immediate attention and a timely detection could make a difference in increasing the survivability of patients with these conditions. Signs and symptoms are not always present in patients with aortic injury and other severe injuries could interfere with its early detection. The proper triage could help identify possible patients with aortic injury after being exposed to motor vehicle crashes. Efforts in identifying the characteristics of motor vehicle crashes that present aortic injuries have been done to contribute to the triage process of emergency responders.

Aortic injuries are present in frontal crashes and side-impact crashes. This thesis will focus only on the near-side-impact cases. I will compare the crash factors that may contribute to aortic injuries in low- and high-severity accidents. Previous studies focused on the contributing factors to aortic injuries in near-side-impacts. This study will focus on the low-severity impacts where there is a higher opportunity to save lives by alerting the possibility of aortic injuries early in the diagnosis.

There are several tests used for screening for aortic injuries. The primary screening study is the Chest Radiograph (CXR). With these tests a wide variety of signs can suggest the presence of an aortic injury. A widened mediastinum caused by the presence of blood from the artery is the most common sign for detecting an aortic injury with a Chest Radiograph. Blurring of the aortic knob contour, presence of a left apical cap and a tracheal displacement are other signs that could screen patients with a high suspicion for aortic injury (Chiesa, et al., 2003). If there are any abnormalities found in the Chest Radiograph additional tests are performed to confirm the diagnosis.

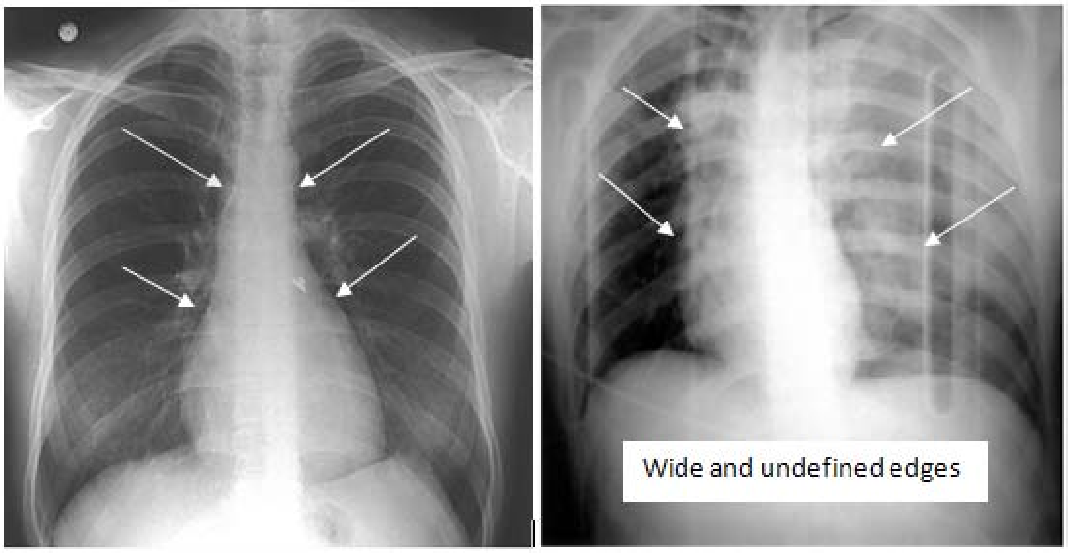

Figure 12 – Normal Chest Radiograph with a proportional mediastinum (left) and Chest Radiograph showing a wide mediastinum caused by aortic injury (right). (Chiesa, et al., 2003)

The Spiral Computer Tomography of the chest (STC) is another screening method to identify patients with aortic injuries and it is considered a definitive diagnostic method. It can identify aortic injuries and ruptures and it is a less invasive, faster and less expensive procedure than the Angiography. Some signs of an aortic injury are an intimal flap, an intramural hematoma or dissection, an aortic wall or contour irregularity and a pseudoaneurysm (Chiesa, et al., 2003).

Figure 13 – SCT demonstrates: thoracic aortic injury at the descending part with vessel wall irregularity and left hemothorax (Chiesa, et al., 2003)

The Angiography is the “gold standard” for detecting aortic injury, defining its location and extent. Angiography is also known as arteriography and it is a technique using medical imaging. An X-ray is taken after a radio contrast agent is added to the blood stream to visualize the cardiovascular structures. The injury shows as an irregular or discontinued contour of the aortic lumen, intimal flap, aortic dissection, posttraumatic coarctation or luminal outpouching as shown in Figure 11 (Chiesa, et al., 2003).

The Trans-esophageal Echocardiography (TEE) is another test, but it requires very specific training and expertise, so it may not be available widely like the SCT or angiography. However, this test can help see small intimal injuries which cannot be detected by the angiography or used for patients that are too critical to move to the angiography room.

Once the aortic injury diagnosis is confirmed the treatment that follows is usually a surgical repair. Not all patients can be treated immediately as other injuries may prevent the patient from going into surgery. (Trauma.org, 1989)

3 Real-World Case Analysis

The National Highway Traffic safety Administration's (NHTSA) main focus is the reduction of the human fatalities, injuries and property damage that car accidents inflict on our society. With 42,000 annual fatalities (NHTSA 2005) in the United States due to automotive crashes and hundreds of thousands serious injuries, the NHTSA has developed and implemented various highway safety programs to reduce these statistics. Among their safety initiatives are databases of motor vehicle crashes.

Studying real-world crashes gives us the opportunity to improve our understanding of injury mechanisms in car accidents. The National Automotive Sampling System/Crashworthiness Data System was created by NHTSA to gather data on car crashes throughout the United States. This system has two main components, the General Estimate System (GES) and the Crashworthiness Data System (CDS). The cases selected in the NASS sampling system are selected from police accident reports (PARS). The GES data has a larger sample of cases but more generic information is gathered to study general trends.

CDS data consists of crashes involving passenger vehicles. Data such as vehicle damage, restraint usage, occupant injuries, environmental conditions, object contacted, etc are collected by crash investigators. The data is collected at twenty four sites in seventeen states. This data helps scientists and engineers analyze these crashes and improve vehicle design to prevent or lessen the number of fatalities and injuries.

3.1 National Automotive Sampling System/ Crashworthiness Data System (NASS/CDS)

The National Automotive Sampling System/Crashworthiness Data System (NASS/CDS) for the years 1993-2007 was used to study the near-side-impact vehicle-to-vehicle cases and examine the characteristics of the aortic injury environment. Near-side occupants in side-impacts are defined as occupants that are seated on the side of the damage of the vehicle. For example, if the damage is on the right side, the right side passenger is the near-side occupant and vice versa for the left side damage.

For the data analysis, SAS Business Intelligence V9.1 was used. This software was used to create the appropriate data sets for the analysis. With SAS it is possible to run logistical regression analysis not only for models involving categorical response variables and a set of independent variables but it can also be used for complex data with stratification, clustering and unequal weighting. Since the NASS data is weighted and clustered, SAS is a suitable and available tool to use for this analysis.

3.1.1 Near-Side-Impact – High & Low-severity (DELTA V) Distribution

In this thesis, near-side-impacts can be categorized based on their severity as high and low. High-severity crashes are those that have a lateral Delta V higher than 30 km/h. Low-severity ones have a lateral Delta V lower or equal to 30 km/h. The data below shows that 5 percent of all severities near-side-impacts weighted data result in aortic injury, out of which only 1 percent are from low-severity impacts.

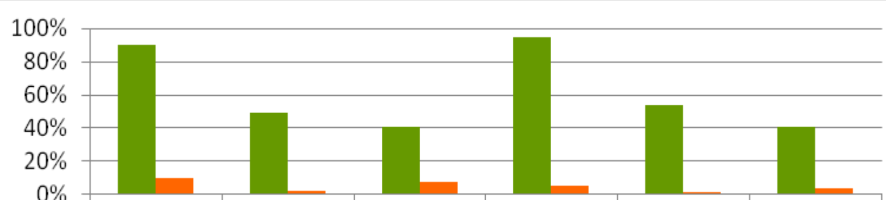

	UNWEIGHTED			WEIGHTED		
	Near *	Low Severity	High Severity	Near *	Low Severity	High Severity
Near Side Impacts (No AI)	90%	49%	41%	95%	54%	41%
Near Side Impacts (AI)	10%	2%	8%	5%	1%	4%

Figure 14 – Aortic Injury in High and Low-severity Near-Side-Impacts (AI = Aortic Injury and *= All Severities)

There are 783 cases of near-side-impacts in the NASS database between the years of 1993 and 2007 that have a Delta-V recorded. Out of which, 77 cases resulted in aortic injuries. After applying the weighting factors we now work with 59,112 near-side-impact cases with 2,913 cases presenting aortic injury. The baseline rates of incidence of aortic injury in all near-side-impacts of un-weighted and weighted data are 0.0983 and 0.049, respectively. The baseline rates of incidence of aortic injury for high and low-severity cases are shown in Table 3. We can see that the incidence of aortic injury is more elevated in high-severity cases than in the low ones. Given this correlation, we can consider Delta V as a factor that could contribute to causing aortic injuries.

Table 3 – Baseline Rates of Aortic Injuries in Near-Side-Impacts

	Un-weighted			Weighted		
	Near-side Crashes	Aortic Injuries	Baseline Rate	Near-side Crashes	Aortic Injuries	Baseline Rate
All Severities	783	77	0.0983	59,112	2,913	0.049
High Severity	385	59	0.1532	26,602	2,108	0.079
Low Severity	398	18	0.0452	32,510	805	0.025

3.1.2 Near-Side-Impact – Contacted Vehicle or Fixed Object Distribution

The following graphic shows the distribution of side-impacts against other vehicles or fixed objects. Fixed objects range from trees, posts, mailboxes, cement pillars, buildings, etc. Fixed objects are only involved in 17 and 9 percent of the side-impact cases with only one crash event for un-weighted and weighted data respectively.

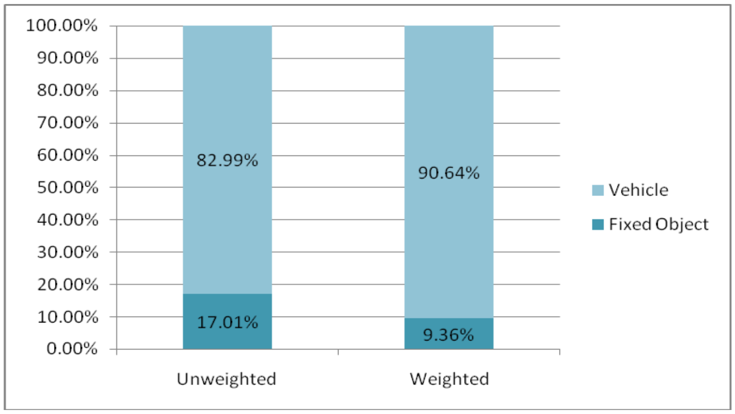

Figure 15 - Distribution of objects contacted in side-impacts

3.2 Case Selection Criteria

The following criterion is followed to select the appropriate cases for the study:

- All data and results use un-weighted and weighted data.
- The data set was built using only vehicle-to-vehicle near-side-impacts.
- Rollover cases were excluded.
- Only cases with AIS 3+ injuries were included.
- Only passengers eleven years old or older were included.
- Rear passengers were excluded from the study.
- Only passenger car cases were examined.
- Cases with one event were included in the data set to isolate the side-impact effects.

3.3 NASS Cases with Aortic Injury Analysis

The crash factors analysis can be categorized in two major areas:

- Occupant : weight, height, age, gender
- Crash Factors: belt usage, PDOF, damage pattern, damage extent.

3.3.1 Occupant Factors

This section studies the effect of occupant factors such as age, gender, height and weight on the pattern of aortic injury in side-impact motor vehicle crashes. Analyzing the injury rates will help us call attention to the effect of these parameters on the aortic injury rate.

3.3.1.1 Near-Side-Impact – Occupant: Weight

In the table below we can see the rates of aortic injuries in near-side-impacts based on weight distribution. For all severity cases, the incidence of aortic injuries increases as the weight of the occupant increases. The heavier the occupant is, the more likely it is for him/her to get an aortic injury in the event of a side-impact.

The results in Table 4 show that the occupants weighing more than 90 Kg are more likely to have an aortic injury than the less heavy occupants. Examining the low-severity cases, we can see that the rate of aortic injuries is about the same for occupants with a weight lower than 90 kg while the heavier occupants show a significant spike in the incidence rate. In the high-severity cases, occupants with a weight lower than 90 kg also have less chance of having aortic injury than the ones over 90 kg.

Comparing these aortic injury rates based on weight to the aortic injury rates in side-impacts we can see that the all severity rate weighted cases for the 90 + Kg group reaching 0.060 is higher than the overall side-impact rate of only 0.049. For weighted low-severity cases we also see an increased rate of 0.035 for the heaviest group compared to a 0.025 aortic injury rate in low-severity near-side-impacts. The rate numbers in bold are the rates that are higher to the reference rate of aortic injury in near-side-impacts for the correspondent severity.

Given these results for both un-weighted and weighted data and the different severity categories we can see an evident correlation between age and rate of aortic injury. This brings to our attention the age parameter as a possible predictor of aortic injury. The statistical significance of this parameter will be analyzed in a later section of this thesis.

Table 4 – Rate of Aortic Injury: Occupant Weight Distribution

	Weight (Kg)	All Severities	Aortic Injury	Rate	Low Severity	Aortic Injury	Rate	High Severity	Aortic Injury	Rate
Base rate				**0.0983**			**0.0452**			**0.1532**
UN-WEIGHTED	**0-54**	169	11	0.065	83	3	0.036	86	8	0.093
	55-75	290	34	**0.117**	140	4	0.029	150	30	**0.200**
	76-89	140	11	0.079	82	4	**0.049**	58	7	0.121
	90+	114	21	**0.184**	74	7	**0.095**	40	14	**0.350**
Base rate				**0.049**			**0.025**			**0.079**
WEIGHTED	**0-54**	15,058	496	0.033	6,699	109	0.016	8,359	387	0.046
	55-75	21,923	1,423	**0.065**	11,465	330	**0.029**	10,458	1,093	**0.105**
	76-89	9,774	366	0.037	6,710	124	0.018	3,064	242	**0.079**
	90+	10,394	624	**0.060**	6,788	240	**0.035**	3,606	384	**0.106**

The weight distribution shows that occupants between 55 and 75 kilograms are present in 40 percent of the cases, and it is also highest percentage when separated into low and high-severity cases. The second most commonly injured group are ones weighting less than 55 kilograms.

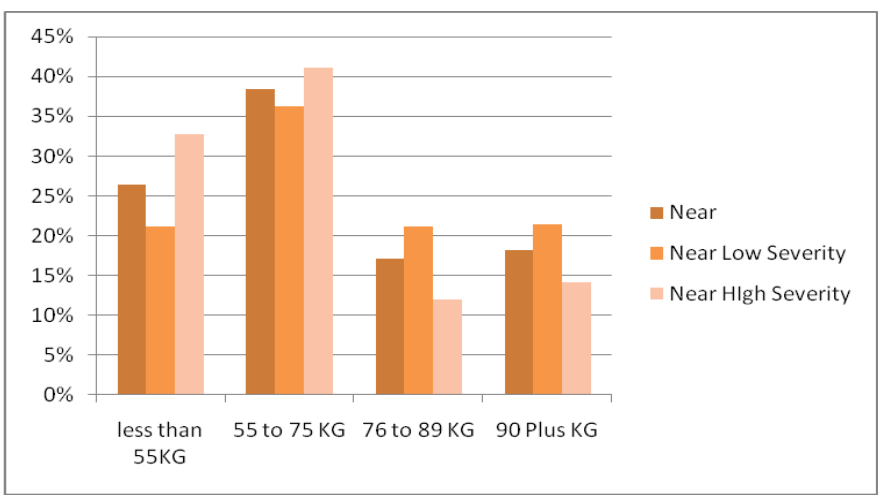

Figure 16 - Weight Distribution

3.3.1.2 Near-Side Impact – Occupant: Height

The following table shows the relationship between traumatic aortic ruptures and occupant height in near-side impacts. The results of this analysis are mixed. The occupants within the 151-170 cm range and the 181 plus cm range have the higher incidence of aortic injury exceeding the 0.049 reference for weighted data. The low-severity cases also present the same groups having a higher incidence of aortic injury compared to the 0.025 near-side aortic injury reference. The un-weighted data presents a similar pattern having the 151-170 cm range and the 181 plus cm range as the most vulnerable for all severity categories. The shortest group seems to always have the lowest injury rate for all cases.

Table 5 – Rate of Aortic Injury: Occupant Height Distribution

	Height (cm)	All Severities	Aortic Injury	Rate	Low Severity	Aortic Injury	Rate	High Severity	Aortic Injury	Rate
Base rate				**0.0983**			**0.0452**			**0.1532**
UN-WEIGHTED	**0-151**	98	4	0.041	46	2	0.043	52	2	0.038
	151-170	333	45	**0.135**	174	11	**0.063**	159	34	**0.214**
	171-180	183	17	0.093	94	3	0.032	89	14	**0.157**
	181+	96	11	**0.115**	62	2	0.032	34	9	**0.265**
Base rate				**0.049**			**0.025**			**0.079**
WEIGHTED	**0-151**	6,467	104	0.016	2,278	28	0.012	4,189	76	0.018
	151-170	27,752	1,923	**0.069**	16,766	509	**0.030**	10,986	1,414	**0.129**
	171-180	16,127	492	0.031	8,364	177	0.021	7,763	315	0.041
	181+	5,804	391	**0.067**	4,255	89	0.021	1,549	302	**0.195**

The 151-170 cm group is also the one with the most incidences reaching almost 50 percent of the cases. There is no clear trend on this injury rate analysis; it does not clearly show a correlation between height and aortic injury. However, it will be furthered studied in a later section to establish its statistical significance in predicting aortic injury.

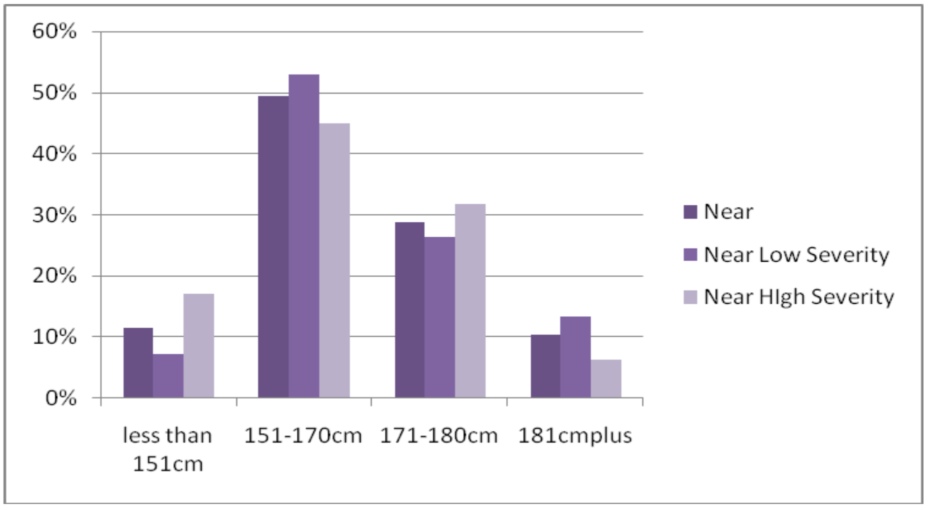

Figure 17 - Height Distribution

3.3.1.3 Near-Side-Impact – Occupant: Age

In the table below we can see the rates of aortic injuries in near-side-impacts based on age distribution. This table shows that the incidence of aortic injuries increases as the age of the occupant increases. The older the occupant is, the more likely it is for him to receive an aortic injury in the event of a side-impact. The rate of aortic injury in the age groups of 35-64 and 65 plus years of age are higher than the baseline rate for all severities and high-severity cases both un-weighted and weighted. Low-severity cases show only the 65 plus age group as the one exceeding the baseline aortic rate or 0.0452 and 0.025 for un-weighted and weighted cases.

The age parameter shows a clear correlation between age and aortic injury with the injury rate increasing as the age group increases. The statistical significance of this age-injury rate correlation will be studied in a later section.

Table 6 – Rate of Aortic Injury: Occupant Age

	Age (years)	All Severities	Aortic Injury	Rate	Low Severity	Aortic Injury	Rate	High Severity	Aortic Injury	Rate
Base rate				**0.0983**			**0.0452**			**0.1532**
UN-WEIGHTED	**15-34**	282	22	0.078	131	3	0.023	151	19	0.126
	35-64	258	29	**0.112**	137	4	0.029	121	25	**0.207**
	65+	168	26	**0.155**	111	11	**0.099**	57	15	**0.263**
Base rate				**0.049**			**0.025**			**0.079**
WEIGHTED	**15-34**	20,184	741	0.037	9,205	102	0.011	10,979	639	0.058
	35-64	18,049	1,021	**0.057**	10,715	208	0.019	7,334	813	**0.111**
	65+	17,270	1,149	**0.067**	11,743	494	**0.042**	5,527	655	**0.119**

The 65+ age group is the most vulnerable in low and high-severity cases. Age is a possible contributing factor to aortic injuries in near-side-impacts. The age distribution shows that the 65 plus years age group is the biggest one with 38 percent while the 35-64 years group and the 15-34 years group are 35 percent and 26 percent respectively in all severity cases. For low-severity cases the 65 plus years age group reaches a frequency of 61 percent. We can see that the older range of occupants are more likely to have a low-severity impact than the high-severity one as only 31 percent of the cases in high-severity cases are in this group range.

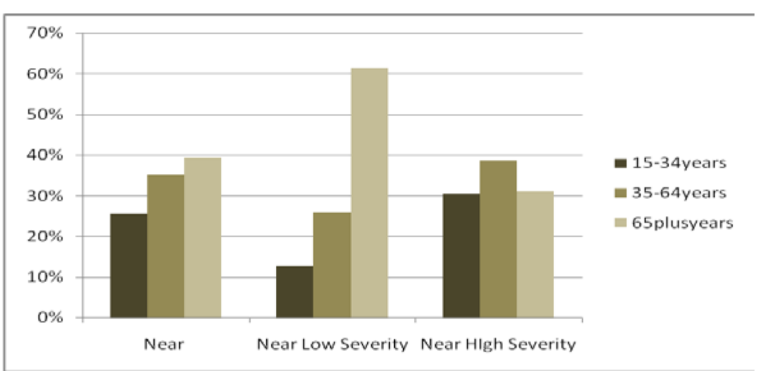

Figure 18 - Age Distribution

3.3.1.4 Near-Side-Impact – Occupant: Gender

Next we analyze the rates of aortic injuries in near-side-impacts based on gender distribution. The rates of aortic injury in all severity near-side-impacts between female and male occupants show little difference. In the low-severity cases there is almost no difference between males and females for the un-weighted data. This parameter shows no correlation between gender and aortic injury. There is no trend showing that one gender is more vulnerable to aortic injury for any of the severity categories. The statistical significance of this parameter will be further analyzed in a later section of this thesis; however, we can expect that the results will show that gender is not a good predictor of aortic injury.

Table 7- Rate of Aortic Injury: Occupant Gender

	Gender	All Severities	Aortic Injury	Rate	Low Severity	Aortic Injury	Rate	High Severity	Aortic Injury	Rate
Base rate				**0.0983**			**0.0452**			**0.1532**
UN-WEIGHTED	**Male**	341	38	**0.111**	190	9	**0.047**	151	29	**0.192**
	Female	368	39	**0.106**	186	9	**0.048**	182	30	**0.165**
Base rate				**0.049**			**0.025**			**0.079**
WEIGHTED	**Male**	25,136	1,194	0.048	13,973	258	0.018	11,163	936	**0.084**
	Female	30,918	1,718	**0.056**	17,612	546	**0.031**	13,306	1,172	**0.088**

In the gender distribution we can see that women were involved in 59 percent of the low-severity cases, somewhat higher than males. The gap is narrower in the high-severity cases where 55 percent of the cases were with female occupants.

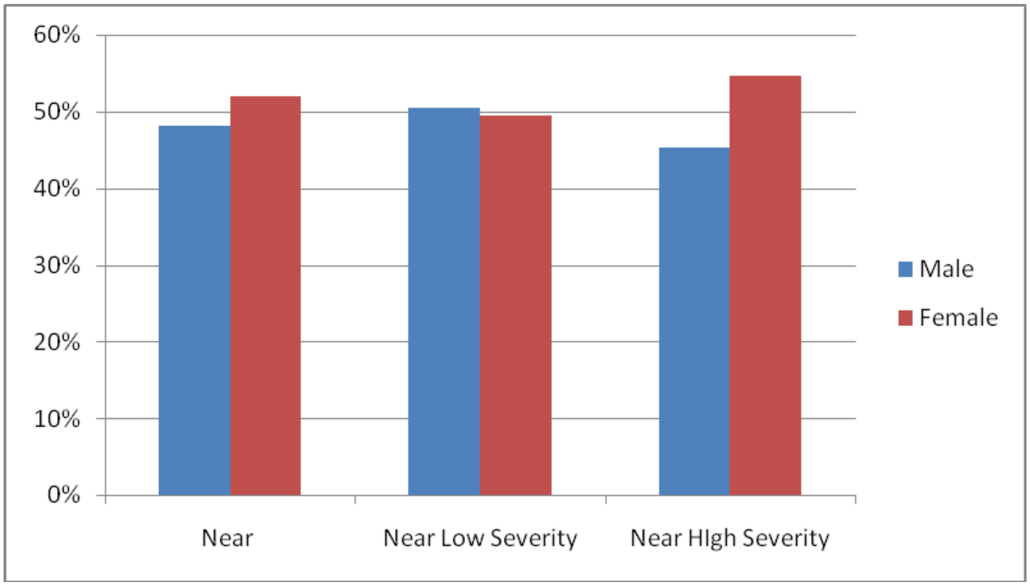

Figure 19 - Gender Distribution

3.3.2 Crash Factors

This section explores the effect of crash factors belt usage, direction of force, damage pattern and damage extent on the incidence of aortic injury in side-impact in motor vehicle crashes. Analyzing the injury rates will help us call attention to the effect of these parameters on the aortic injury rate.

3.3.2.1 Near-Side-Impact - Crash Factors: Belt Usage

Table 8 shows the rates of aortic injuries in near-side-impacts based on belt usage distribution. We can see that none belted occupants are at a slightly higher risk of getting an aortic injury than occupants that are belted. In all severity cases the incidence of aortic injury of non belted subjects is 0.056 for weighted data, slightly higher than the 0.049 reference rate. Similarly in the low-severity cases the injury rate reaches a value of 0.027, while the reference rate is only of 0.025. Analyzing the cases with belted occupants we see that the aortic injury rates are below the reference.

However, in both cases of belted or unbelted occupants the rates are very close to the reference rates which means that belt usage does not influence the outcome of an aortic injury by a large margin. The injury rate analysis does not show a clear correlation between belt usage and aortic injury. This parameter, however, will be analyzed with logistic regression in a later section to study its statistical significance in predicting aortic injury.

Table 8 – Rate of Aortic Injury: Belt Usage

		All Severities	Aortic Injury	Rate	Low Severity	Aortic Injury	Rate	High Severity	Aortic Injury	Rate
Base rate				**0.0983**			**0.0452**			**0.1532**
UN-WEIGHTED	**Belted**	408	42	**0.103**	218	10	**0.046**	190	32	**0.168**
	Not Belted	293	32	**0.109**	155	8	**0.052**	138	24	**0.174**
Base rate				**0.049**			**0.025**			**0.079**
WEIGHTED	**Belted**	35,810	1,677	0.047	19,275	469	0.024	16,535	1,208	0.073
	Not Belted	20,044	1,121	**0.056**	12,269	335	**0.027**	7,775	786	**0.101**

3.3.2.2. Near-Side-Impact - Crash Factors: PDOF

One other crash factor in the rates of aortic injuries in near-side-impacts is based on principal direction of force (PDOF). The PDOF with highest incidence according to the NASS weighted data are the nine, ten and eleven o'clock directions. Out of these three common PDOF's the ten o'clock direction has the highest aortic injury rate at 0.048 overall, 0.026 in low-severity and 0.087 in high-severity cases for weighted cases. The highest aortic injury rate in high-severity cases is for the eleven o'clock direction. One and two o'clock directions have the highest aortic injury rates reaching 0.176 and 0.163 in all severities weighted cases. These two directions have a much lower incidence.

The principal direction of force (PDOF) rates show that the 1 and 2 o'clock directions have a high risk of aortic injury. This angle has a longitudinal and lateral component to it as it is not a 90 degree impact. This is also typical in the Y and D damage patterns which involve the frontal 2/3 of the vehicle. These types of patterns also have a high risk of aortic injury.

Table 9 - Rate of aortic injury: PDOF

	PDOF	All Severities	Aortic Injury	Rate	Low Severity	Aortic Injury	Rate	High Severity	Aortic Injury	Rate
Base rate				**0.0983**			**0.0452**			**0.1532**
UN-WEIGHTED	**1**	14	3	**0.214**	12	3	**0.250**	2	0	0.000
	2	66	16	**0.242**	29	2	**0.069**	37	14	0.000
	9	183	14	0.077	64	2	0.031	119	12	0.101
	10	320	30	0.094	181	8	0.044	139	22	**0.158**
	11	75	5	0.067	70	2	0.029	5	3	**0.600**
Base rate				**0.049**			**0.025**			**0.079**
WEIGHTED	**1**	1,451	255	**0.176**	1,373	255	**0.186**	78	0	0.000
	2	4,115	672	**0.163**	1,674	28	0.017	2,441	644	**0.264**
	9	19,794	672	0.034	6,916	103	0.015	12,878	569	0.044
	10	21,474	1,030	0.048	13,819	362	**0.026**	7,655	668	**0.087**
	11	6,357	34	0.005	6,280	24	0.004	77	10	**0.130**

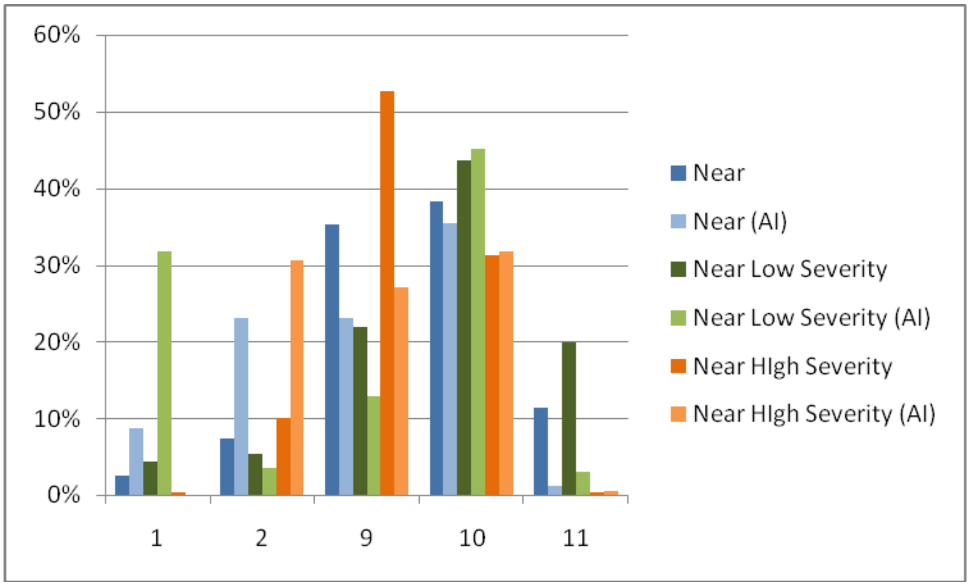

Figure 20 - PDOF Distribution

3.3.2.3 Near-Side-Impact - Crash Factors: Damage Pattern

The damage pattern refers to the extent and location of the damage. The figure below shows the different damage patterns coded in the NASS Database. The most common damage patterns in near-side-impacts with aortic injuries are the P, D, Z and Y type. The graphic below shows the location and extent of these types of damage patterns.

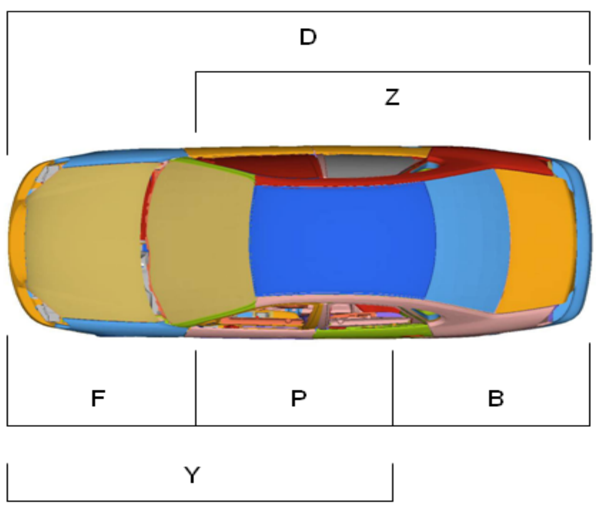

Figure 21 – CDS Damage Patterns

In the table below we can see the rates of aortic injuries in near-side-impacts based on damage pattern distribution. We can see that the D, Y and P damage types are the ones with higher rates of aortic injury for all severities weighted and un-weighted data. This trend is also seen in both low- and high-severity cases. The Y damage pattern is the damage pattern most commonly found in near-side-impacts in real-world cases as seen in the damage distribution figure having a 52% incidence.

However, the damage pattern D and P are the only ones with a consistently higher rate than its base rate throughout the different severity categories. This parameter will be studied further with logistic regression in a later section to see if a specific damage pattern has a greater chance of presenting aortic injury.

Table 10 – Rate of Aortic Injury: Damage Pattern

	Damage Pattern	All Severities	Aortic Injury	Rate	Low Severity	Aortic Injury	Rate	High Severity	Aortic Injury	Rate
Base rate				**0.0983**			**0.0452**			**0.1532**
UN-WEIGHTED	**B**	2	0	0.000	2	0	0.000	0	0	0.000
	D	120	27	**0.225**	48	7	**0.146**	72	20	**0.278**
	F	13	0	0.000	12	0	0.000	1	0	0.000
	P	120	12	**0.100**	72	4	**0.056**	48	8	**0.167**
	Y	350	32	0.091	175	5	0.029	175	27	**0.154**
	Z	107	6	0.056	70	2	0.029	37	4	0.108
Base rate				**0.049**			**0.025**			**0.079**
WEIGHTED	**B**	133	0	0.000	133	0	0.000	0	0	0.000
	D	7,885	1,065	**0.135**	3,380	255	**0.075**	4,505	810	**0.180**
	F	1,431	0	0.000	1,331	0	0.000	100	0	0.000
	P	9,622	505	**0.052**	7,763	330	**0.043**	1,859	175	**0.094**
	Y	29,009	1,188	0.041	12,784	192	0.015	16,225	996	0.061
	Z	8,042	153	0.019	6,270	26	0.004	1,772	127	0.072

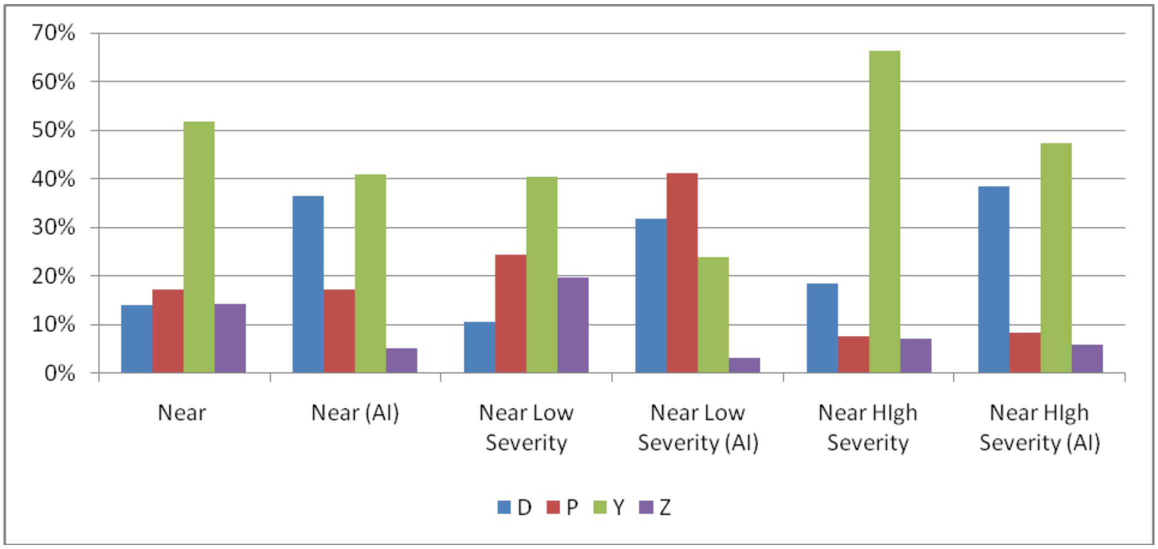

Figure 22 - Damage Location

3.3.2.4 Near-Side-Impact - Crash Factors: Damage Extent

Using the damage extent zones as coded by the NASS/CDS system, we can analyze the extent of the damage. The different numbers represent the intrusion extent of the damage. The higher the number the more intrusion is present. The vehicle is divided into nine damage extent zones.

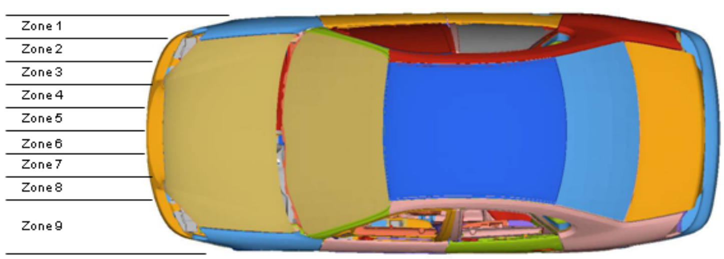

Figure 23 – Damage Extent Zones

Now we compare the nine damage zones from Figure 23 against the rate of aortic injury. As expected, the rate of aortic injury increases when there is more intrusion in the occupant's compartment. The higher the damage extent zone the more intrusion exists. Zones one and two which have the least amount of intrusion have no aortic injuries. Aortic injuries are mostly present in zones 3-6 and there is a clear increasing injury rate.

The damage extents from 4 to 6 present a higher incidence rate of aortic injury than the 0.049 reference in all severity cases. Damage extent 4 presents a 0.048 aortic injury rate for low-severity cases higher than the 0.025 reference aortic injury rate on near-side-impacts. There is a clear correlation between damage extent and aortic injury rate. Damage extent could be a possible predictor of aortic injury and will be further studied in a later section where it will be analyzed with intrusion and crush levels.

Table 11 – Rate of Aortic Injury: Damage Extent

	Damage Extent	All Severity	Aortic Injury	Rate	Low Severity	Aortic Injury	Rate	High Severity	Aortic Injury	Rate
Base rate				**0.0983**			**0.0452**			**0.1532**
UN-WEIGHTED	**1**	2	0	0.000	2	0	0.000	0	0	0.000
	2	74	0	0.000	68	0	0.000	6	0	0.000
	3	317	15	0.047	229	9	0.039	88	6	0.068
	4	240	38	**0.158**	69	9	**0.130**	171	29	**0.170**
	5	53	15	**0.283**	8	0	0.000	45	15	**0.333**
	6	19	7	**0.368**	2	0	0.000	17	7	**0.412**
	7	1	0	0.000	0	0	0.000	1	0	0.000
	8	1	1	**1.000**	0	0	0.000	1	1	**1.000**
	9	1	0	0.000	0	0	0.000	1	0	0.000
Base rate				**0.049**			**0.025**			**0.079**
WEIGHTED	**1**	319	0	0.000	319	0	0.000	0	0	0.000
	2	5,170	0	0.000	4,968	0	0.000	202	0	0.000
	3	31,073	875	0.028	20,078	523	**0.026**	10,995	352	0.032
	4	15,355	1,296	**0.084**	5,911	281	**0.048**	9,444	1,015	**0.107**
	5	3,187	529	**0.166**	299	0	0.000	2,888	529	**0.183**
	6	693	183	**0.264**	53	0	0.000	640	183	**0.286**
	7	103	0	0.000	0	0	0.000	103	0	0.000
	8	16	0	0.000	0	0	0.000	16	16	**1.000**
	9	100	0	0.000	0	0	0.000	100	0	0.000

3.4 Injuries

The injuries analysis can be done by studying fatalities and injuries occurring in conjunction with aortic injuries. These concurrent injuries can be categorized by body region or by organs.

3.4.1 Near-Side-Impact - Injuries: Fatalities

The most dramatic parameter to analyze on near-side-impacts is the fatality rates. The fatal cases in all near-side-impacts, is only 17 percent however in cases with aortic injury the fatality rate increases dramatically to 92 percent. The fatality rates for accidents with aortic injury do not vary much for low and high-severity cases.

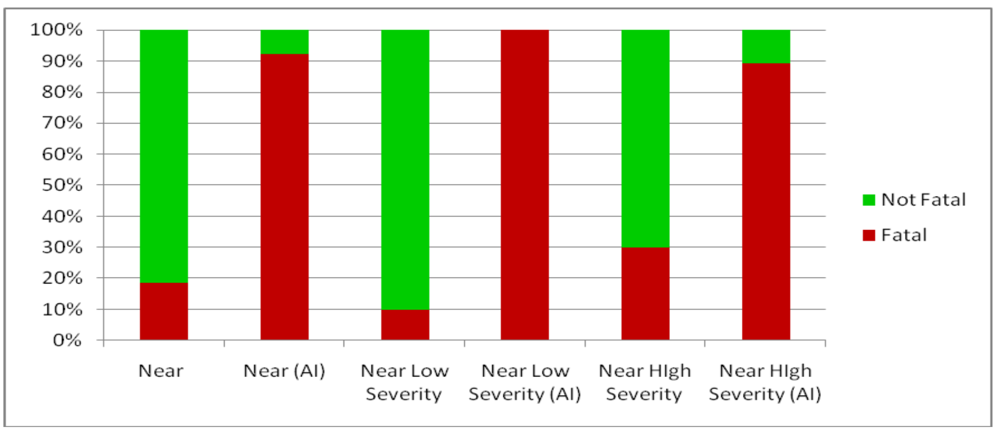

Figure 24 – Fatality Rates

3.4.2 Near-Side-Impact – Injuries: Body Region

The following table shows concurrent injuries by body region in occupants with aortic injuries. The correlation of thoracic and head injuries is the most common in near-side-impacts. Ninety nine percent of the occupants had thoracic injures in low-severity cases, while 43 percent of them also sustained head injuries. Thoracic injuries consist of single and multiple rib fractures, heart and lungs injuries, etc. About thirty percent of low-severity cases present abdomen and lower extremity injuries.

Figure 25 - Concurrent injuries in occupants with aortic tear by body region

3.4.3 Near-Side-Impact – Injuries: Organs

Another important injury to analyze in conjunction with aortic injuries is those to organs. Eighty six percent of the occupants had skeletal injuries. These skeletal injuries are mostly comprised of pelvis, rib and skull fractures. The heart and lungs are the most injured organs in the thoracic area. The liver injuries had lower incidence in the abdominal area. As expected, the brain also shows a high occurrence reaching over 40 percent. As we can see in Figure 26 lung injuries are very common in low-severity cases when compared to the all severity cases reaching over 80 percent of the cases.

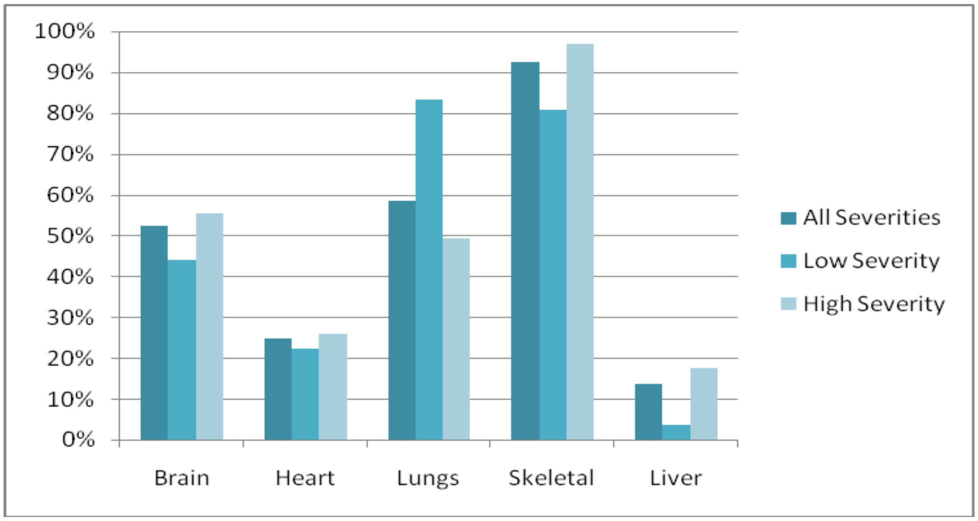

Figure 26 - Concurrent injuries in occupants with aortic tear by organs

3.5 Logistic Regression Analysis of Selected NASS Cases

This section gives a brief background on logistic regression and presents the results of the logistic regression applied to a data set based on the NASS/CDS database to identify possible factors that contribute to aortic injuries in side-impact motor vehicle crashes.

3.5.1 Linear Regression and Logistic Regression Models

A linear regression analysis helps us examine if two variables are linearly related to each other. The linear relationship between the variables can be described by the following equation:

$$Y = \alpha + \beta X \qquad \text{Equation 2}$$

where Y is the dependent variable (variable being predicted), X is an independent variable (variable used to predict Y) and α and β are population parameters to be estimated. The intercept, called α, represents the value of Y when X equals zero. The change in Y, called β, represents the slope of the line that provides the relationship best estimate.

Several independent variables exist in multiple regressions. The following equation is used for modeling multiple regressions:

$$Y = \alpha + \beta_1 X_1 + \beta_2 X_2 + \beta_3 X_3 + \ldots ++ \beta_k X_k + \epsilon \qquad \text{Equation 3}$$

Where k represents the number of independent variables and $\beta_1, \beta_2, \ldots, \beta_k$ are the partial slope coefficients. Having these partial slopes explains that each independent variable has only a partial explanation of the prediction for the value Y. The term ϵ represents the error in predicting Y from X.

The method of ordinary least squares is used to estimate the intercept and the slope coefficients. This method helps choose the best fit curve by picking the curve that has the minimal sum of the deviations squared from a given data set.

Linear regression is used in many cases and can be very accurate for certain applications. However, it is not suitable for studying aortic injuries. In aortic injuries we have the dependent variable having two outcomes; occupant injured or not injured. It is a dichotomous variable as the outcomes are represented by 0 and 1. The relationship of aortic injuries appears to be nonlinear.

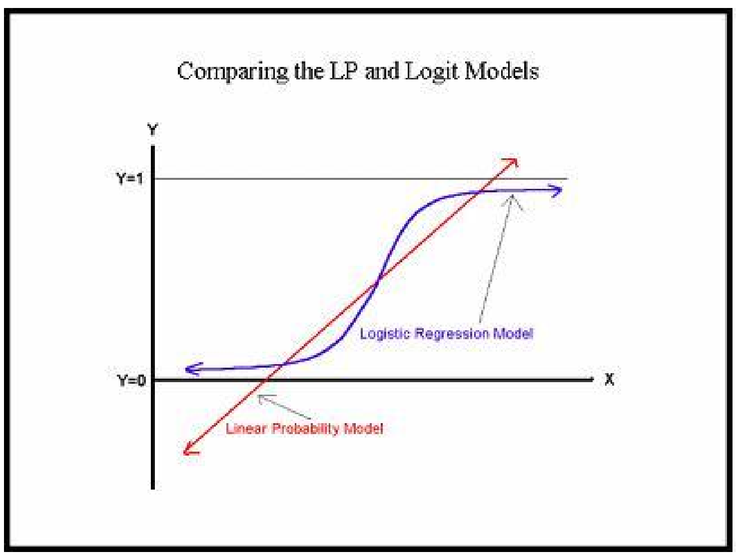

Figure 27 - Linear Regression and Logistical Regression Curves (Whitehead n.d.)

Logistic regression is more adequate for this application. In logistic regression the probability (P) of an event is represented by the logarithm of the odds, also called logit (Equation 4). Odds ratio helps compare if the probability of an event is the same for two groups. (Equation 5)

Logit (Y) = ln [p1 / (1-p1)] = b0 + b1x1 + b2x2 + ...+ bkxk + E **Equation 4**

Odds = p1 / (1-p1) **Equation 5**

There are several measures for evaluating the best fit model for the data set. The chi square goodness of fit test helps us determine how close the observed values are to those which would be expected under the model. The p-value is the probability that the results observed in a data set could have occurred by accident. The null hypothesis is rejected if the P-value is smaller than the significance level. Convention dictates a P-value of 0.05 or below as being statistically significant. In other words, there is a relationship between the independent variables and dependent variable that cannot be attributed by chance.

Another measure is the Receiver Operating Characteristic (ROC) curve which is a function of a model's specificity and sensitivity. Sensitivity is the proportion of true positives as meeting a certain condition. Specificity is the proportion of true negatives as not meeting a certain condition. The interpretation of the areas is the following:

0.50 to 0.75 = fair

0.75 to 0.92 = good

0.92 to 0.97 = very good

0.97 to 1.00 = excellent.

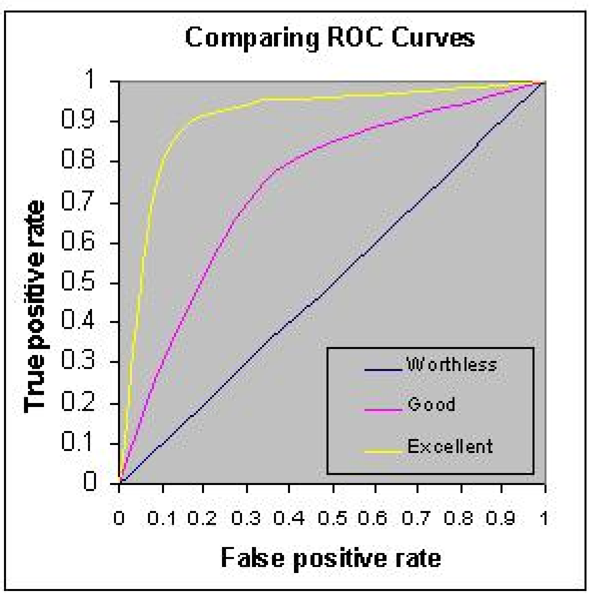

Figure 28 - ROC Curves (University of Nebraska n.d.)

3.5.2 NASS Cases

In the analysis, the cases were separated into two severity groups: low-severity and high-severity. Low-severity cases have a lateral Delta-V of 30kmph or less while the high-severity cases have a lateral Delta-V greater than 30kmph. High-severity cases present many severe injuries and therefore the chances of making a difference in the individual's survivability by a proper accurate triage for aortic injuries decreases. The analysis of low-severity cases would allow for more opportunities to improve proper triage by identifying the most relevant factors that could cause an aortic tear. Also, low-severity aortic injuries are more common in side-impacts than in any other type of impact. That is why the following analysis focuses on all near-side-impact cases for low-severity near-side cases. In addition, this was done for weighted and un-weighted and for individual variables as well as with a combination of those variables to see the effect of weighted data and the different variables.

3.5.2.1 All Near-Side-Impact Cases

Twenty three percent of NASS aortic injury cases occurred with a delta-v below thirty kilometers per hour (30 km/h) or less. For some cases without delta-v the damage extent was used as a parameter to categorize the cases in low-severity and high-severity cases. Cases with damage extent between 1 and 3 were categorized as low-severity and the ones with damage extent between 4 and 9 were selected for high-severity cases. Some cases were eliminated as they did not have a delta-v or damage extent reported in the NASS database. Low-severity cases deserve more attention because there is a higher survivability chance. The data consisted of 398 low-severity cases out of which 18 presented aortic injury and 387 high-severity cases with 59 presenting aortic injuries.

We start with the univariate logistic regression analysis. This analysis will help us understand the role of individual independent variables in cases with aortic injuries. The following table lists the independent variables selected for the logistic regression analysis.

Table 12 - Independent variables for logistic regression

Variable	Type	Description
Age	Continuous	Age of Occupant in years
Sex	Binary	Gender of Occupant
Height	Continuous	Height of Occupant in meters
Weight	Continuous	Weight of Occupant in Kilograms
Belt Usage	Binary	Usage of 3 point belt
Lateral Delta- V	Continuous	Lateral Delta V in kmph
Total Delta-V	Continuous	Total Delta V in kmph
Intrusion	Continuous	Maximum intrusion into occupant compartment in centimeters
Crush	Continuous	Maximum vehicle crush in centimeters
Damage Location	Category	Damage location

In the univariate logistic regression for all severity cases, we found that the age, weight, Total Delta-V, Intrusion, crush and damage location parameters are the significant variables with a P-Value below 0.05 in the non-weighted data. When the weighting factor is applied the age variable is no longer significant.

Analyzing the odds ratio for the non-weighted data we see that for the age variable there is a 1.1 percent increased chance of aortic injury for every year of the occupant's age, showing that the older the individual is the more chance it has of being injured. The weight variable we see a 1.2 percent increased chance of aortic injury for every 1 kg of the occupant's weight. The total delta v, crush and intrusion have a greater chance of aortic injury as the value of each variable increases. We can see that the intrusion variable has a 60 percent increased chance for every centimeter of intrusion.

Comparing the un-weighted damage location patterns against its different categories we see that the Y pattern has about half the chance of presenting an aortic injury than the D pattern. The D pattern has almost twice the chance of aortic injury as the P pattern. For the weighted data the D pattern has a much greater chance of presenting an aortic injury compared to the Y pattern and also against the P pattern.

For the weighted data, we can see that Weight, Total Delta V, Intrusion, Crush and Damage Location remain as significant variables with a P-value less than 0.05. The odds ratios for these variables vary but are in the same ranges except for the intrusion variable which has a very high value of 1.963. The Receiver Operating Characteristic (ROC) values for these models are all in the 0.50 to 0.75 range which make them fair models. This means that the models do not have very good specificity and sensitivity values.

Table 13 - Univariate Odds Ratio and P-Value Results – All Severities

	UN-WEIGHTED			WEIGHTED		
Parameter	**Odds Ratio**	**P-VALUE**	**ROC**	**Odds Ratio**	**P-VALUE**	**ROC**
Age	1.011	**<0.0001**	0.564	1.006	0.1941	0.57
Sex	0.914	0.4051	0.508	1.03	0.8456	0.494
Belted	0.940	0.5598	0.515	0.877	0.5545	0.517
DV Lateral	1.000	0.9763		1.002	0.7038	0.528
DV Total	1.047	**<0.0001**	0.697	1.059	**<0.0001**	0.697
Height	0.998	0.7917	0.511	0.997	0.7048	0.508
Weight	1.012	**<0.0001**	0.557	1.008	**<0.0348**	0.553
Crush	1.023	**<0.0001**	0.677	1.031	**<0.0001**	0.676
Intrusion	1.603	**<0.0001**	0.646	1.963	**<0.0001**	0.644
Damage Location		**<0.0001**	0.593		**<0.0001**	0.587
Damage Location Yvs.D	0.493			0.279		
Damage Location Yvs.P	0.924			0.911		
Damage Location Dvs.P	1.874			3.262		
Damage Location YDvs.BZFP	1.396			1.706		
Damage Location Pvs.BZFYD	0.974			0.85		

In the non-weighted multivariate logistic regression, age, weight, Total Delta V, intrusion and damage location are the statistically significant independent variables showing a P-value under 0.05. When the regression is applied to the weighted data the Total Delta V variable is no longer significant compared to the non-weighted data. The Receiver Operating Characteristic

(ROC) results show a fair model with values near 0.75. The damage location analysis of the univariate and multivariate analysis show a similar pattern. The D pattern has a greater chance of presenting aortic injury when compared to the P and Y patterns for both weighted and un-weighted data.

Table 14 - Multivariate Odds Ratio and P-Value Results-All Severities

	UN-WEIGHTED			WEIGHTED		
Parameter	**Odds Ratio**	**P-VALUE**	**ROC**	**Odds Ratio**	**P-VALUE**	**ROC**
Age	1.0220	**<0.0001**		1.0200	**0.0041**	
Sex	0.9130	0.639		1.1450	0.6909	
Belted	1.0000	0.9999		1.2150	0.5055	
DV Lateral	1.0010	0.7019		1.0010	0.6619	
DV Total	1.0280	**0.0011**		1.0190	0.1149	
Height	0.9800	0.0694		0.9890	0.5425	
Weight	1.0180	**0.0001**		1.0140	**<0.0001**	
Crush	1.0090	0.1419		1.0150	0.0671	
Intrusion	1.3160	**0.0045**		1.4810	**0.0084**	
Damage Location		**0.0360**			**<0.0001**	
Damage Location Yvs.D	0.5040			0.2550		
Damage Location Yvs.P	1.0790			1.1110		
Damage Location Dvs.P	2.1410			4.3610		
Damage Location YDvs.BZFP	1.2100			1.6900		
Damage Location Pvs.BZFYD	0.7710			0.6410		
			0.761			0.746

3.5.2.2 Low-Severity Near-Side-Impacts

In the univariate logistic regression for non-weighted low-severity cases, the age, Lateral Delta V, Total Delta V, Weight, Crush, Intrusion and Damage Location are the statistically significant variables with a P-Value of less than 0.05. When the logistic regression is applied to the weighted data we can see that weight and age are no longer significant variables. All of these univariate models show Receiver Operating Characteristic (ROC) results higher than 0.5 but are only fair models. Examining the damage location, the D pattern is the one with the highest chance of presenting aortic injury.

Table 15 - Univariate Odds Ratio and P-Value Results – Low Severities

	UN-WEIGHTED			WEIGHTED		
Parameter	**Odds Ratio**	**P-VALUE**	**ROC**	**Odds Ratio**	**P-VALUE**	**ROC**
Age	1.009	**0.0027**	0.554	1.003	0.5359	0.554
Sex	0.901	0.4161	0.511	1.041	0.8346	0.492
Belted	0.946	0.6537	0.515	0.891	0.6498	0.515
DV Lateral	0.983	**<0.0001**	0.623	0.98	**0.0014**	0.618
DV Total	1.049	**<0.0001**	0.706	1.065	**<0.0001**	0.706
Height	0.998	0.7175	0.508	0.999	0.9009	0.494
Weight	1.011	**0.0022**	0.558	1.007	0.0905	0.55
Crush	1.024	**<0.0001**	0.679	1.033	**<0.0001**	0.679
Intrusion	1.696	**<0.0001**	0.667	2.09	**<0.0001**	0.665
Damage Location		**<0.0001**	0.613		**<0.0001**	0.608
Damage Location Yvs.D	0.437			0.252		
Damage Location Yvs.P	0.814			0.796		
Damage Location Dvs.P	1.862			3.162		
Damage Location YDvs.BZFP	1.389			1.691		
Damage Location Pvs.BZFYD	1.069			0.939		

In the multivariate logistic regression for non-weighted low-severity cases, the results showed that age, height, weight, intrusion and damage location are the statistically significant variables, but only age, weight, intrusion and damage location for the weighted data.

In the odds ratio analysis, there is a significant risk of aortic injury if the odds ratio is greater than one. The odds ratio value explains the percentage risk increase or decrease of injury per unit. In this case we can see that an occupant is 2.0 percent more likely to have an aortic injury for each year of the occupant's age.

In both the univariate and multivariate, weighted and non-weighted results for low-severity cases, the intrusion always shows a very high odds ratio which means that the probability of injury increases significantly for every unit increase in the intrusion variable. The Y pattern damage has less than half the chance of presenting an aortic injury compared to the D pattern damage. The D pattern shows a higher chance of resulting in an aortic injury than any other pattern in side-impacts.

Table 16 - Multivariate Odds Ratio and P-Value Results- Low-Severity

	UN-WEIGHTED			WEIGHTED		
Parameter	**Odds Ratio**	**P-VALUE**	**ROC**	**Odds Ratio**	**P-VALUE**	**ROC**
Age	1.022	**<0.0001**		1.018	**0.0225**	
Sex	0.946	0.8177		1.814	0.1325	
Belted	1.098	0.6536		1.184	0.6200	
DV Lateral	0.999	0.7924		0.998	0.7384	
DV Total	1.022	0.0774		1.016	0.2554	
Height	0.972	**0.0443**		0.997	0.8678	
Weight	1.017	**0.005**		1.015	**0.0018**	
Crush	1.01	0.2069		1.009	0.4535	
Intrusion	1.494	**0.0011**		1.828	**0.0041**	
Damage Location		**0.0379**			**<0.0001**	
Damage Location Yvs.D	0.406			0.205		
Damage Location Yvs.P	0.949			0.986		
Damage Location Dvs.P	2.336			4.799		
Damage Location YDvs.BZFP	1.28			2.037		
Damage Location Pvs.BZFYD	0.849			0.697		
			0.779			0.758

3.5.3 Discussion

Previous studies done with un-weighted data and other data sets have concluded that age, delta V, intrusion and damage location are good predictors of aortic injuries (Steps, 2004) (Bertrand, et al., 2008). This analysis reiterates the same findings; however, we can see that in some of the weighted data the results are not completely consistent. Some of these differences can be attributed to the amount of cases that do not have a delta V or damage extent reported. A lot of these cases are discarded when doing the analysis in low-severity cases. This type of truncation of data can also impact the weighting ratios which may no longer be the ones intended with the complete data set. It is also important to mention that this analysis was done with eighteen low-severity cases and fifty nine high-severity cases with aortic injury.

Damage location and intrusion are the parameters that are consistently significant for any severity category. Age appears to be another parameter that is significant but only in the multivariate analysis. Although Delta V is a significant parameter for predicting aortic injury for all severity cases, for the low-severity cases Delta V does not seem to be a significant parameter. This could be attributed to the fact that the range of Delta V on low-severity cases is a lot smaller. Over all, the analysis done for the NASS data (1993-2007) revealed that damage location, intrusion, age and Delta V are the most significant variables for predicting aortic injury.

4 Side-Impact Crash Modeling

The primary software packages used in the side-impact modeling for this study were LS-DYNA and MADYMO. LS-DYNA is a software package developed by Livermore Software Technology Corporation; it is used in the automobile, aerospace, military and bioengineering industries. It is capable of solving many complex problems including ones with large deformations and non-linear materials.

MADYMO is a software package that is commonly used in the automotive and aerospace industries. It is developed by TNO (*Netherlands Organization for Applied Scientific Research)*. Its solver allows analysis on multi-body dynamics and finite element models using Newtonian equations of motion. MADYMO allows engineers to improve occupant safety systems in a more efficient and cost effective way by reducing the need for prototypes. A MADYMO model was created to analyze occupant response on side-impact collisions. Finite Element Analysis was also used to model the impact between vehicles. This analysis was important to obtain the following:

a. Prescribed Structural Motion of the Door
b. Longitudinal and rotational accelerations of the vehicle.

The prescribed structural motion will help us analyze the door intrusion while the longitudinal and rotational accelerations will provide the dynamics of the vehicle at a certain location. The finite element models developed by the National Crash Analysis Center of the 2001 Taurus, NHTSA's moving deformable barrier and IIHS' moving deformable barrier were used.

The Finite Element model for the 2001 Taurus has 951,321 nodes, 805,105 shell elements and 111,255 solid elements. NHTSA's Moving Deformable Barrier has 54,581nodes, 24,633 shell elements and 31,938 solid elements.

Table 17 - Finite Element Model Description

	Taurus 2001	NHTSA 214 MDB
Nodes	951,321	54,581
Shell Elements	805,105	24,633
Solid Elements	111,255	31,938

Figure 29 - Finite Element Taurus 2001 Model by NCAC

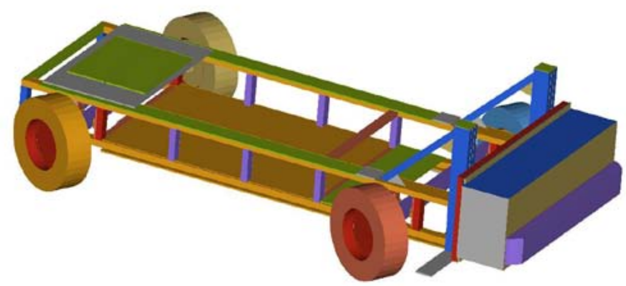

Figure 30 - NHTSA - FMVSS 214 Moving Deformable Barrier by NCAC

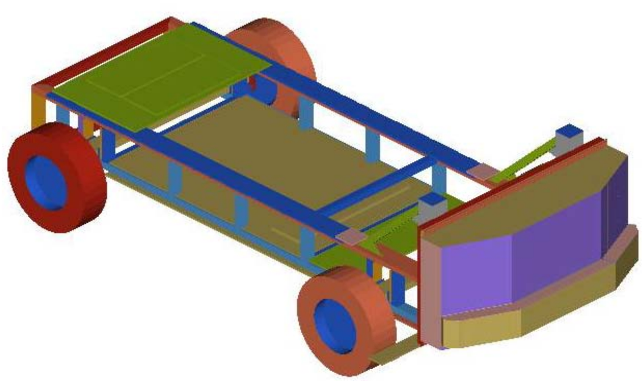

Figure 31 - IIHS Moving Deformable Barrier by NCAC

Different simulations for side-impact were performed including: Side-impact NCAP and Side-impact NCAP Y-Damage using NHTSA moving barrier. For purpose of this study, it was important to have a different range of speeds and damage patterns to see differences in occupant response.

An Accelerometer was placed on the Center of Gravity of the Taurus Model to measure the longitudinal and rotational accelerations of the vehicle. These accelerations will give us the pulse needed for the dynamic simulation in MADYMO.

Also with this simulation we have the structural deformation. Using Visual-Viewer, a post-processing software developed by ESI Group, we are able generate a Prescribed Structural Motion file which extracts the displacement of all the nodes in the selected parts for each time step used. In this case we extract the information of all the nodes in the door parts.

4.1 Vehicle Dynamics Modeling using MADYMO

In the MADYMO modeling, the TNO 50th percentile Human Facet Model and a generic vehicle model were used. The vehicle model which consists of planes and ellipsoids was modified to adapt it to the dimensions of the Ford Taurus.

A joint was placed in the same location as the accelerometer in the center of gravity of the FE model. Then the acceleration on the lateral direction (Y) and the rotation on the vertical axis were assigned using the results from the accelerometers in the LS-DYNA simulation. These accelerations give the longitudinal and rotational motion to the vehicle model.

4.2 Prescribed Structural Motion (PSM) Integration with MADYMO

Full vehicle Finite Element model simulations for structural analysis are common. Prescribed Structural Motion is used to integrate a structural model with an occupant simulation subsystem model. The prescribed structural motion is taken from the full vehicle structural analysis results. The sub-system model is usually used to improve occupant's performance.

The advantage of using the Prescribed Structural Motion Method is the short computation time. The MADYMO multi-body sub system model helps save a lot of computation time as opposed to the higher computation times of structural analysis. The difficulty of occupant performance in near-side-impacts is the door intrusion velocity and the intrusion profile. Prescribed Structural Motion helps input the velocity and intrusion profile to interact with the occupant model.

MADYMO allows the integration of the LS-DYNA Finite Element Structural analysis and the occupant sub model analysis. This is done by creating a finite element model in MADYMO. The location of all the nodes in the door model is specified as well as all the elements that are part of it. Material properties are assigned accordingly. This information is obtained from the LS-DYNA Finite Element Input Deck.

The first step for creating a Prescribed Structural Motion is to identify the PSM Boundaries. In this case, the outer door panel, inner door panel and door trim are selected as the main PSM boundaries.

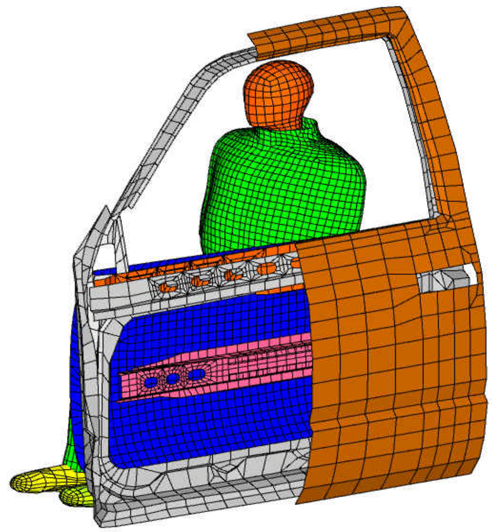

Figure 32 – PSM Boundaries (TNO Automotive-PSM)

The second step is to derive the nodal time histories from the LS-DYNA results. This can easily be done by using Altair Hyper-mesh or Visual Viewer. This software applications help create the PSM file which contains the list of nodes from the selected parts and their nodal displacements.

We identified the PSM boundaries as the Outer door panel, the inner door panel and the door trim. The displacement of the outer door panel nodes as well as all the flush surfaces on it are all prescribed. The outer door has the displacement caused by the striking vehicle.

Critical structural parts that exist between the outer and inner door panel are not totally prescribed. Part of the deformation will take place in the MADYMO run so only the nodes of small areas on the critical parts are prescribed to make a proper connection certain. The nodes in other non critical parts that exist between the door panels should be prescribed.

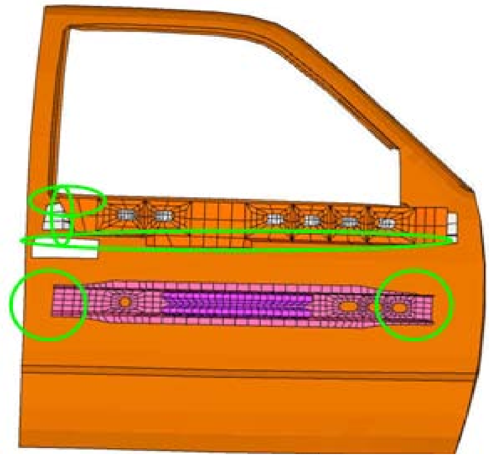

Figure 33 – Structural Parts prescribed areas. (TNO Automotive-PSM)

It is recommended to prescribe the outer nodes in the outer edge of the inner door panel. This functions as a tie between the outer and inner door panel. The rest of the nodes will be deformed during the MADYMO run. Similar to the inner door panel, the outer nodes of the door trim edge are prescribed. This also ensures the tie between the inner door panel and the door trim.

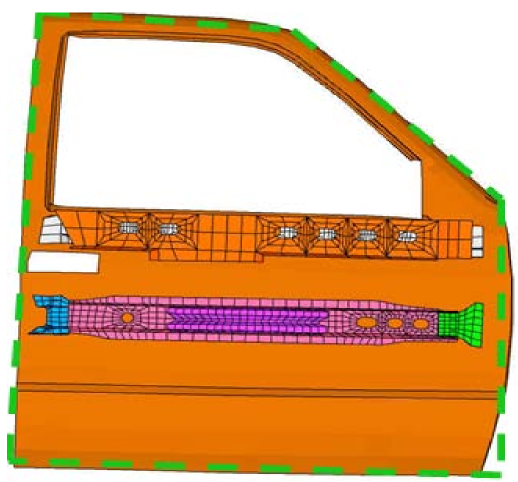

Figure 34 – Inner Door Panel Edge (TNO Automotive-PSM)

The PSM file is created once the nodes that need to be prescribed are selected. This PSM file can be integrated into the MADYMO model by using the MOTION.STURCT_DISP option where you specify the file name with the nodal time history.

Another important step is to specify the contact between the different parts in the door. There should be FE.FE (Finite Element to Finite Element) contacts for the Outer door panel and any deformable structures (critical elements and inner panel), the inner door and the door trim and any other deformable structure as well.

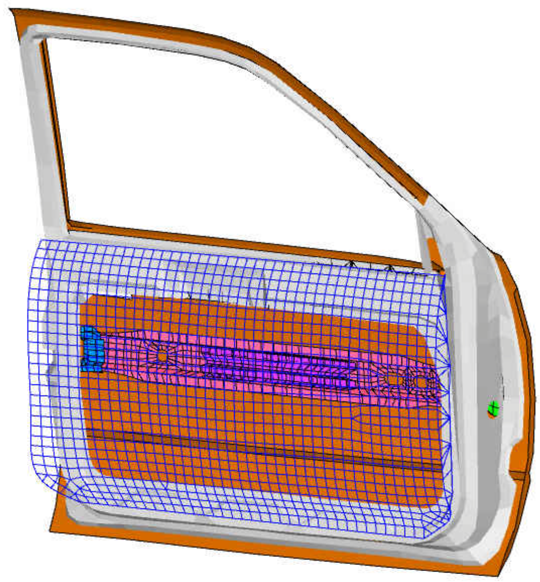

Figure 35 – Door Trim (TNO Automotive-PSM)

This completes the PSM integration with the model, however, contacts between the trim and the dummy should be also specified in the model.

4.3 MADYMO Occupant Model Types

MADYMO allows occupant simulations by representing the occupants as a system of rigid bodies connected by joints. These bodies interact with the interior of the vehicle sometimes represented by planes, cylinders, ellipsoids, etc. or in this case by a finite element model. These simulations allow us to study the behavior of the occupant within a certain environment.

MADYMO works with three model types: ellipsoid models, facet models and finite element models. The three models differ in the modeling application.

These models are different as their geometry and mechanical properties are designed using different modeling techniques. All of MADYMO models are based on chains of rigid bodies connected by kinematic joints called multi-body modules. The rigid bodies have inertial properties.

Ellipsoid models – These models consists of rigid bodies. Their geometry is represented by ellipsoids, cylinders and planes. These bodies have inertia properties and constant mass. Deformations are represented by force-based contact characteristics that are defined for each ellipsoid. These interactions can be within the model or between the model and its environment.

Facet models – These models also consists of multi-body models but they have a more advanced multi-body and rigid surface finite element technology. Inertial properties are also incorporated into the rigid and deformable bodies. The facets are generally the outer surface of the model and are represented by meshes of shell-type elements with no mass. These facets are connected to rigid or deformable bodies. This allows a more complex interaction than simple force-deflection interaction. Structural deformation of flexible parts, such as ribs are represented by deformable bodies which give a more biofidelic response.

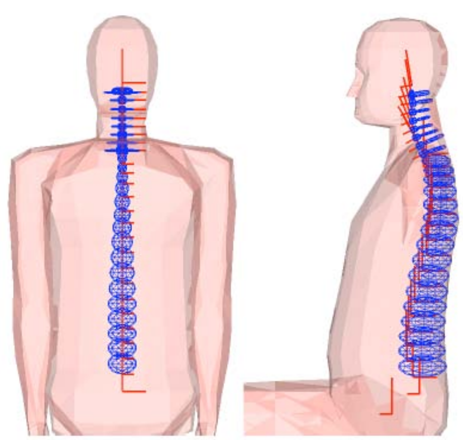

Figure 36 - TNO's Human Facet Model (TNO Automotive-AM, 2005)

Finite Element Models – These models have the most important parts modeled with finite elements. FE models are able to provide accurate results of local deformations of components as well as kinematics and global deformations.

Ellipsoid models are the most CPU time efficient. However, facet models provide more realistic responses than ellipsoid models. Facet models require more CPU time but are still a lot more efficient than FE models. For this study, we used the Human Facet Model which provides a more accurate response.

4.4 NCAP MADYMO Modeling with Human Facet Model

TNO's 50^{th} percentile Human Facet Model was used for this study. This model was chosen because it is important to have a representative response of the human biomechanics. Compared to other TNO Dummy models the Human Facet Model is the one with the most biofidelic response and therefore used in this analysis.

This model has been used in studies by Steps and Alonso (Steps, 2004) (Digges, et al., 2005) analyzing near-side-impacts and far-side-impacts respectively. The Human Facet Model shows a better biofidelity over the EuroSID2 in a near-side-impact configuration (Steps, 2004). One of the main advantages of the Human Facet Model is that it allows multidirectional responses not only lateral while the Euro SID2 allows only lateral direction. Alonso (Alonso, 2004) also found that, the TNO Human Facet model showed good correlation in the kinematics with a human cadaver test under a far-side crash configuration. The Human Facet Model was validated for far-side crashes by duplicating the cadaver test performed by Fildes (Fildes, et al., 2002).

The model was first compared to the results of the NCAP test (TEST #3263). The first step for this was running the Finite Element Model in LS-DYNA with the most updated models of the

2001 Ford Taurus and the NHTSA Deformable Barrier. The velocity of the deformable barrier was set up at 61.95 km/h (43.4709mph) with a 27 degree crabbed angle.

Table 18 - Comparison of NCAP Test vehicle with Finite Element Model

	NCAP Test	Finite Element Model
Make	Ford	Ford
Model	Taurus	Taurus
Year	2000	2001
Weight	1507 Kg	1740 Kg
Body Type	4 Door	4 Door

The Ford Taurus model was equipped with accelerometers throughout the vehicle according to the test report. The velocities and crush profiles of the door of the test results and the simulation results were then compared to make an assessment of the quality of the model for a side-impact.

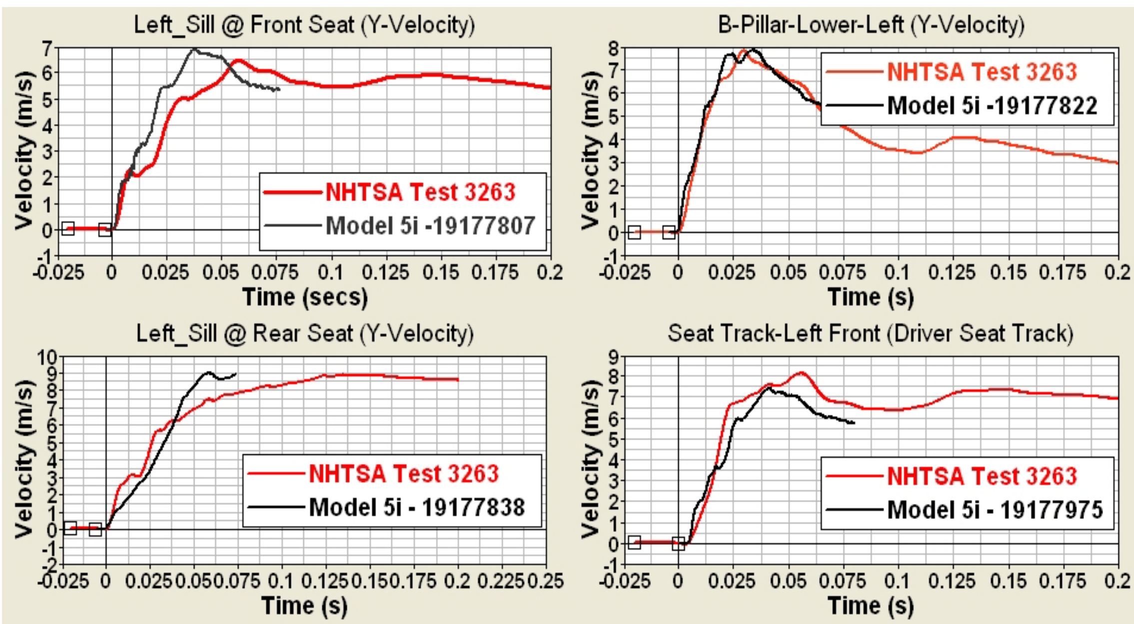

Figure 37 - Comparison of Near-side Velocities between the NCAP test and the NCAP Simulation test.

In Figure 37 we can see the velocities at four different locations of the vehicle from the NCAP test and the NCAP simulation. The velocities of the NCAP simulation are slightly higher at the left sill at front seat and left sill at rear seat locations. The velocities at the Lower B-Pillar on the left side of the vehicle and the velocity at the left front seat track are very similar between the NCAP test and the NCAP simulation. Overall, these velocities indicate that the NCAP simulation with the NCAC models is a good approximation for the NCAP test.

The comparison of the external crush profiles at 4 different heights or levels for the NCAP test and the NCAP simulation are shown in Figures 38 through 41. Levels 2 through 4 show a very good correlation between both tests. Figure 41 illustrates that the simulation has a higher external crush at Level 1 but is still a good correlation.

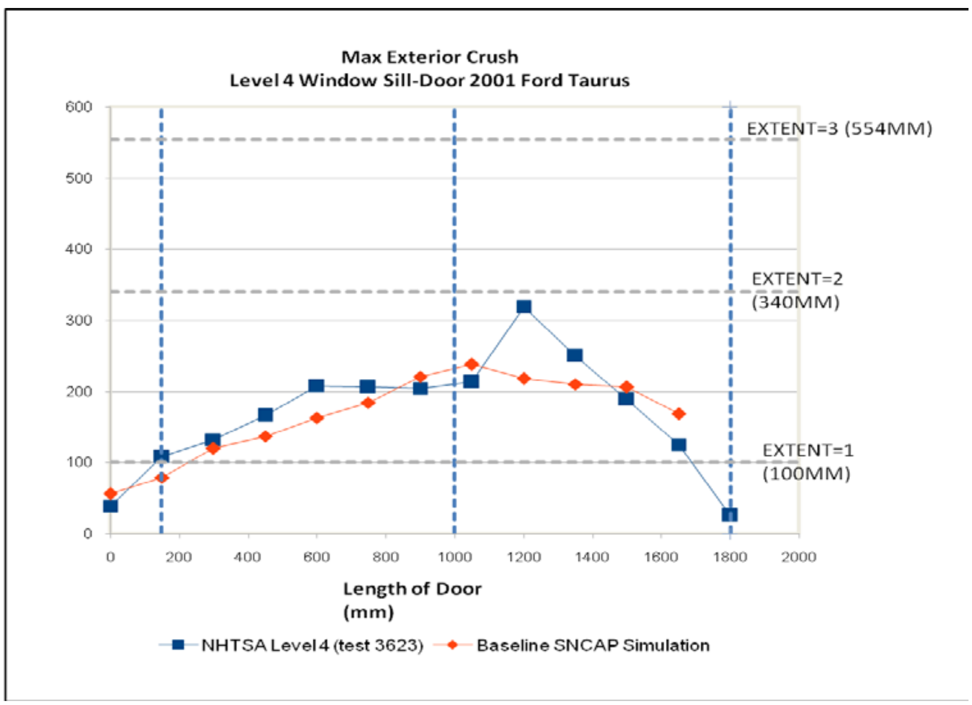

Figure 38 - Comparison of Exterior Crush (Level4) between NCAP test and NCAP Simulation

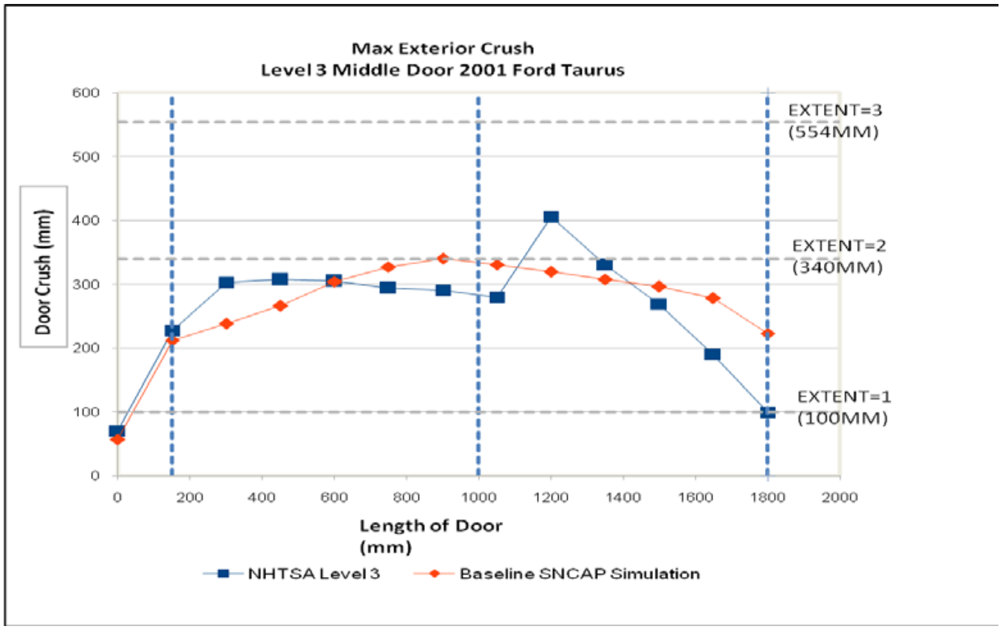

Figure 39 - Comparison of Exterior Crush (Level3) between NCAP test and NCAP Simulation

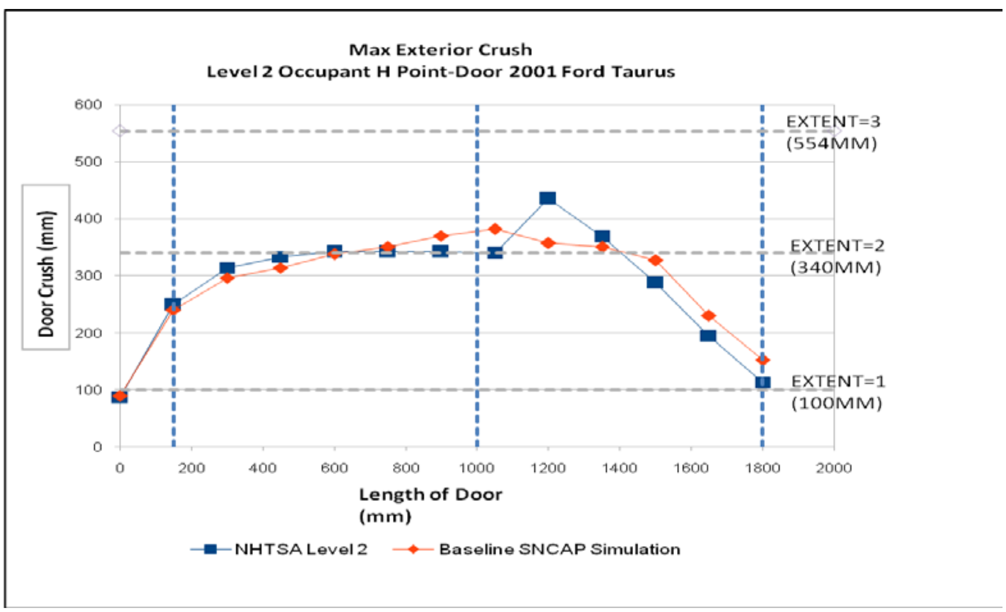

Figure 40 - Comparison of Exterior Crush (Level2) between NCAP test and NCAP Simulation

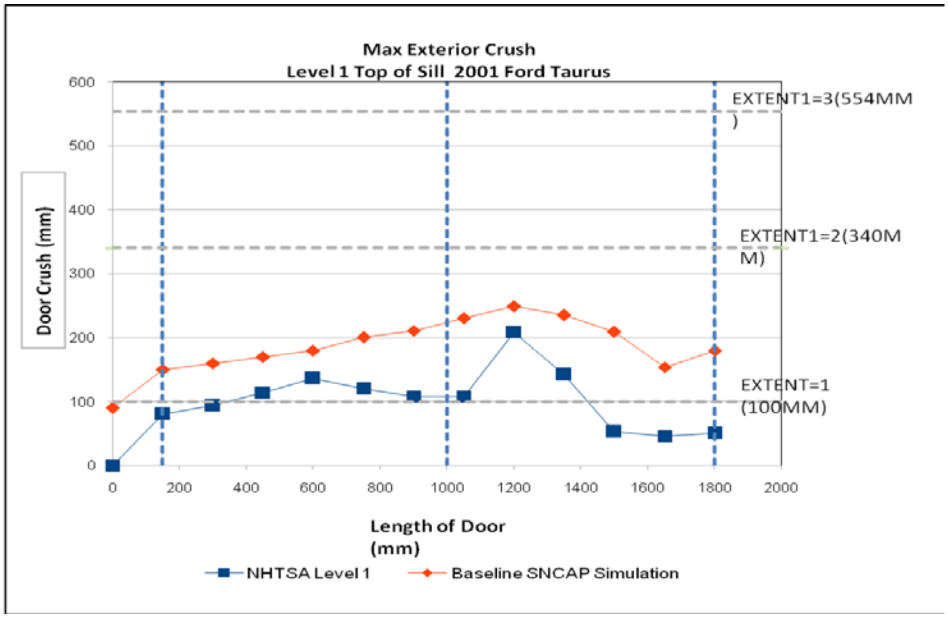

Figure 41 - Comparison of Exterior Crush (Level1) between NCAP test and NCAP Simulation

Given the successful results of the model, the prescribed structural motion of the door parts is extracted to implement them on the MADYMO model. The second step is modifying the MADYMO generic vehicle model in order to represent the Taurus model more accurately. This model only consists of the front-driver seat and passenger seat. Dimensions of the toe pan, the seat position and size, etc were taken from the finite element model and then translated into the MADYMO model.

The finite element door is incorporated into a MADYMO Finite Element model including the prescribed structural motion file, which dictates the displacement of all the nodes in the selected parts of the door.

The 50th percentile Male Human Facet Model was also positioned in the driver seat. The side thorax airbag model was taken from the MADYMO models. It was sized according to the dimensions required by the Taurus model. The contact interactions between the human model and the seat, floor, belt, door and airbag are defined and the contact interactions between the airbag and the door were specified.

There are some general guidelines in choosing the master and slave surfaces for FE.FE contacts. In these types of contacts the penetration will be very small. The choice of the master and slave surface depends on the coarseness of the mesh in the model. The model with coarser mesh should be selected as the master surface.

The contact between the arm, leg and pelvis facets and a finite element airbag was defined using a CONTACT.FE_FE. In this case it is recommended to use a Contact_Method.Node_To_Surface_Char. The Human model arms, legs and pelvis are chosen as the master surface and the airbag group is chosen as the slave surface. The contact is based on contact characteristics of the master surface characteristics. A friction function is also defined in the contact.

The contacts between the seat and/or floor with the Human Model are MB_FE (multi-body/Finite Element) contacts. A force model is used for these interactions. In these cases the vehicle structures were chosen as the master surfaces and the Human model parts were chosen as the slave surfaces.

A FE.FE contact is used between the door and the airbag. The coarseness of the meshes between the airbag and the door are both small. The door surface is selected as the MASTER surface while the Airbag is selected as the SLAVE surface. For this interaction a penalty based Contact Method Surface_To_Surface is used. This model uses the bulk modulus of the master surface to calculate the contact force. This model is designed for non-rigid finite element surfaces and penetrations should be kept as low as possible.

4.4.1 MADYMO NCAP Simulation vs. NCAP Test Results

In this section the results of the MADYMO NCAP simulation are compared to the NCAP Taurus 2001 test results. We expect to see some differences between them because the Human

Facet Model is used in the MADYMO NCAP simulation and a SID III dummy in the NCAP test. These models, besides the fact that one of them is a computer model, are built different and are expected to have different responses.

In the next graphic we can see the accelerations of the lower spine in the NCAP test and the simulation in MADYMO. The lower spine acceleration of the MADYMO model reaches only 659 m/s^2 while the test with a SID III Dummy reaches an acceleration of 804m/s^2. Also the timing of the peaks is slightly different; the MADYMO model has its peak 5.48 milliseconds after the NCAP test.

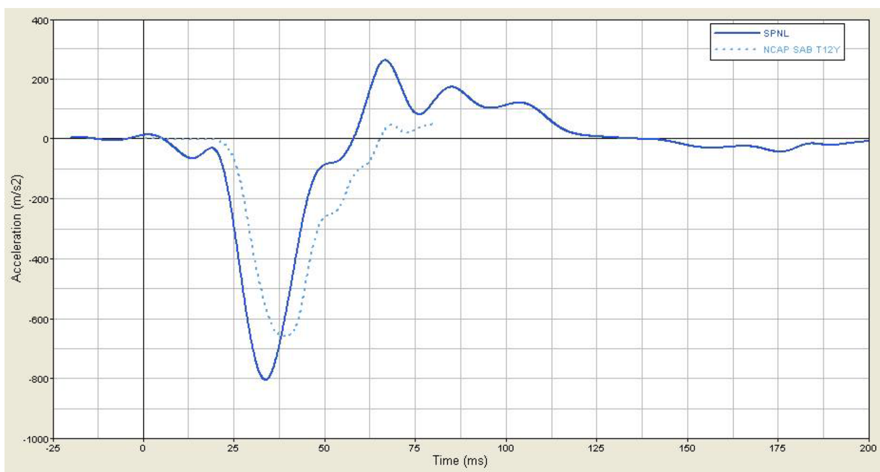

Figure 42 - Lower Spine Acceleration (Y) Response NCAP Test Vs. MADYMO Simulation

Similar to the spine the peak of the Pelvis Acceleration in the MADYMO Model is 7.48 after the NCAP test. The peak Pelvis Acceleration is also lower than the reference test coming only at 797 m/s^2 while the NCAP test reaches 1084 m/s^2.

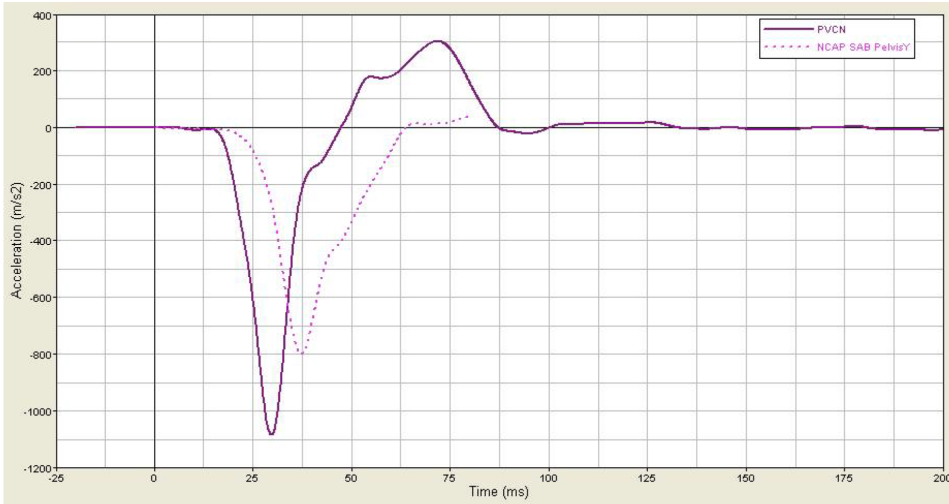

Figure 43 - Pelvis Acceleration (Y) Response NCAP Test Vs. MADYMO Simulation

The signal results have magnitude and peak-timing differences as expected. The different occupant models have slightly different responses. Other factor that could contribute to the difference in the response accelerations is the modeling of the door intrusion. In the previous section we illustrated the differences between the velocities and crush profiles of the NCAP test and LS-DYNA Finite Element simulation. These velocities and crush profiles from the simulation were also slightly different from the physical test. However, this exercise was only done to see if the model behaved similarly to the test, having small accelerations and peak time differences.

5 Injury Analysis with Human Facet Model

In this chapter I present the responses of the Human Facet Model when exposed to sled test with and without 6 inch pelvic offset as well as side-impact tests such as NCAP, NCAP Y-Damage and IIHS test. Some of the Cavanaugh's cadavers testing injury parameters were selected to analyze and compare with the simulations results (Cavanaugh, et al., 2005).

As mentioned in Chapter 3, the aorta tears when it is stretched beyond its tensile strength limit. When the heart shifts positions during Chest Compression, it induces the aorta to stretch along its axis. This stretching usually results in a transverse laceration when the failure strain is exceeded (Shah, 2007).

To explore the longitudinal stretching of the aorta, a simple spring mass model was incorporated within the human model to study the inertial effect of the heart during the sled side-impact test and the vehicle side-impact tests. The spring, which represents the aorta, is attached to the spine on one end and to a mass representing the heart on the other end. The body representing the heart was attached to the spine with a translational joint which limits the degrees of freedom to one. This joint will only allow the heart to move upwards and downwards and will help us to determine the inertial effect of the heart. The stretching of the spring in the Z direction is intended to indicate the inertial effect of the heart on the aorta.

The Maxwell restraint in MADYMO was the most appropriate restraint used to model this spring mass model. This type of restraint is a massless, uniaxial element that can be attached to two bodies. It allows the user to define a non-linear force-relative elongation characteristics of the spring where a positive force represents tension and a negative force compression. No damping was specified and the initial length and the un-tensioned length were the same in the initial state.

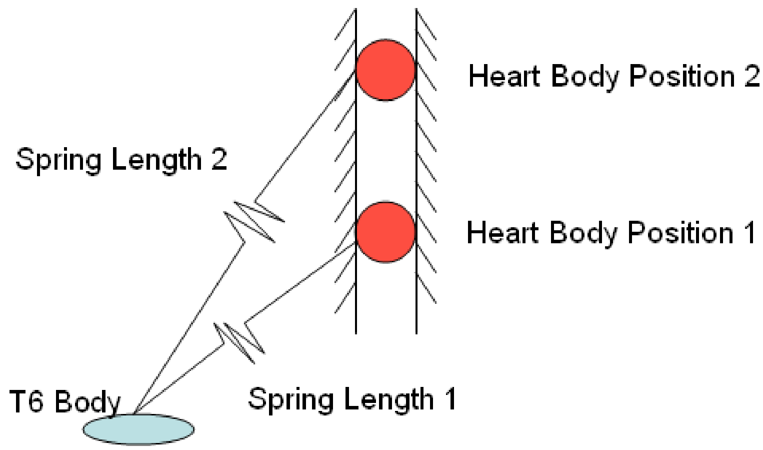

Figure 44 - Spring Mass Model Diagram

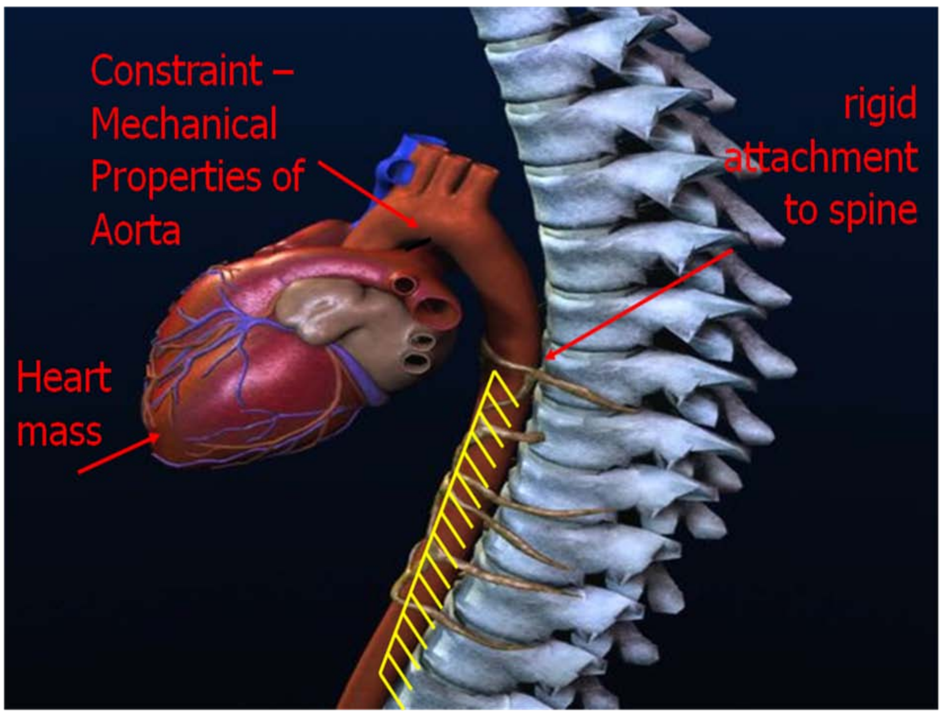

Figure 45 – Anatomy of Heart, Aorta and Spine (Steps, 2004)

The properties of the aortic artery from Shah's study were used as the spring characteristics (Shah, 2007). The per-isthmus aortic properties were selected because it is the most common place of injury and because the spring represents the aorta in that location (Viano, 1983). Figure 46 shows the longitudinal stress-strain response for the per-isthmus region of the aorta according to Wayne State University studies (Shah, 2007).

This test shows a small-strain limit to failure at about 0.175. With this simple model we eliminated the arch of the aorta attaching the heart to the per-isthmus aorta. The strain, also called, relative elongation is defined as the following:

$$\varepsilon = (L_2 - L_1)/L_1 \qquad \textbf{Equation 6}$$

Where ε = strain or relative elongation

L_2 = length after stretching

L_1= Initial length

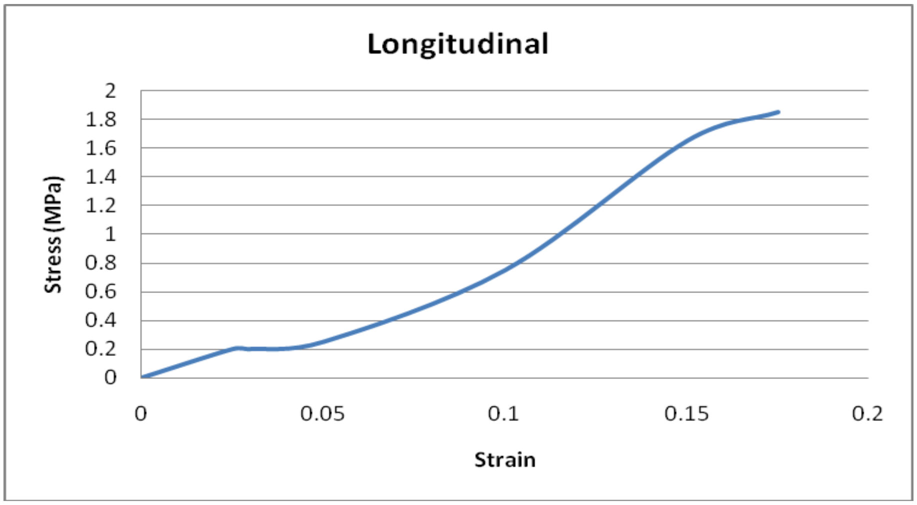

Figure 46 - Longitudinal stress-strain response for the Peri-isthmus region of the aorta (Shah, 2007)

This simple spring mass model isolates the inertial effect of the heart. The mass of the heart was specified at the average of 0.35 kg. This model is not taking into consideration the Chest Compression that has been proposed as a possible injury mechanism. It examines the loading of the acceleration in the vertical axis (Z) in absence of Chest Compression. This model intended to supplement the cadaver tests that induced Chest Compression but without inertial acceleration as observed in crash tests.

There are many existing challenges associated with modeling tissue interactions. It is very important to understand the boundary conditions associated with the aorta and the interaction with other tissues and blood pressure. There is some existing information on tissue mechanical properties, but to incorporate the complexity of the material behavior and motion of the tissues into finite element models is extremely difficult. A more detailed model including all boundary conditions, would introduce many variables and errors into the model that could translate in results that are not much more accurate than a simple spring-mass model. Therefore, the spring mass model was chosen to simply proof that this inertial component was present.

5.1 Sled Test Side-Impact Tests

As discussed earlier, it is important to include cadaver testing to obtain better data in our analysis. For that reason, I have also used the sled testing studies performed by Cavanaugh, who examined the response of the human body to side-impacts. The modeled sled tests were primarily done to validate the human model with the added spring mass model of the aorta against the Cadaver testing, trying to reproduce the same results under the same test conditions.

This series of cadaver tests was the only one that produced aortic injuries and it will be used as a reference to continue the study of aortic injury through modeling. A horizontally accelerated sled that contained a rigid seat fixture was used in the Cavanaugh tests. The cadavers impacted three different surfaces: a flat rigid side wall, a side wall with a six inch pelvic offset and a flat padded wall. The results of these studies have helped us understand the human response to different impact surfaces and configurations. The sled, shown in Figure 58, consists of four beams located so as to impact the shoulder, thorax, abdomen and pelvis and knee.

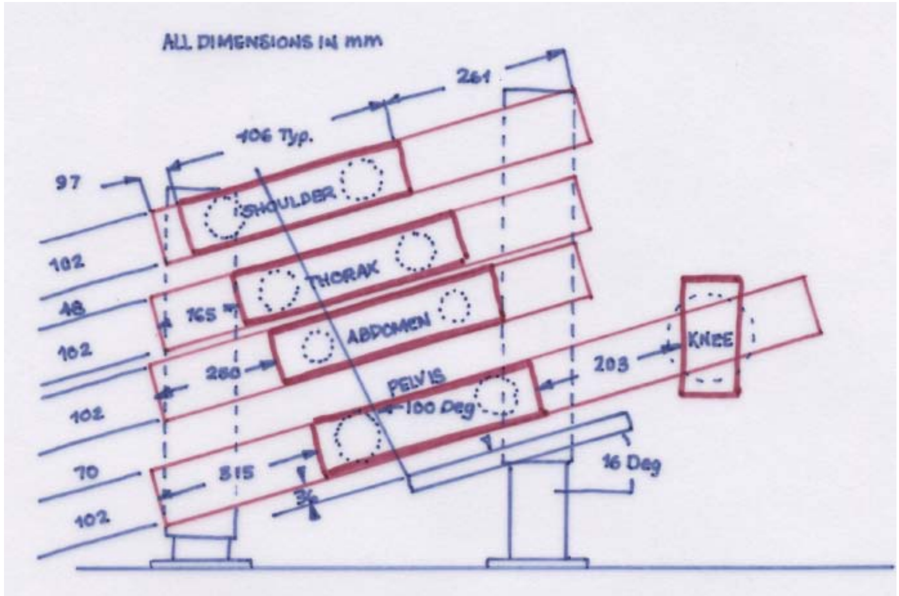

Figure 47 - Diagram of impacted side wall showing beams at shoulder, thorax, abdomen, pelvis and knee. (Cavanaugh, et al.)

A simulation of the sled test was done using MADYMO. The Human Facet Model and a rigid seat sled model were used to model Cavanaugh's test environment. Also, some of the parameters studied by Cavanaugh were used in the Human Facet Model simulations for the analysis and the validation. The injury analysis will help us better understand the lateral impact responses for the chest, abdomen and pelvis. Acceleration readings were taken on the Lower Spine (T12Z, T12Y), Upper Sternum (SternumUpX, SternumUPY), Pelvis (PelvisY) and Upper and lower Ribs, as well as the [VC]Max and CMax readings of the Human Facet Model.

The Human Facet Model was impacted against the rigid beams as described in Figure 47 with and without a six inch pelvis offset. Cavanaugh's studies were done at speeds of approximately 9 m/s (Cavanaugh, et al., 2005). The simulations done in MADYMO were done at 12m/s to reach the T12Z accelerations, Chest Compressions and Viscous Criterion in Cavanaugh's study. The differences in the acceleration, compression and VC differences between the model and cadavers can be attributed to several factors. The cadaver testing done by Cavanaugh was done with older cadavers and cadavers of different heights, body shapes and weights factors that are not well represented in the simulations. There is evidence that hardened arteries, usually present in older individuals, are more vulnerable to aortic tears (Hardy, et al., 2008). Also, rib fracture was present in all cadavers. This factor cannot be reproduced in with the Human Facet Model. However, we can focus on the differences between the model with and without pelvic offset to make an assessment on this environmental condition.

When comparing tests with the same speed but with and without offset we see that the offset tests have a higher [VC]max and CMax values. This is consistent with Cavanaugh's studies where he was able to reproduce aortic injuries mostly on offset tests (Cavanaugh, et al., 2005).

Table 19 – Injury Parameters for Sled tests with and without 6 inch Pelvic Offset

	Units	SLED	SLED with Pelvic Offset
[VC]Max R8 Res	m/s	1.6090	2.2129
[VC]Max R4 Res	m/s	0.4536	1.6704
CMax R8 Res		43%	45%
CMax R4 Res		21%	40%
P(T12Z&[VC]maxResR8)		14%	76%
P(T12Z&[VC]maxResR4)		0%	23%
P(T12Z&CMaxResR8)		1%	3%
P(T12&CMaxResR4)		0%	0%
T12 Z	(g)	32.02	44.46
Sternum UP X	(g)	27.02	20.50
Pelvis Y	(g)	287.36	440.62
T12Y	(g)	129.61	144.80
Sternum Y	(g)	180.08	142.76
RIB8L(Lower)	(g)	173.25	323.56
RIB4L (Upper)	(g)	143.98	209.65
TTI = 0.5 (Rib8y+T12y)	(g)	151.43	234.18
TTI = 0.5 (Rib4y+T12y)	(g)	136.79	177.23
Relative Elongation		0.0153	0.1946
Percentage Failure		9%	111%

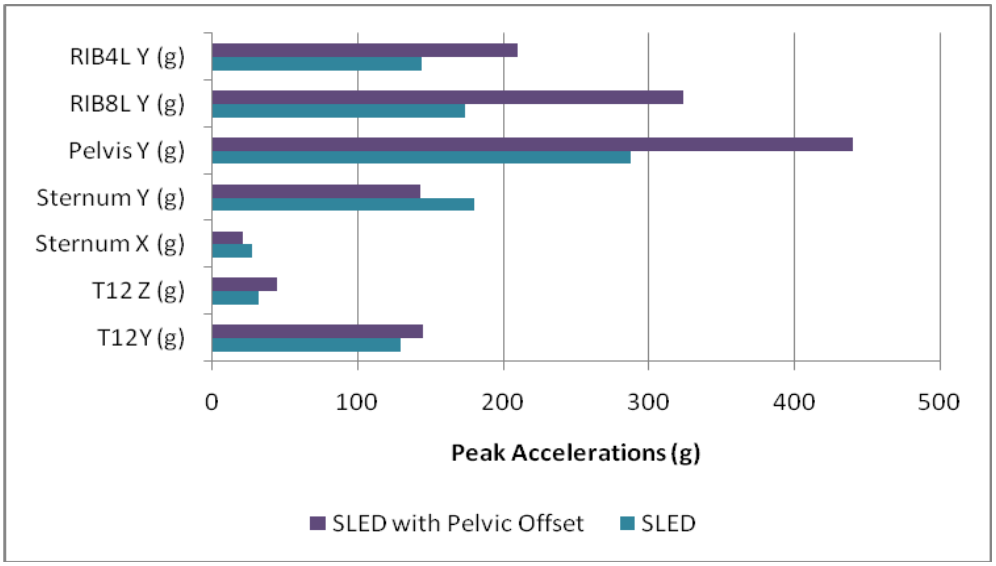

Figure 48 – Peak Accelerations of Sled test simulations with and without pelvic offset

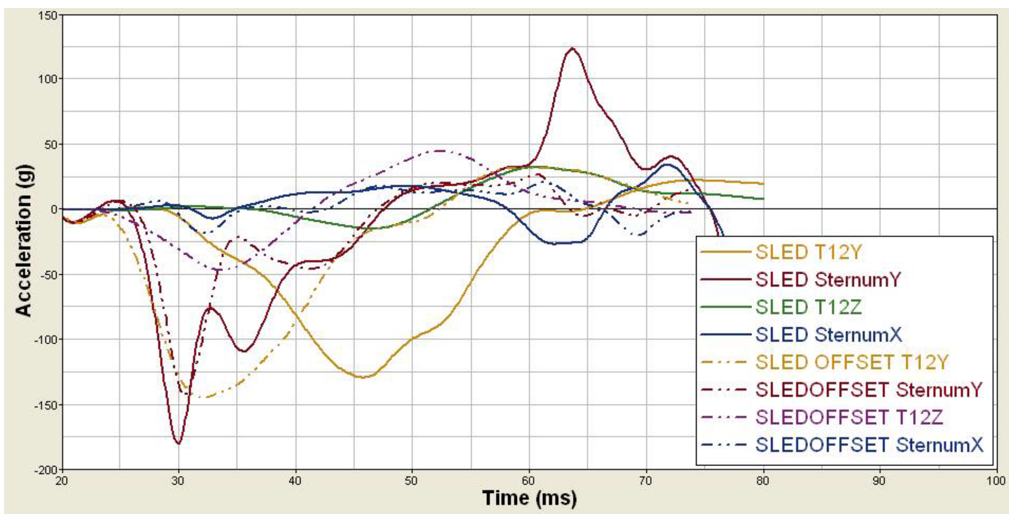

Figure 49 – Sled tests T12 (Y&Z) and Sternum (X&Y) Accelerations

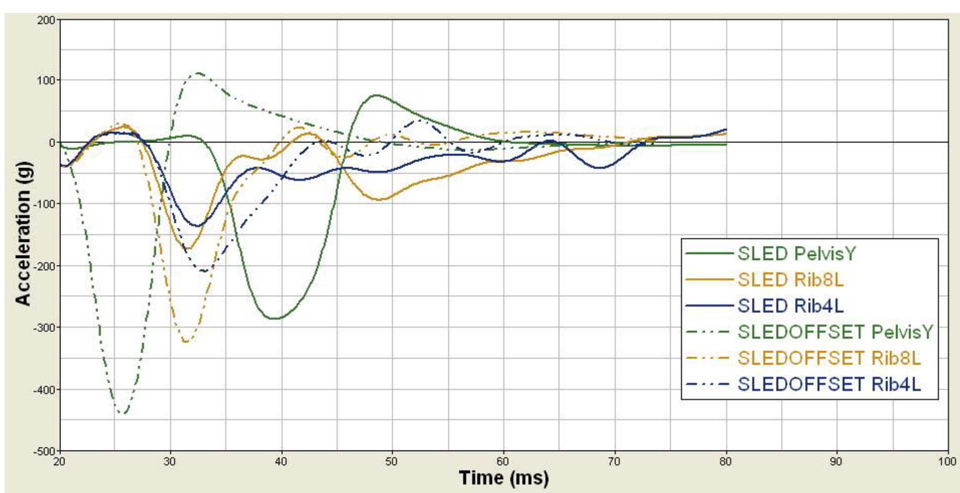

Figure 50 – Sled tests Pelvis and Ribs accelerations

Examining the accelerations measured in the specified points in the model, the lower spine in the Z direction presents higher values on the pelvic offset test. We also see that the accelerations in the pelvis and ribs are higher in this same test. Only the Sternum accelerations on the Y and X direction are higher in the non offset tests. The MADYMO captions for the sled tests can be found in Appendix C.

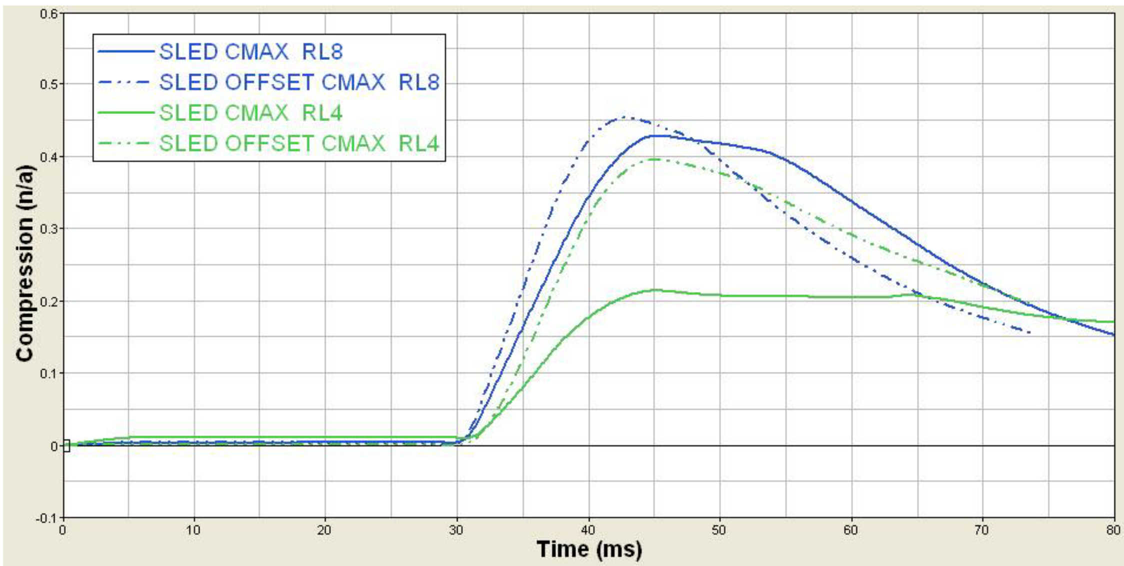

Figure 51 – CMax for Sled tests @ 12m/s with and without 6" pelvic offset

Comparing the sled tests we can see that the offset test has a greater relative elongation than the non-offset test. The non-offset sled test shows a 0.0153 relative elongation, while the offset-sled test has a 0.1946. According to the aorta characteristics used, 0.175 is the limit to failure. The sled offset test is higher than the failure value while the non-offset test is far from reaching the failure value. This is consistent with the Cavanaugh sled test results where he was able to reproduce aortic injury with offset sled tests better than with non-offset ones. The offset causes a greater inertial component in the positive Z-direction than the non-offset test.

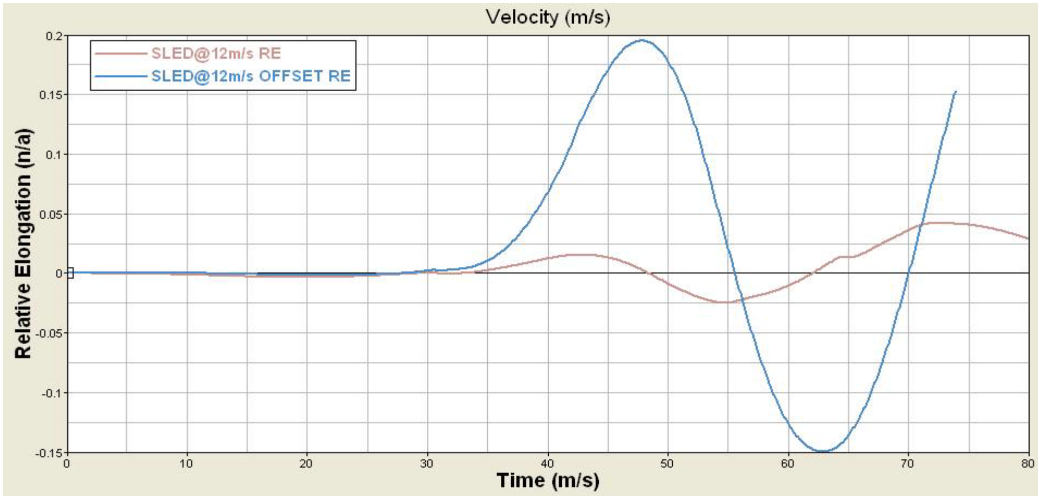

Figure 52 - Relative Elongation of spring Sled and Sled Offset tests.

Again we can see a correlation between the T12Z component and the longitudinal elongation of the aorta. Cavanaugh's injury criteria show a lower probability of injury in the non offset sled test and higher percentage on the offset test (T12Z and [VC]Max), reaching 111% probability of failure. Analyzing the T12Z and [VC]Max combination injury criteria we can see that the sled model was able to reproduce the cadaver results finding that the offset tests are more conducive for reproducing aortic injury.

A sensitivity analysis on Cavanaugh's injury probabilities of the combination of T12Z and VC is discussed in the section to follow. This analysis explores the effects of various parameters and the changes on the system behavior. Sensitivity analysis will help us determine how sensitive the injury probability is when one of the parameters is changed while the other one is kept constant. Cavanaugh's logistic regression was used. The constant values in table 22 were used and one of the parameters was varied while the other one was kept constant.

Table 20 – Logistic Regression –Linear Combination Analysis (Cavanaugh, et al., 2005)

Combination	K1	K2	K3	Chi-Square	P-Value
K1*T12Z+K2*[VC]Max+K3	0.0294	4.6622	-10.4518	9.760	0.0018

Figure 53 shows that varying the VC values have a greater impact in the outcome (P-Value) than varying T12Z. In this sensitivity plot, the gradient of the VC curve indicates the effect that the parameter has on the P-Value. A steep curve indicates a greater influence on the P-Value. A flat curve indicates that the variable has a small effect on the outcome such as the T12Z curve in Figure 53. The ranges of the values were taken from the vehicle simulations having the Spinal Acceleration T12Z varying from 2 to 38g. While the VC parameter varied from 0.673 to 2.973.

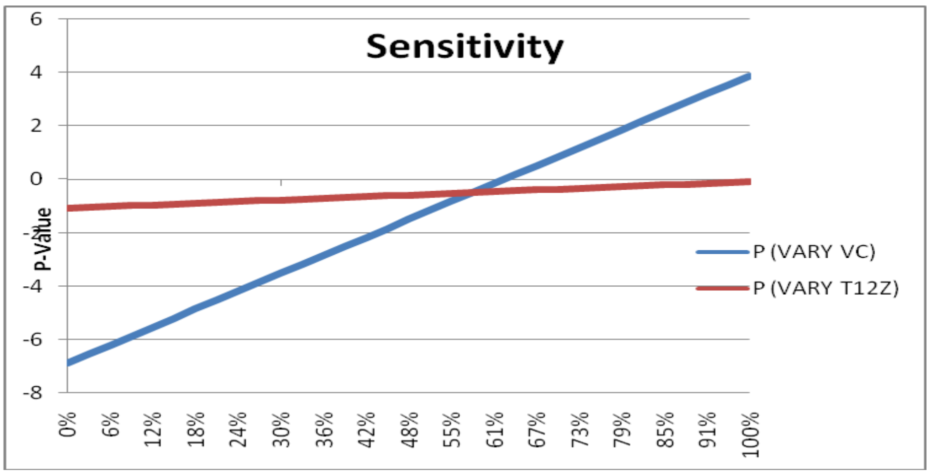

Figure 53 – Sensitivity analysis VC vs. T12Z

The same variations were plotted for the probability values and we can see that while varying the VC parameter the injury probability ranges from 0 to 100 percent while when varying the T12Z parameter it only varies between 35 and 50 percent.

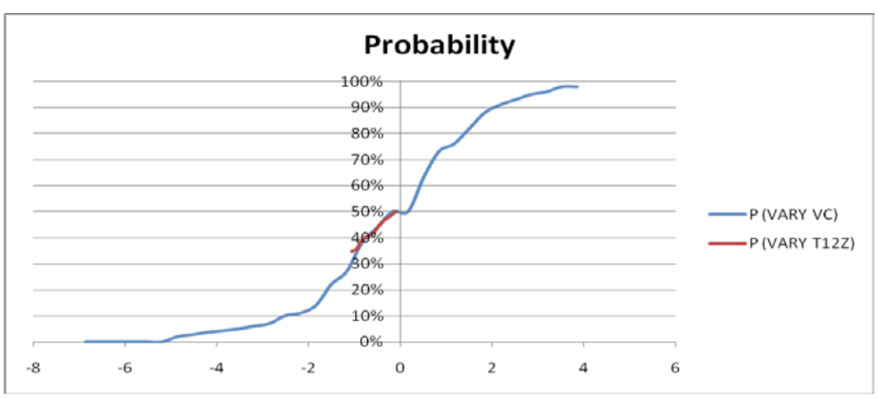

Figure 54 – Probability VC vs. T12Z

5.2 *Taurus Side-Impact Tests*

Having the MADYMO model in conjunction with the LS-DYNA Prescribed Structural Motion we can now see the response of the TNO Human Facet Model in different environments. The impact configurations that were used for this analysis are described in Table 19.

Table 21 - Impact Configurations

	NCAP	NCAP Y-Damage	IIHS
Impact Velocity	61.95 Km/h (38.5mph)	61.95Km/h (38.5mph)	50 Km/h (31.06mph)
Impact Angle	270	270	270
Crab Angle	27	27	0
Moving Deformable Barrier	NHTSA	NHTSA	IIHS
Impact Location	Middle of Vehicle	Front of Vehicle	Middle of Vehicle

In the captions below the LS-DYNA Finite Element simulations with the same configurations are shown. The progress of the impact is shown every 10 milliseconds from the top view and the door intrusion from the frontal view.

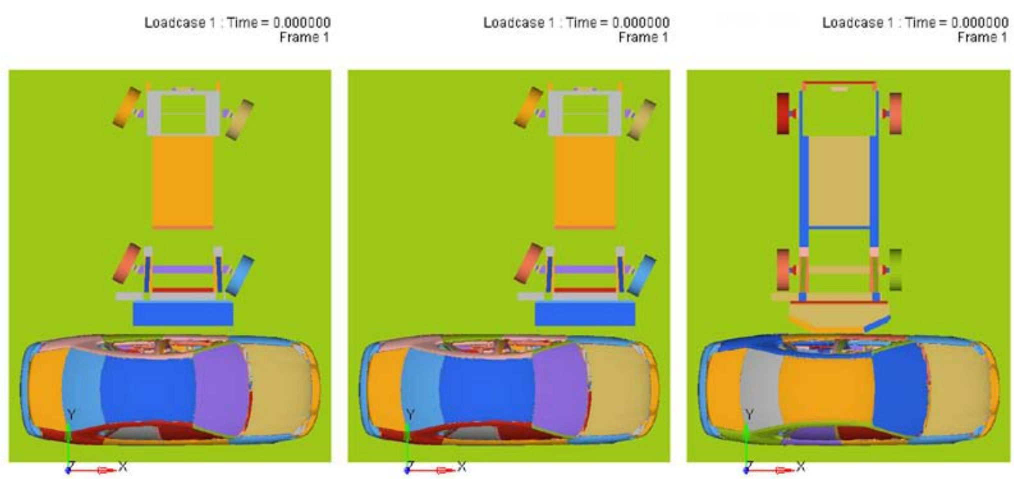

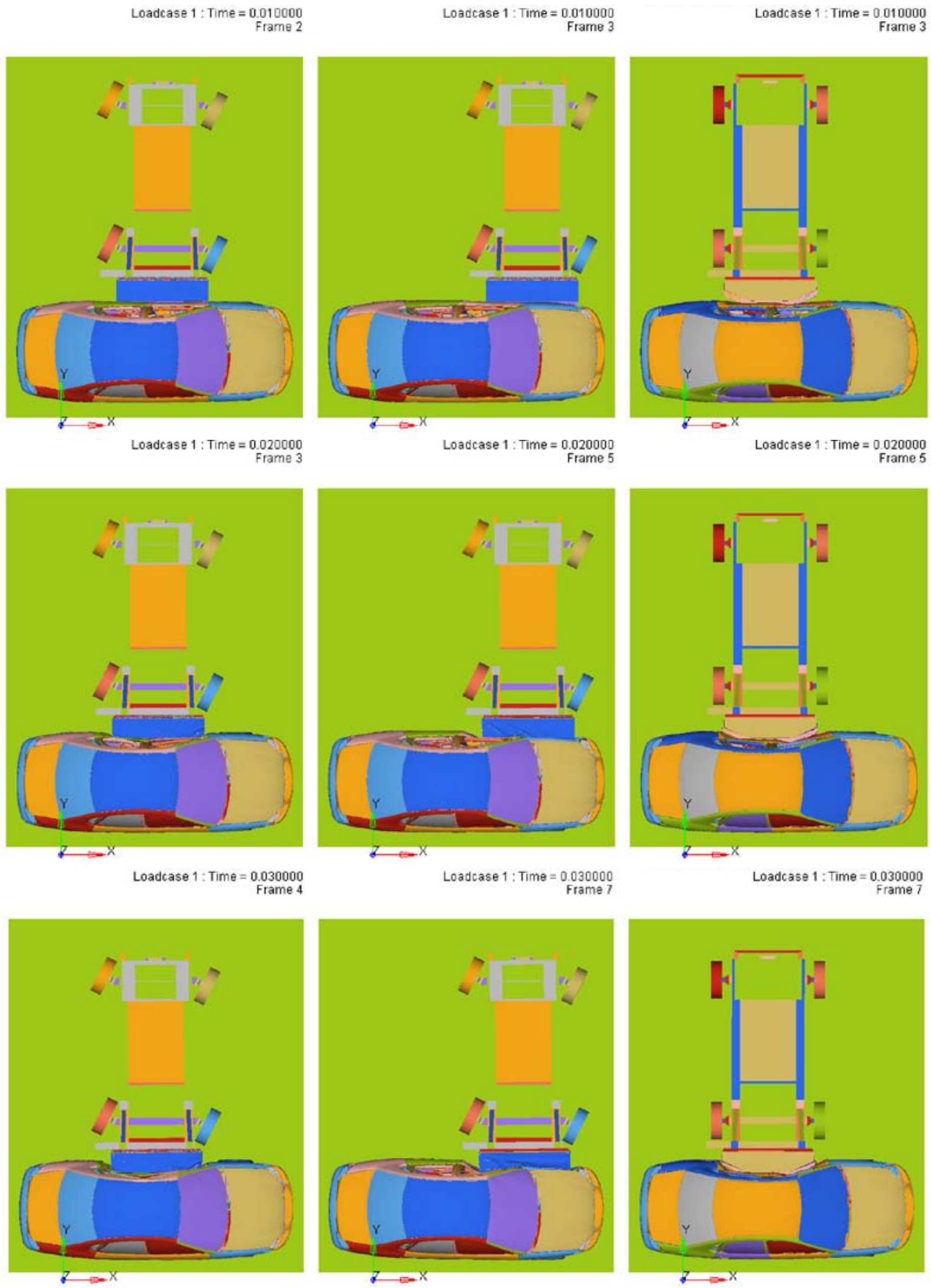
Loadcase 1 : Time = 0.010000
Frame 2
Loadcase 1 : Time = 0.010000
Frame 3
Loadcase 1 : Time = 0.010000
Frame 3
Loadcase 1 : Time = 0.020000
Frame 3
Loadcase 1 : Time = 0.020000
Frame 5
Loadcase 1 : Time = 0.020000
Frame 5
Loadcase 1 : Time = 0.030000
Frame 4
Loadcase 1 : Time = 0.030000
Frame 7
Loadcase 1 : Time = 0.030000
Frame 7

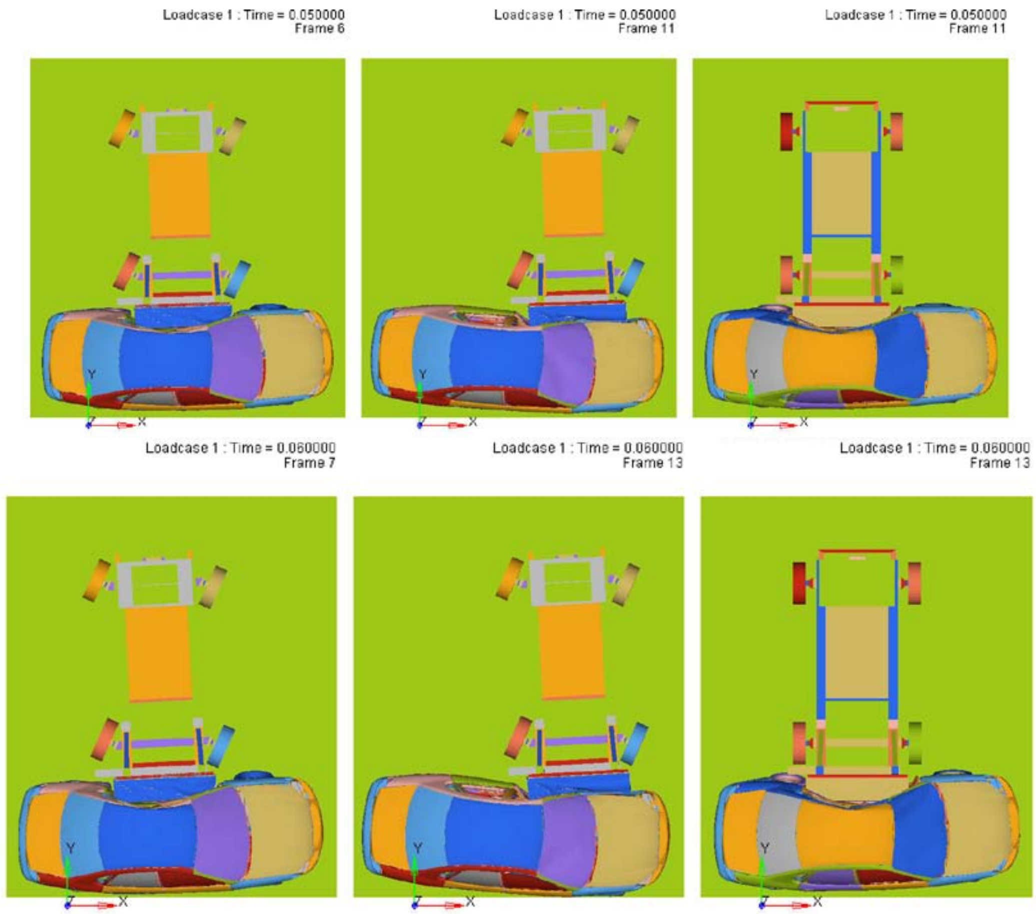

Figure 55 - Top view of FE simulations NCAP Side-impact (left), Y-Damage (middle) and IIHS (right)

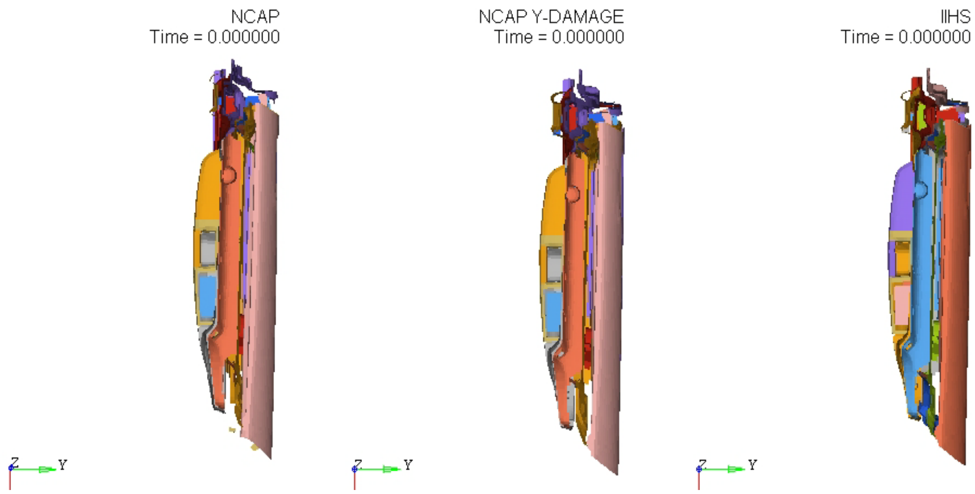

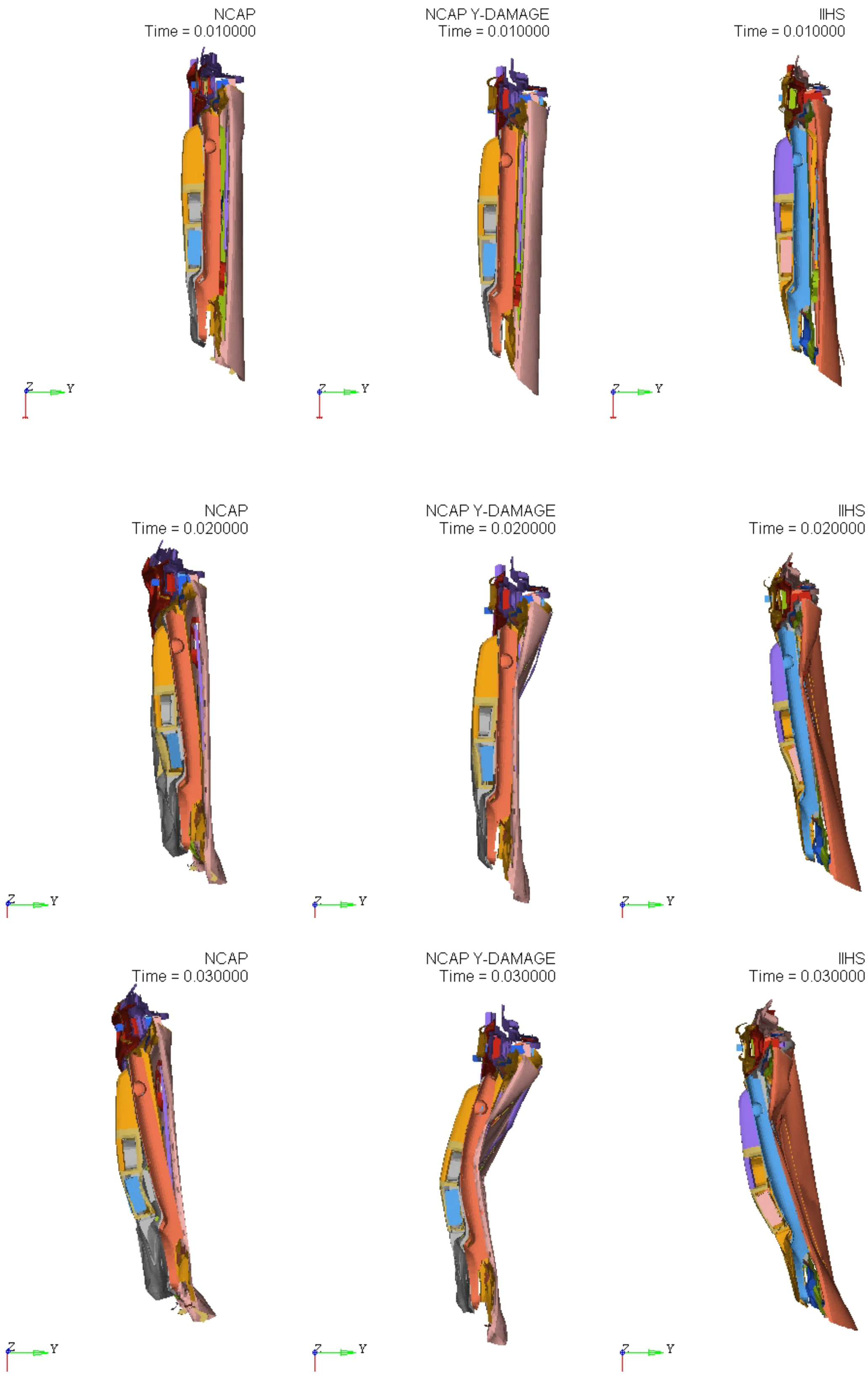
NCAP
Time = 0.010000
NCAP Y-DAMAGE
Time = 0.010000
IIHS
Time = 0.010000
NCAP
Time = 0.020000
NCAP Y-DAMAGE
Time = 0.020000
IIHS
Time = 0.020000
NCAP
Time = 0.030000
NCAP Y-DAMAGE
Time = 0.030000
IIHS
Time = 0.030000

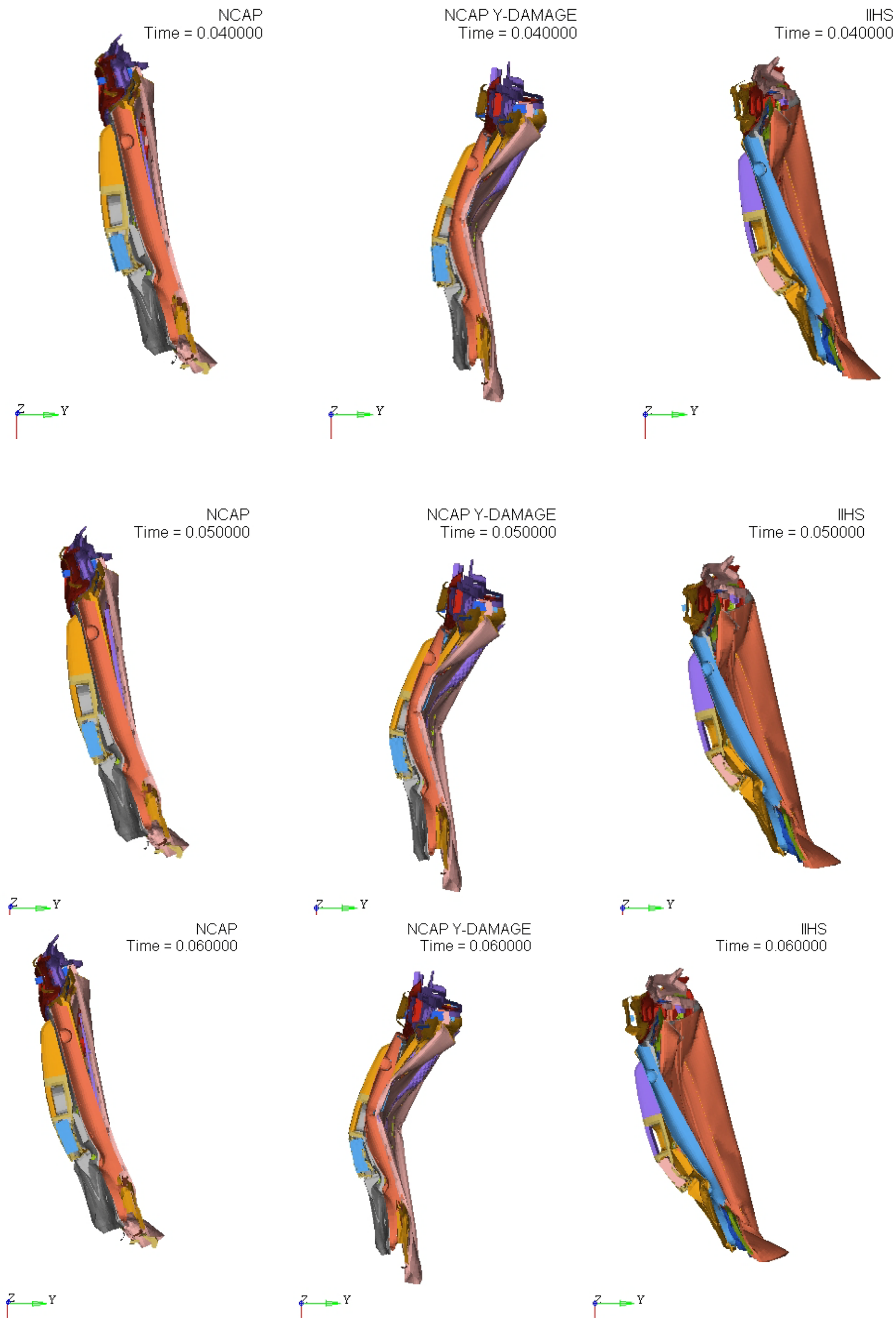

Figure 56 – Door top view of FE simulations of NCAP Side-impact (left), Y-Damage (middle) and IIHS (right)

We can see that as a result of the crash, the vehicles sometimes have a rotation. The rotation depends on the vehicle's center of gravity and the position of the impact as seen in Figure 55. The NCAP test is in the middle of the vehicle but the velocity has a longitudinal and lateral component. The Y-Damage case is the one with a higher rotation because the impact is in front of the vehicle and the striking vehicle also has a longitudinal and lateral velocity component. The IIHS test shows little rotation but a lot of intrusion in the door as seen in Figure 56.

Figures 58 and 59 show the peak crush and intrusion velocity values of the vehicle-to-vehicle tests measured at several tracking points on the front door of the Taurus finite element model as shown in Figure 57. These points were selected at three different heights (shoulder, ribs and pelvis) and two levels along the front door (back and middle). The graphics show how the highest crush point occurs in the IIHS test at the Rib/BackFDoor location (Node 3541526) reaching a 375 mm of crush. The intrusion velocity in that same location reaches 9,800mm/s.

Between the NCAP and NCAP Y-Damage tests, the crush levels appear to be higher in the NCAP test reaching 310 mm of crush while the maximum crush in the NCAP Y-Damage only reaches 212 mm. However, looking at the intrusion velocities, we can see that the highest intrusion velocity, occurs in the NCAP Y-Damage test at the Shoulder/MidFDoor location (Node 3540563) reaching a velocity of 10,000 mm/s. This velocity exceeds the intrusion velocities of the IIHS test in any of the six control locations.

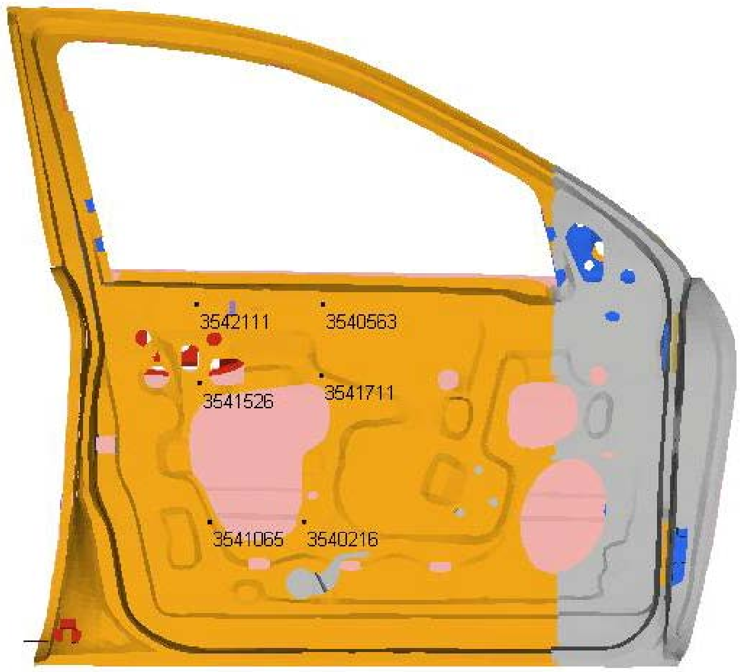

Figure 57- Front Door Tracking Points

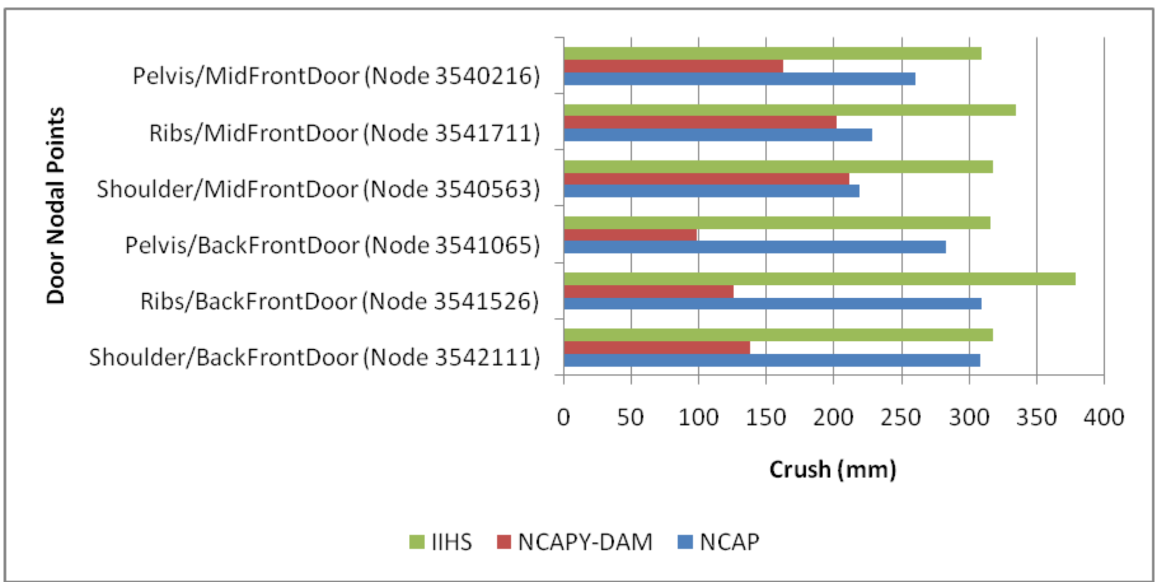

Figure 58 – Peak Values of Door Crush at selected nodal points.

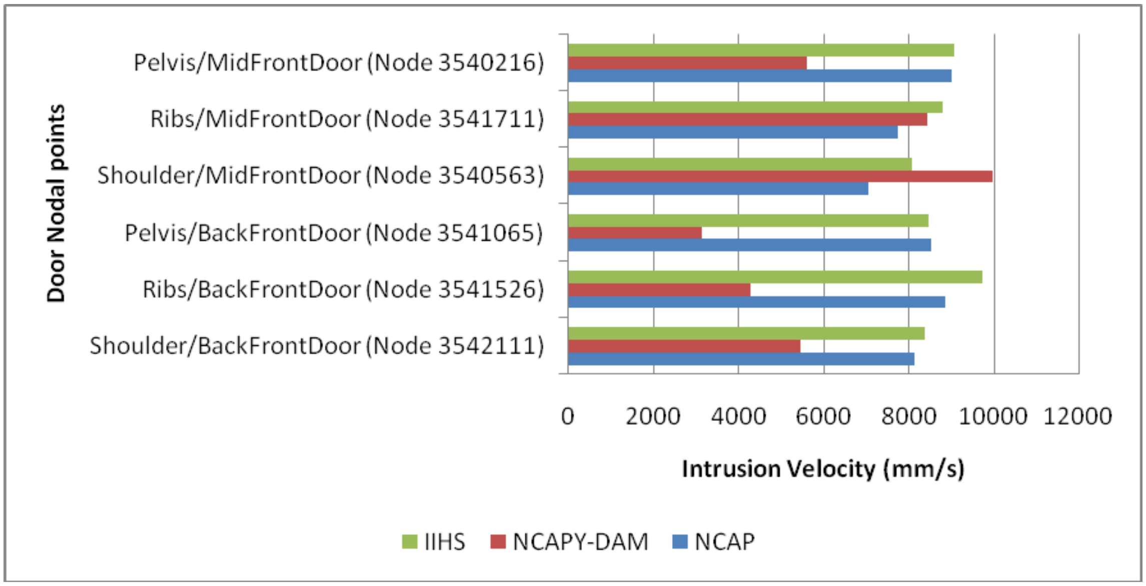

Figure 59 – Peak Values of Door Intrusion Velocity at selected nodal points.

The EUROSID and SID dummies have different responses from the human ones. The Human Facet Model, which was used in this study, has characteristics more representative to humans. Earlier research by Steps (Steps, 2004) found that the Human Facet Model was able to distinguish the crash modes most likely to produce aortic injuries where as the side-impact dummy models could not. One of the main goals in studying side-impact crashes is human occupant protection, not dummy protection. Understanding the crash environment and interior contacts that cause injury to humans is essential to identify the causes of such serious and/or fatal injuries in lateral impacts.

Anthropomorphic test devices such as EUROSID and SID dummies are generally used to study side-impact interactions. However, these dummies do not have a sufficiently accurate human-like response to permit their use in the study of the causes of aortic injury. The Human Facet Model was used in this analysis to provide more human like response. The Human Facet Model also allows the measurement of VC and Chest Deflection. In addition, this model has a representation of a flexible spine, having a rigid body for each vertebra in the spine.

In Figure 60 we see a graphic of the vehicle and occupant response to side-impact. At impact, the exterior door and striking vehicle have the same velocity. Initially the occupant is motionless until the door comes in contact with the occupant (See graph 3 and 4 at time t_0). The struck vehicle is also accelerated as a result of the impact and reaches the striking vehicle velocity (See graphs 1 and 5). The door intrusion ends when the door velocity and the struck vehicle reach a common velocity (See graphs 1 and 5 at t_2). The occupant separates from the door when its velocity becomes greater than the door intrusion velocity (t_1). During the time period between t_0 and t_1 , the occupant is accelerated by door contact. The occupant acceleration may have both x and y components, depending on the direction of the door intrusion. Some vehicle designs may employ "pelvic lead" to increase the percentage of crash energy transmitted to the pelvic region (Hobbs, 1995). Pelvic lead is accomplished by establishing load paths through the door that cause the pelvic to be loaded before the chest. One result may be increased rotation about the occupant's center of gravity resulting in increased Spinal Z Acceleration. Some of the cadaver tests conducted by Cavanaugh incorporated load paths to induce pelvic lead. A purpose of the Cavanaugh research was to evaluate the consequence of pelvic lead on occupant response.

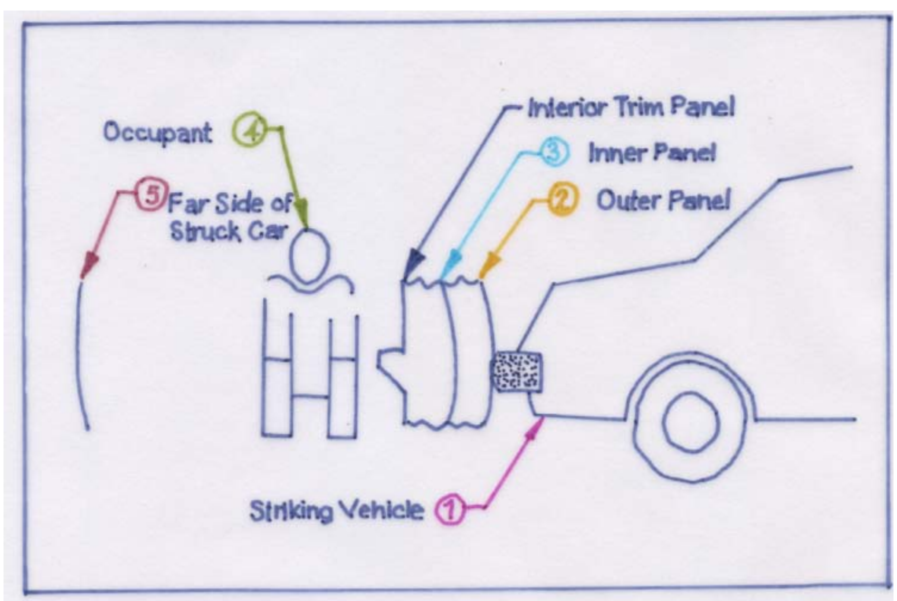

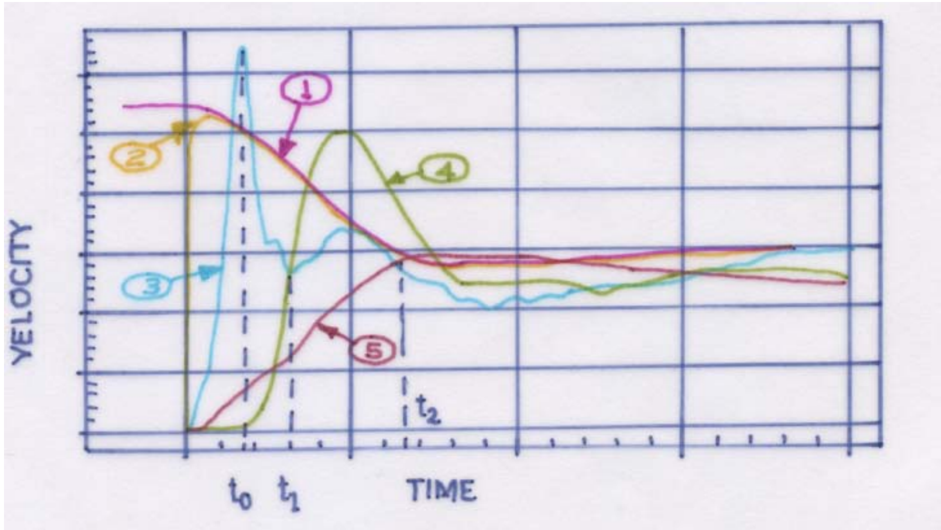

Figure 60 - Side-impact Velocity Vs. Time Diagram and Plot (Chan, et al., 1998)

As previously mentioned, side-impact protection consists of vehicle side stiffness, interior geometry, airbags and padding. The injury analysis in this thesis was done not only by varying the crash set up but by varying some of these countermeasures. The NCAP, NCAP Y-Damage and IIHS tests were modeled with and without a side airbag.

The injury analysis shows the lateral impact responses for the Chest, Abdomen and Pelvis. Accelerations readings were taken on the Lower Spine (T12Z, T12Y), Upper Sternum (SternumUpX, SternumUPY), Pelvis (PelvisY) and upper and lower Ribs, as well as the [VC]Max and CMax readings of the Human Facet Model.

The selection of these parameters was based on the Cavanaugh's sled testing study previously mentioned. One important note on the Human Model Simulations is that it cannot reproduce rib fracture. The captions of these simulations are shown in Appendix C. All cadaver cases in Cavanaugh's study sustained rib fracture, which changes the stiffness of the chest. This makes prediction of cadaver injuries by the Human Facet Model more challenging.

In Table 20, the peak values of the selected injury parameters for the analysis are shown. The table displays the peak values of injury measures for all the tests proposed for this study. The injury measures were: Viscous Criterion [VC]Max, Chest Compression (CMax), Cavanaugh's logit values and probabilities, Spinal (T12Y and T12Z), Upper Sternum (SternumX and SternumY), Pelvis (PelvisY) and Ribs (RibL8 and RibL4) accelerations, TTI, relative elongation and percentage elongation.

We first compare the NCAP, NCAPY-Damage and IIHS tests. The IIHS, being the most severe test presents the highest [VC]Max and CMax with values reaching 2.973 and 72%. Between the NCAP and NCAPY-Damage which are performed at the same speed but in a different impact point, the NCAPY-Damage test show higher values of [VC]Max than the NCAP test.

Based on the Cavanaugh's combined injury parameters for predicting aortic injury we see that the IIHS test presents the highest probabilities for AIS 4+ aortic injury, with 98% and 100% chance of injury for the T12Z and [VC]Max and T12Z and CMax combination respectively. The second highest is the NCAPY-Damage with 75% (T12Z and [VC]Max) and 48% (T12Z and CMax) probability of AIS 4+ aortic injury compared to the NCAP test having an 11% (T12Z and [VC]Max) and 35% (T12Z and CMax) probability.

Parameter	Units	NCAP	NCAP SAB	NCAP YDam	NCAP YDam SAB	IIHS	IIHS SAB
[VC]Max LR8 (m/s)	**m/s**	1.358	1.922	0.673	1.165	2.973	1.933
[VC]Max LR4 (m/s)	**m/s**	1.630	2.550	2.270	1.200	1.095	1.923
CMax LR8		39%	54%	27%	44%	72%	57%
CMax LR4		54%	58%	55%	47%	42%	51%
K1*T12Z+K2*[VC]MaxRL8+K3		-3.694	-0.848	-6.638	-4.618	4.516	-1.389
K1*T12Z+K2*[VC]MaxRL4+K3		-2.425	2.082	0.808	-4.455	-4.237	-1.435
K1*T12Z+K2*CMaxRL8+K3		-6.289	-0.658	-10.558	-4.675	6.312	0.139
K1*T12Z+K2*CMaxRL4+K3		-0.852	0.949	-0.183	-3.282	-4.503	-2.108
P (T12Z&[VC]MaxRL8)		4%	74%	0%	3%	98%	83%
P(T12Z&[VC]MaxRL4)		11%	15%	75%	2%	3%	84%
P(T12Z&CMaxRL8)		0%	41%	0%	2%	100%	52%
P(T12Z&CMaxRL4)		35%	75%	48%	4%	1%	12%
T12 Z	(g)	15	22	23	14	38	2
Sternum UP X	(g)	-19	-6	-7	-12	-13	-14
Pelvis Y	(g)	-134	-83	-160	-181	-130	-58
T12Y	(g)	-82	-66	-86	-85	-64	-55
Sternum Y	(g)	-51	-50	-48	-35	-37	-39
RIB8 Y L	(g)	-95	-141	-100	-95	-182	-114
RIB4L	(g)	-233	-141	-115	-120	-225	-91
TTI = 0.5 (Rib8y+T12y)	(g)	-89	-103	-93	-90	-123	-84
TTI = 0.5 (Rib4y+T12y)	(g)	-158	-103	-100	-103	-144	-73
TTI (average)= 0.5 (((Rib4y+Rib8y)/2)+T12y)	(g)	-123	-103	-97	-96	-134	-79
Relative Elongation		0.036	-0.050	0.110	0.108	0.132	0.064
Percentage Elongation (Failure @0.175)		21%	-29%	63%	62%	76%	37%

Table 22 – Injury Parameters for NCAP, NCAP Y-Dam and IIHS Test with and without SAB

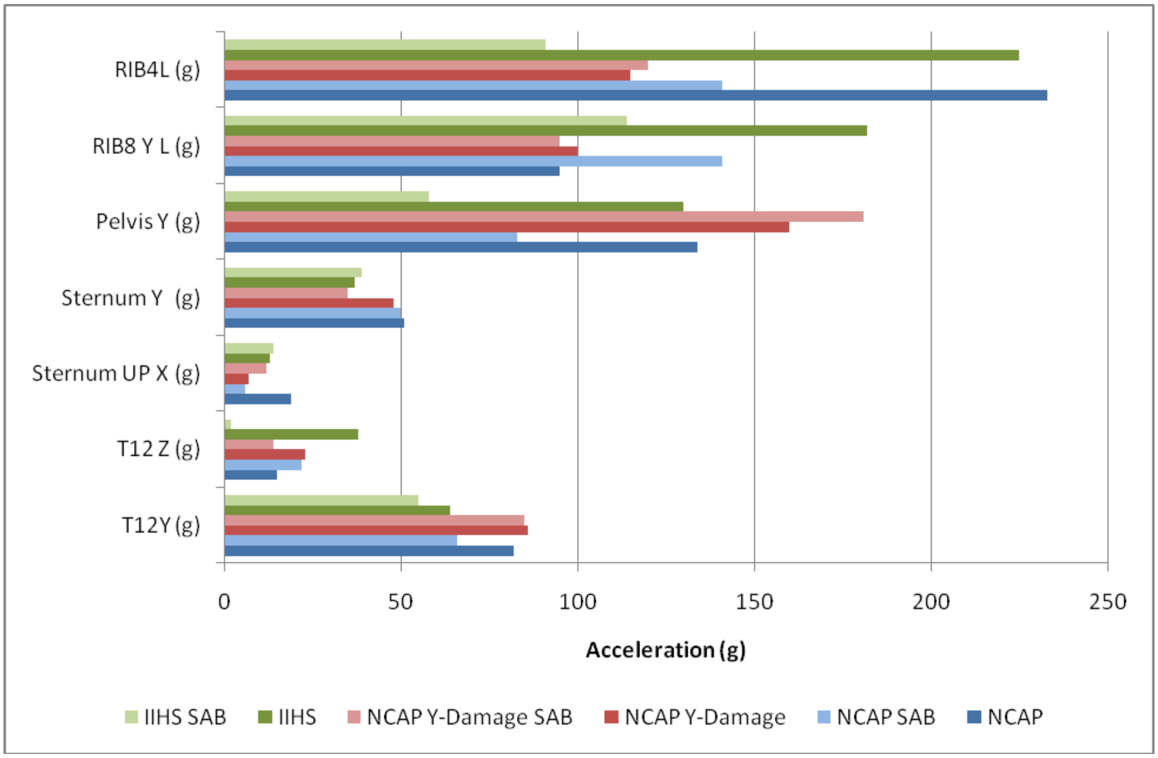

Figure 61 – Peak Acceleration in vehicle-to-vehicle tests with and without side airbag.

The NCAP test with airbag, presents higher values of [VC]Max and CMax than the test without the airbag. In the other two tests there is an improvement in the Viscous Criterion and Chest Compression values when using a side airbag. The graphics for CMax can be found in Figure 62 and 63. Cavanaugh's probabilities improve in the NCAPY-Damage and IIHS tests with a side airbag but are worse for the NCAP tests. This could be attributed to the extended loading of the chest due to the airbag.

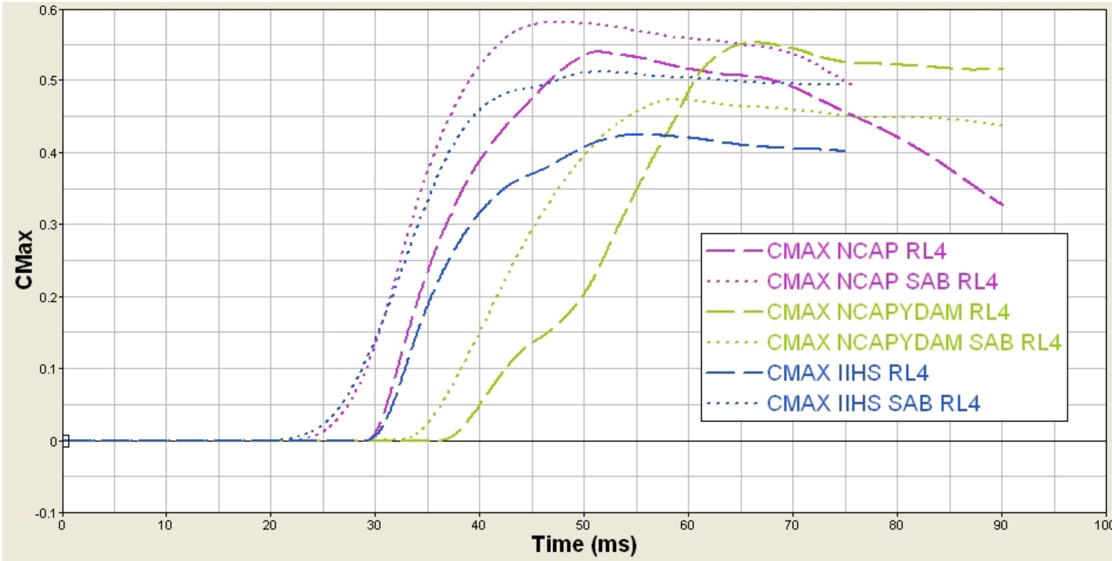

Figure 62 – NCAP, NCAPYDam and IIHS with and without SAB CMax RL4

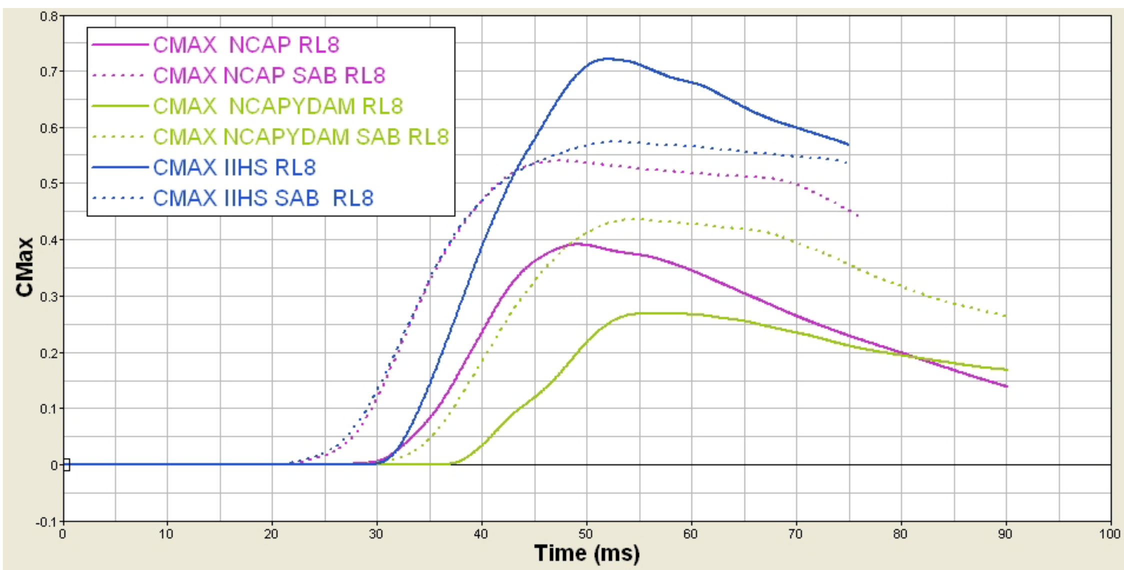

Figure 63 – NCAP, NCAPYDAM and IIHS with and without SAB CMax RL8

A comparison of the vehicle side-impact tests displayed in Figure 64 shows that the IIHS configuration has the highest relative elongation reaching a value of 0.132, followed by the NCAP Y-Damage tests with a 0.109 relative elongation. The IIHS tests 0.132 relative elongation value is the one closest to the failure limit of 0.175. These values are significantly higher than the one from the NCAP test where the relative elongation is only 0.036 while the NCAPY-Damage is closer to the IIHS test reaching a 0.110 relative elongation.

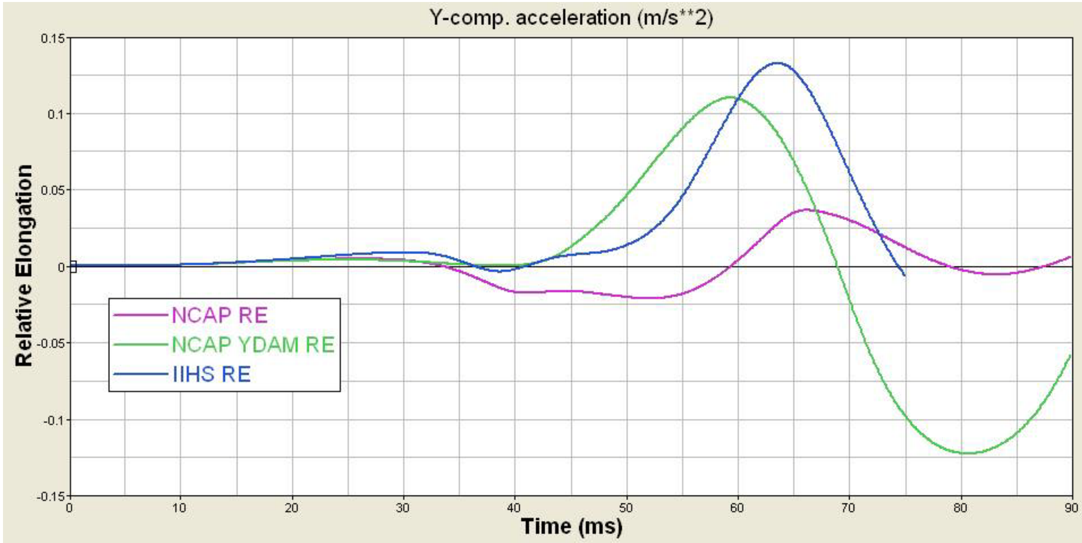

Figure 64 – Spring Relative Elongation for NCAP, NCAPYDAM and IIHS tests.

The IIHS test is a very severe impact. Since this is the most severe of the selected tests, it is consistent with the real-world results where we found that severity or Delta-V is one of the contributing factors for aortic injury. On the other hand, we have the NCAP test and the NCAP Y-Damage test, which are performed at the same speed but different location. A comparison of these tests shows a significant difference in the spring relative elongation. In the real-world analysis the location of the damage was a contributing factor for aortic injury and the results of these tests were also consistent with this statement. The NCAP Y-Damage test has a higher inertial effect than the NCAP test. This is also true for Cavanaugh's injury criteria where the NCAPY-Damage test has a 75% and 48% chance of injury while the NCAP test has an 11% and 35% chance.

The higher the relative elongation is the higher the chance of receiving an aortic injury. As mentioned before, this addition only focuses on the inertial effect of the heart without taking into consideration the Chest Compression. Additional studies will be needed to combine the Chest Compression with the inertial effect of the heart to better understand the injury mechanism. This simple spring-mass model simply helps us get an insight on how the aorta can be stretched longitudinally.

The vehicle-to-vehicle tests were modeled with and without side airbags and we now explore the impact of these devices on the inertial effect of the heart in a side-impact event. In the Figure 65 we see a variation in relative elongation of the IIHS test with and without the airbag. The relative elongations of these two tests are 0.064 and 0.132 respectively. In this case, similar to the NCAP test where the relative elongations are -0.050 when done with airbag and 0.036 without airbag, the tests with the airbag present a lower relative elongation than the ones without it.

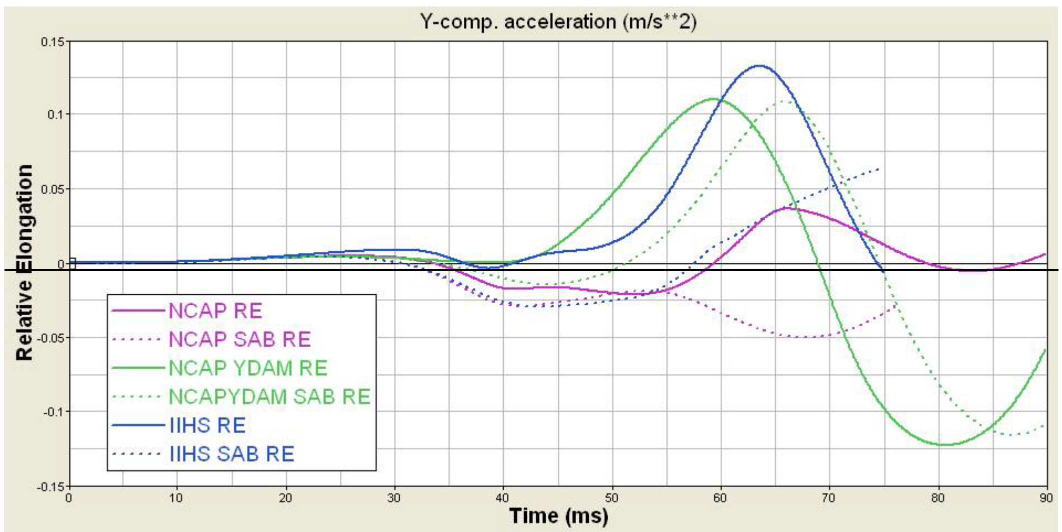

Figure 65 -Comparison of relative elongation for tests with and without side airbag

On a different note, the airbag in the NCAPY-Damage test has little effect on the inertial component. The NCAPY-Damage test with airbag has a 0.110 relative elongation, while the same test without the airbag reaches only a 0.108 relative elongation value.

We can see that the relative elongation is following Cavanaugh's injury probabilities. The IIHS test has the highest injury probabilities, then the NCAPY-damage test and lastly the NCAP test. The relative elongation of the spring-mass model shows the same trend. The IIHS has the highest relative elongation and the NCAP test has the lowest. The highest rib accelerations are present on the NCAP test but this test has the lowest injury probability. Now, examining the T12Z component, we see that the NCAP test has the lowest value of the three tests.

5.3 Limitations

One of the main limitations of the Human Facet Model is that the age of the human cannot be taken into consideration. There is evidence that shows older persons with hardened arteries are more likely to have an aortic rupture than younger healthier persons. Also, in Cavanaugh's sled testing all the cadavers sustained rib fracture. The rib fracture cannot be reproduced in the Human Facet Model. These and other parameters might affect the biomechanical response of the model making it less like the cadaver.

The spring mass model added to the Human Facet Model is limited by the condition that the heart-mass has no interaction with the thoracic cavity. Chest Compression, compression velocity and vascular pressure are known to influence aortic injury, but are not considered by the model. For this reason, the elongations shown in the results are not an accurate representation of the actual elongation, but for the purpose of this study it does show the existence of the inertial component. The aorta is represented by a spring with the mechanical properties of the aorta according to Shah.

6 Conclusions

The purpose of this research study is to explore the possible injury mechanisms that can contribute to aortic injuries in side-impact crashes. Different resources and previous studies were used to improve the understanding of the causes of aortic injury. Real-world Data (NASS) was analyzed with statistical tools to identify possible variables influencing aortic injury. Multiple previous studies were used to identify environments conducive to aortic injuries. These environments were reproduced through computer modeling using LS-DYNA and MADYMO. Finally, the extensive results were analyzed.

As discussed previously in this work, aortic injuries do not have an established injury criterion that has been accepted by the safety community. The task of studying the injury mechanisms of aortic tears is difficult because of the complexity of the thoracic cavity organs, as well as the forces and accelerations involved in a side-impact. It seems that not only one but several injury mechanisms are relevant in the study of aortic ruptures.

The cadaver tests done by Cavanaugh, show that a pelvis offset in the sled tests increases the incidence of aortic injuries. His studies also show that the combination of T12Z and VC and T12Z and Chest Compression are good predictors of aortic injury (Cavanaugh, et al., 2005). Studies done by Shah tested the mechanical properties of the aortic tissue establishing its limits to failure (Shah, 2007).

6.1 Contributions

Several environments inductive to aortic injury were modeled. These environments were selected and designed as the result of a variety of research studies that used cadaver testing, real-world data analysis and vehicle tests. The results of these computer simulations were then analyzed and compared with some of the previously proposed aortic injury predictors. The models recreated two different test scenarios: (1) vehicle-to-vehicle and (2) sled tests of cadavers.

In both cases the Cavanaugh injury criteria that used the combination of T12Z and VCMax was good predictor of aortic injury (Cavanaugh, et al., 2005). The IIHS test has the highest probability of producing aortic injury followed by the NCAP Y-Damage. When comparing the NCAP Y-Damage test with the NCAP test we see that the probability is higher in the NCAP Y-Damage test. This result is also consistent with Step's findings that the Y pattern damage had a higher incidence of aortic injury based on real-world data (Steps, 2004).

In the sled tests we also notice that the probability of injury using Cavanaugh's injury criteria based on the combination of T12Z and VC is higher in the pelvic offset test. This also is consistent with the cadaver tests where aortic injuries were mostly reproduced with the pelvic offset condition.

The analysis of the intrusion velocities shows that the highest intrusion velocity, occurs in the NCAP Y-Damage test at the Shoulder/MidFDoor location (Node 3540563) reaching a velocity of 10,000 mm/s. This velocity exceeds the intrusion velocities of the IIHS test in any of the six control locations. This suggests that the loading in some areas of the door could be more severe in the Y-Damage configuration than in any of the other two configurations explored in this study. This result might give us some insight on why the Y-Damage pattern shows a higher aortic injury rate.

A spring-mass model was added to the human model to further explore aortic injuries in side-impact, exploring the inertial effect of the heart. The NCAPY-Damage and pelvic offset sled tests have a higher inertial effect than other scenarios. This inertial effect increases the chances of stretching the aorta past its failure limits, resulting in an aortic injury. The use of a side airbag seems to lower the inertial effect in the vehicle-to-vehicle tests. This result is not observed in the NCAP test where the probabilities of injury increased when using an airbag. The increase in injury risk with an air bag is possibly due to the higher percentage of the crash energy being transmitted to the chest as compared to the pelvic region. This loading would result in chest lead rather than pelvic lead.

6.2 Future Studies

The Y-Damage pattern is not currently being addressed in current U.S. regulations even though Y-Damage pattern is the most common in real-world cases and is the largest source of serious injuries. The modeling suggests that the Y-Damage test produces the highest intrusion velocity and is more likely to produce aortic injuries than the current NCAP test. This finding needs to be further confirmed by crash tests. If confirmed, regulatory agencies should consider changing the test configuration.

Further cadaver studies should include the interaction of the Chest Compression and the inertial effect of the heart in a near-side-impact event. The ability to study the interaction between the Chest Compression and the inertial effect can be crucial in the development of an appropriate dummy and an associated injury criterion for aortic ruptures. Research has shown that Chest Compression and compression velocity are factors that predict aortic injury. This study opens the likelihood of inertia on the Z (upward) direction is a possible injury mechanism that should be studied in conjunction with Chest Compression.

7 Bibliography

Alonso, B. (2004). MADYMO Human Facet Model Validation for Far-side. William Lehman Injury Research Center.

Bertrand, S., Cuny, S., Petit, P., Trosseille, X., Page, I., Guillemot, H. and Drazetic, P. (2008). Traumatic Rupture of Thoracic Aorta in Real World Motor Vehicle Crashes. *Traffic Injury Prevention* . Taylor & Francis Group.

Burkhart, H., Gomez, G., Jacobson, L., Pless, J., & Broadie, T. (2001). Fatal blunt aortic injuries: a review of 242 autopsy cases. *J Trauma* .

Buzztrader.com, & CyberWebInc. (2007). *Current U.S. Side Impact Standard*. Retrieved 2008, from http://buzztrader.com/articles/crashtesting/euus-6.html

Cavanaugh, J. M., Koh, S.-W., Kaledhonkar, S. L., & Hardy, W. N. (2005). An Analysis of Traumatic Rupture of the Aorta in Side Impact Sled Tests. *SAE International* . Wayne State University Bioengineering Center.

Cavanaugh, J. M., Waliko, T. J., Malhotra, A., Zhu, Y., & King, A. I. Biomechanical Response and Injury Tolerance of the Thorax in Twelve Sled Side Impacts. Bioengineering Center Wayne State University.

Cavanaugh, J. M., Zhu, Y., & King, A. I. Injury and Response of the Thorax in Side Impact Cadaveric Tests. *933127* . Wayne State University Bioengineering Center.

Chan, H., Hackney, J. R., Morgan, R. M., & Smith, H. E. (1998). An Analysis of NCAP Side Impact Crash Data. National Highway Traffic Safety Administration.

Chiesa, R., Ruettimann, M., de Moura, L., Lucci, C., Castellano, R., Civilini, E., (2003). Blunt trauma of the thoracic aort: mechanisms involved, diagnosis and management. *Jornal Vascular Brasileiro , 2 (3)* .

Digges, K., Gabler, H., Mohan, P., & Alonso, B. (2005). Characteristics of the injury environment in far side crashes. *Annual Proceedings/Association for the Advancement of Automotive Medicine* . The National Crash Analysis Center, George Washington University, USA.

Fildes, B., Sparke, L., Bostrom, L., Pintar, F., Yoganandan, N., & Morris, A. (2002). Suitability of Current Side Impact Test Dummies in Far side Impacts. *Proceedings of the 2002 IRCOBI Conference* .

Foreman, J., Staceya, S., Evans, J., & Kent, R. (2008). Posterioracceleration as a mechanism of blunt traumatic injury of the aorta. *Short communication, Journal of Biomechanics (41:1359-1364)* .

Gray, H. (2000). *Anatomy of the Human Body.* Retrieved 2008, from Bartleby.com: http://www.bartleby.com/107/illus505.html

Gray, H. (2000). *Anatomy of the Human Body.* Retrieved 2008, from Bartleby.com: http://www.bartleby.com/107/illus506.html

Halloquist, J. O. (2007). *LS-DYNA Theory Manual.* Retrieved 2008, from http://www.dynamax-inc.com/manuals/ls-dyna_theory_manual_2006.pdf

Hallquist, J. (2003). *LS_DYNA Keyword User's Manual.* Retrieved 2008, from http://www.dynamore.de/download/manual/ls-dyna_970_manual_k.pdf

Hardy, W. N., Shah, C. S., Kopacz, J. M., Yang, K. H., Van Ee, C. A., Morgan, R. and Digges, K. (2006). Study of potential mechanisms of traumatic rupture of the aorta using in situ experiments. *Stapp Car Crash Journal (50:247-265)* .

Hardy, W. N., Shah, C. S., Mason, M. J., Kopacz, J. M., Yang, K. H., King, A. I., Van Ee, C.A., Bishop, J., Banglamaier, R., Bey, M.J., Morgan, R. and Digges, K. (2008). Mechanisms of Traumatic Rupture of the Aorta and Associated Peri-isthmic Motion and Deformation. *Stapp Car Crash Journal , 52* . The Stapp Association.

Hobbs, C. A. (1995). Dispelling the Misconceptions about Side Impact Protection. *SAE Technical Paper Series* . Detroit.

Katyal, D., McLeilan, B. A., Brenneman, F. D., Boulanger, B. R., Sharkey, P. W., & Waddell, J. P. (1997). Lateral impactor motor vehicle collisions: significant cause of blunt traumatic rupture of the thoracic aorta. *42(5):769-772* . Journal of Trauma.

National Heart, Lung and Blodd Institute, USA. *Diseases and Conditions Index: Heart and Blood Vessels Diseases: Aneurysm.* Retrieved 2008, from www.nhlbi.nih.gov: http://www.nhlbi.nih.gov/health/dci/Diseases/arm/arm_types.html

Newman, R., & Rastogi, S. (1984). Rupture of the thoracic aorta and its relationship to road traffic accident characteristics. *Injury* .

NHTSA. (2005). *http://www.nhtsa.dot.gov/portal/site/nhtsa/template.MAXIMIZE/menuitem.f2217bee37fb302f6d7c121046108a0c/?javax.portlet.tpst=1e51531b2220b0f8ea14201046108a0c_ws_MX&javax.portlet.prp_1e51531b2220b0f8ea14201046108a0c_viewID=detail_view&itemID=d3a1275827063010*. Retrieved from www.nhtsa.gov.

NHTSA. (2006). Motor Vehicle Traffic Crashes as Leading Cause of Death in the United States, 2003. *Traffic Safety Facts - Research Note* .

NHTSA. (1997-2007). National Automotive Sampling System.

Shah, C. S. (2007). Investigation of traumatic rupture of the aorta (TRA) by obtaining aorta material and failure properties and simulating real world aortic injury crashes using the whole body finite element (FE) human model. Wayne State University.

Shah, C. S., Yang, K. H., Hardy, W. N., Wang, H. K., & King, A. I. (2001). Development of a computer model to predict aortic rupture due to impact loading. *45th Stapp Car Crash Conference* .

Steps, J. A. (2004). *Near Side Vehicle to Vehicle Crashes.* The George Washington University.

TNO Automotive-AM. (2005). *MADYMO-Applications Manual Version 6.3.*

TNO Automotive-HM. (2005). *MADYMO Human Models Manual. Version 6.3.*

TNO Automotive-MM. (2005). *MADYMO Model Manual. Version 6.3.*

TNO Automotive-TM. (2005). *MADYMO Theory Manual. Version 6.3.*

TNO Automotive-PSM. MADYMO Prescribed Structural Motion (PSM) Advanced Training Course.

TNO Automotive-RM. (2005). *MADYMO Reference Manual. Version 6.3.*

Trauma.org. (1987). *Imaging diagnosis of traumatic aortic rupture. A review and experience at a major trauma center. (22:187-96)*. Retrieved 2008, from Trauma.org: http://www.trauma.org/archive/thoracic/CHESTaorta.html

Trauma.org. (1989). *Role of CT in diagnosis of major arterial injury after blunt thoracic trauma (106:596-602)*. Retrieved 2008, from www.trauma.org: http://www.trauma.org/archive/thoracic/CHESTaorta.html

University of Nebraska. *ROC Curves*. Retrieved 2008, from http://gim.unmc.edu/dxtests/ROC3.htm

Viano, D. C. (1989). Biomechanical Responses and Injuries in Blunt Lateral Impact. Biomedical Science Dept. General Motors Research Labs.

Viano, D. C. (1983). Biomechanics of non penetrating Aortic Trauma: A Review. *27:109-114* . Proceedings of 27th Stapp Car Crash Conference.

Viano, D. C., & Lau, I. V. (1986). The Viscous Criterion - Bases and Applications of an Injury Severity Index for Soft Tissues. *SAE-861882* . Biomedical Science Dept. General Motors Res. Labs.

Whitehead, J. *An Introduction to Logistic Regression.* Retrieved 2008, from Department of economics Appalachian State University: http://www.appstate.edu/~whiteheadjc/service/logit/logit.ppt

8 Appendix A - Glossary

Delta V – Change in velocity.

Lateral Delta V – Change in velocity in the lateral direction.

Logistic Regression – A technique used in statistical analysis that helps find the best fitting relationship between a dependent variable and independent variable.

P-Value – A probability that an event happened by chance.

Odds ratio – Measure of relative risk

PSM – Prescribed Structural Motion

AIS – Abbreviated Injury Scale

NCAP – New Car Assessment Program

FMVSS – Federal Motor Vehicle Safety Standard

NHTSA – National Highway Traffic Safety Administration

G – Acceleration due to gravity

MAIS – Maximum Abbreviated Injury Scale Value

MDB – Moving Deformable Barrier

NASS/CDS - The National Automotive Sampling System - Crashworthiness Data System

NCAC – National Crash Analysis Center (George Washington University)

DOF – Direction of Force

VC – Viscous Criterion

TTI – Thorax Trauma Index

Triage - A process for sorting injured people into groups based on their need for or likely benefit from immediate medical treatment.

9 Appendix B – Side Impact Captions

Loaucase 1 : Time = 0.000000
Frame 1

Loadcase 1 : Time = 0.000000
Frame 1

Loadcase 1 : Time = 0.000000
Frame 1

Loadcase 1 : Time = 0.010000
Frame 3

Loadcase 1 : Time = 0.010000
Frame 3

Loadcase 1 : Time = 0.010000
Frame 3

Loadcase 1 : Time = 0.020000
Frame 5

Loadcase 1 : Time = 0.020000
Frame 5

Loadcase 1 : Time = 0.020000
Frame 5

Loadcase 1 : Time = 0.030000
Frame 7

Loadcase 1 : Time = 0.030000
Frame 7

Loadcase 1 : Time = 0.030000
Frame 7

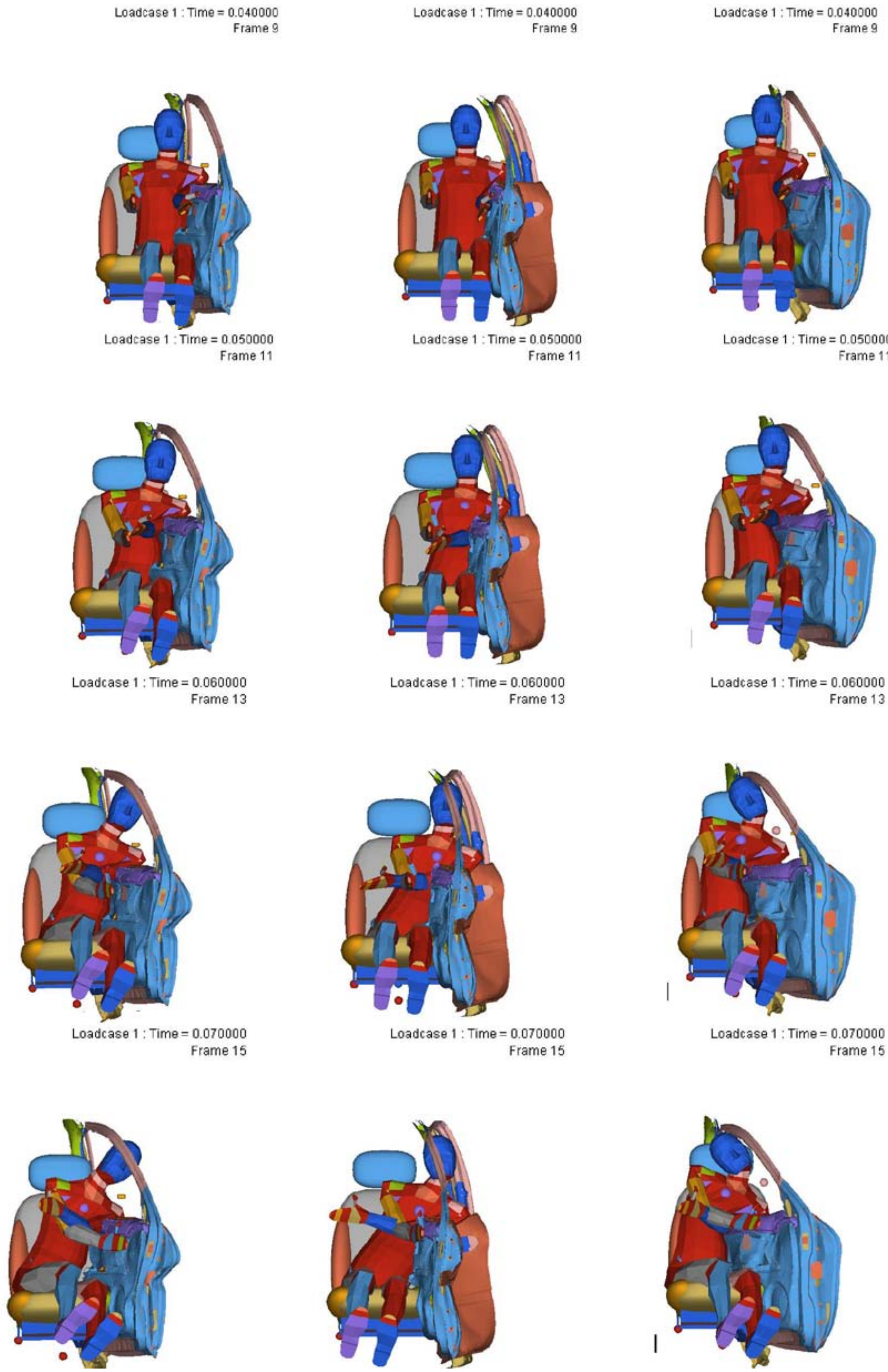

Figure 66. Front View of NCAP(Left) NCAP Y-Damage (Middle) and IIHS(Right)

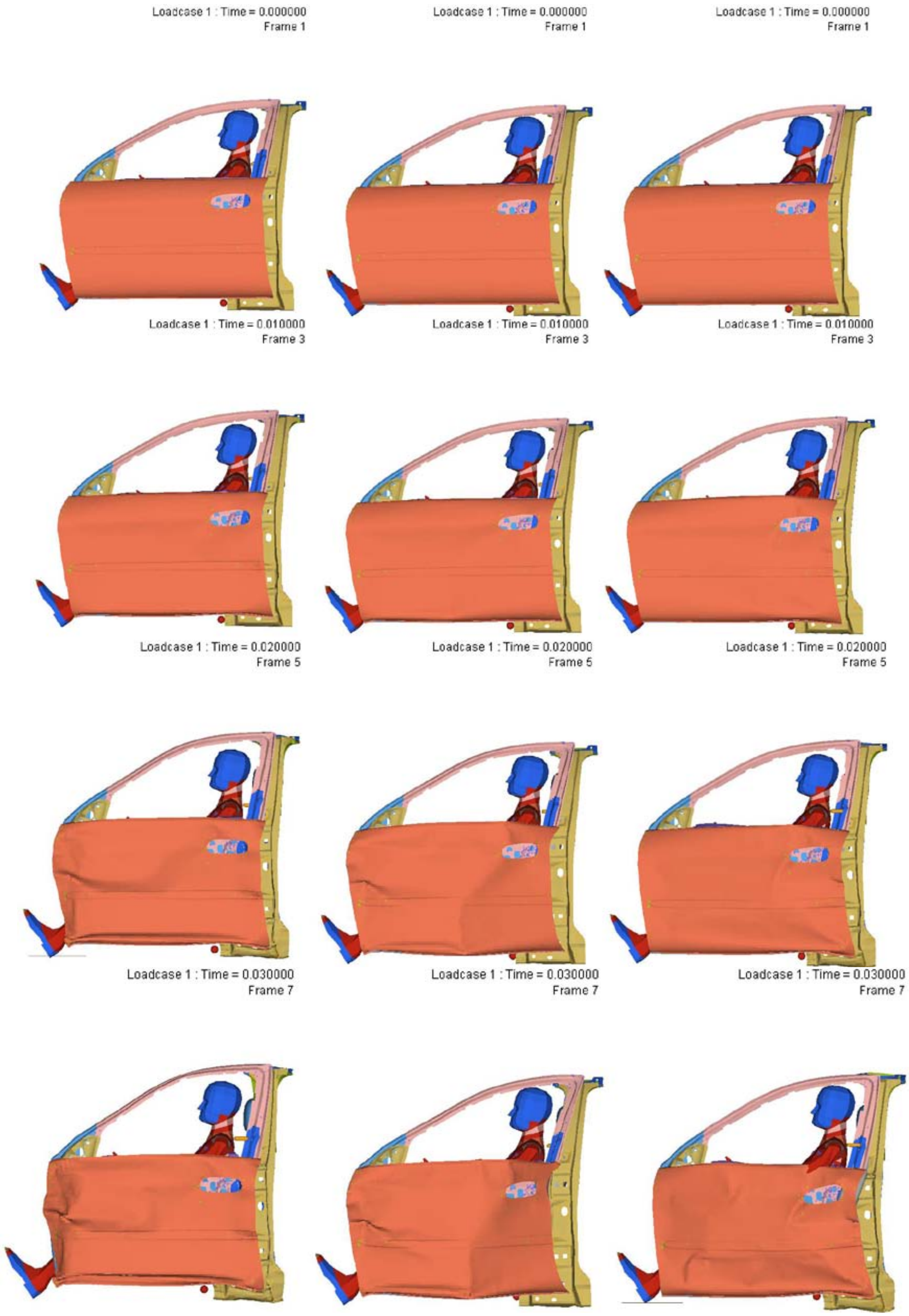
Loadcase 1 : Time = 0.000000
Frame 1
Loadcase 1 : Time = 0.000000
Frame 1
Loadcase 1 : Time = 0.000000
Frame 1
Loadcase 1 : Time = 0.010000
Frame 3
Loadcase 1 : Time = 0.010000
Frame 3
Loadcase 1 : Time = 0.010000
Frame 3
Loadcase 1 : Time = 0.020000
Frame 5
Loadcase 1 : Time = 0.020000
Frame 5
Loadcase 1 : Time = 0.020000
Frame 5
Loadcase 1 : Time = 0.030000
Frame 7
Loadcase 1 : Time = 0.030000
Frame 7
Loadcase 1 : Time = 0.030000
Frame 7

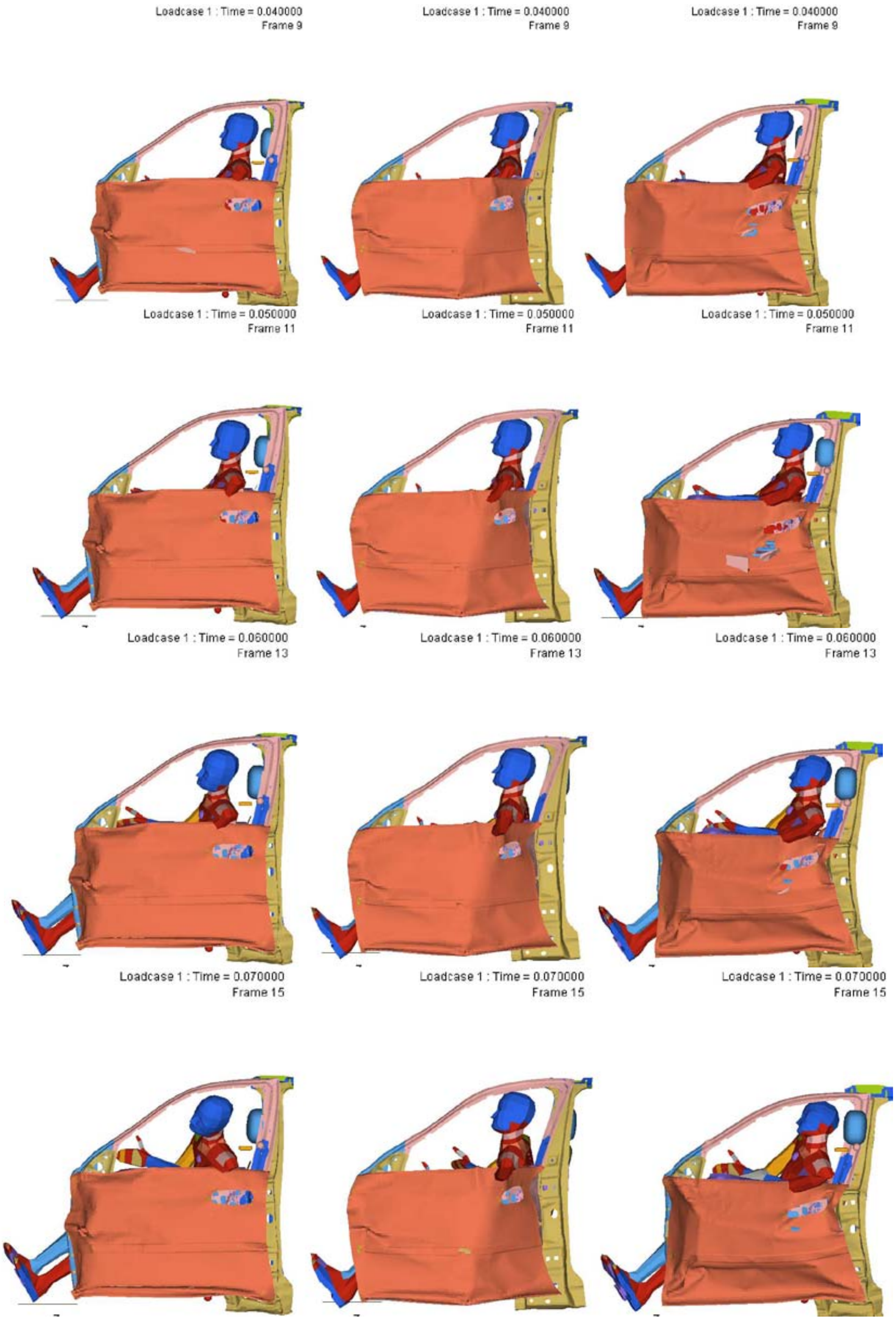

Figure 67. Side View of NCAP(Left) NCAP Y-Damage (Middle) and IIHS(Right)

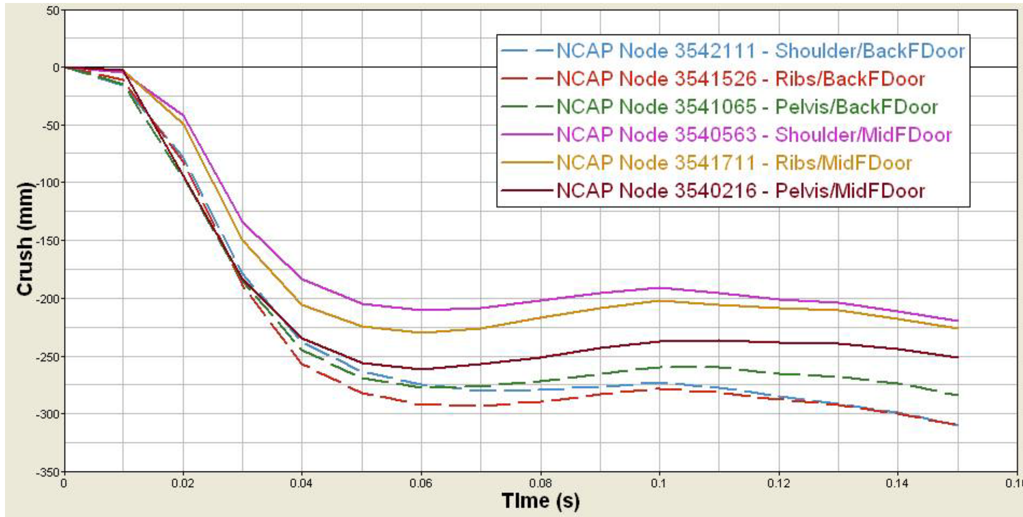

Figure 68 - Door Crush vs. Time plot of selected nodes - NCAP test

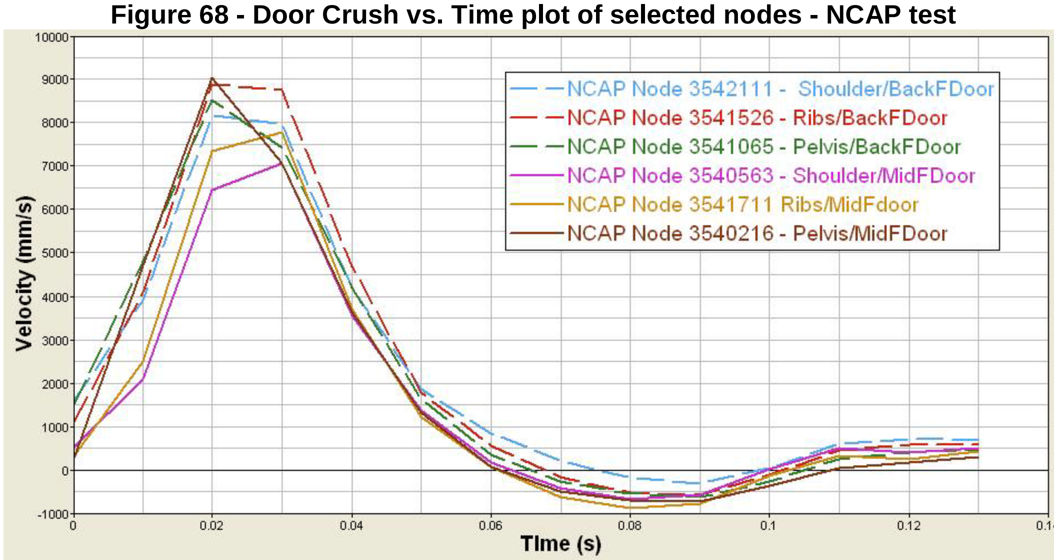

Figure 69 - Intrusion Velocity vs. Time plot of selected nodes – NCAP test

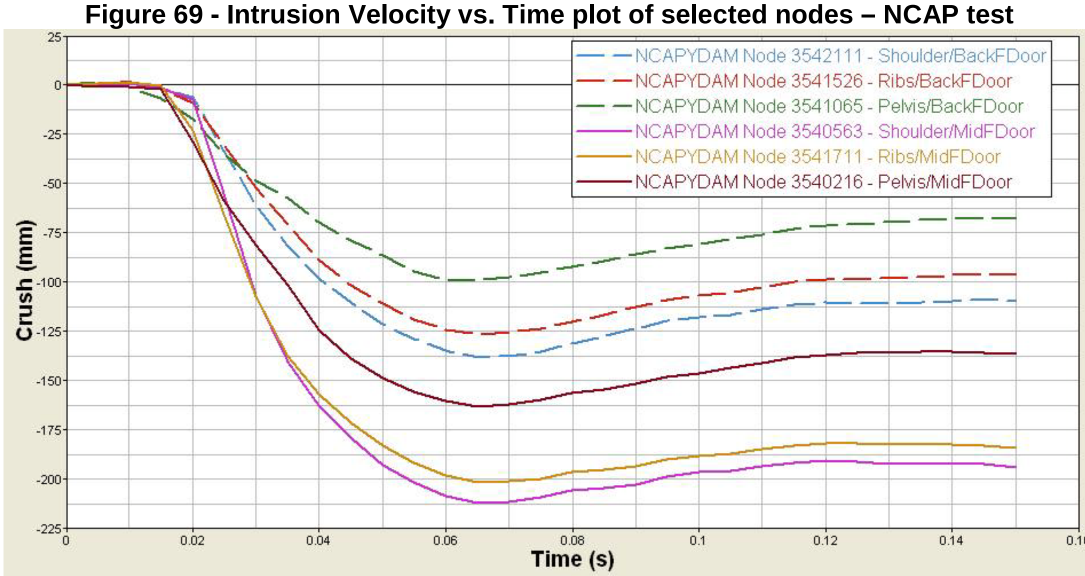

Figure 70 - Door Crush vs. Time plot of selected nodes - NCAP Y Damage test

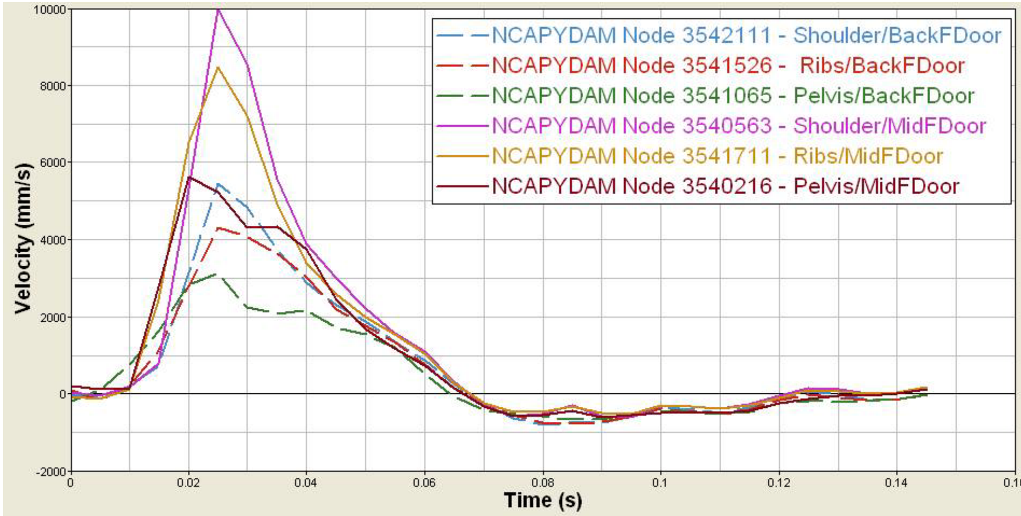

Figure 71- Intrusion Velocity vs. Time plot of selected nodes – NCAP Y Damge test

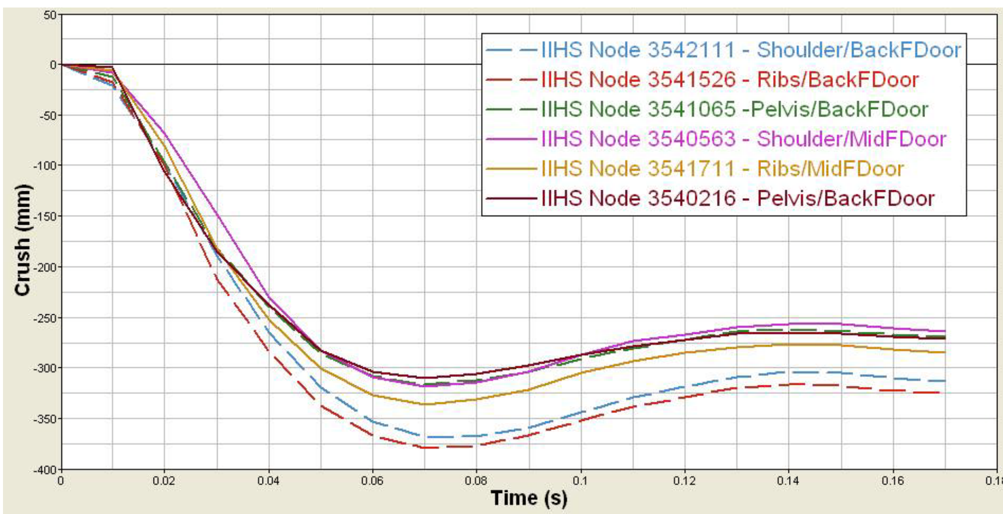

Figure 72 - Door Crush vs. Time plot of selected nodes - IIHS test

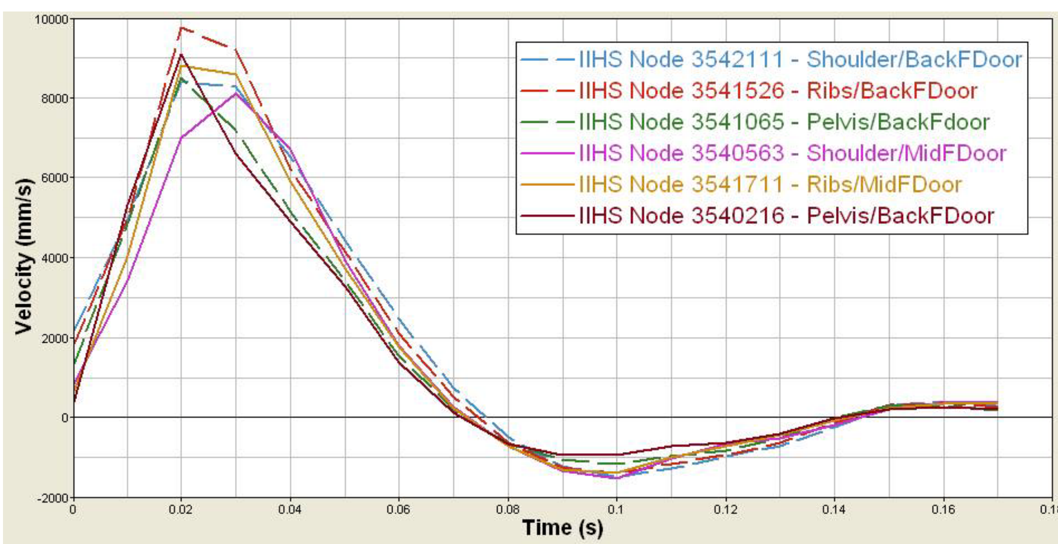

Figure 73 - Intrusion Velocity vs. Time plot of selected nodes – IIHS test

10 Appendix C – Sled Test Captions

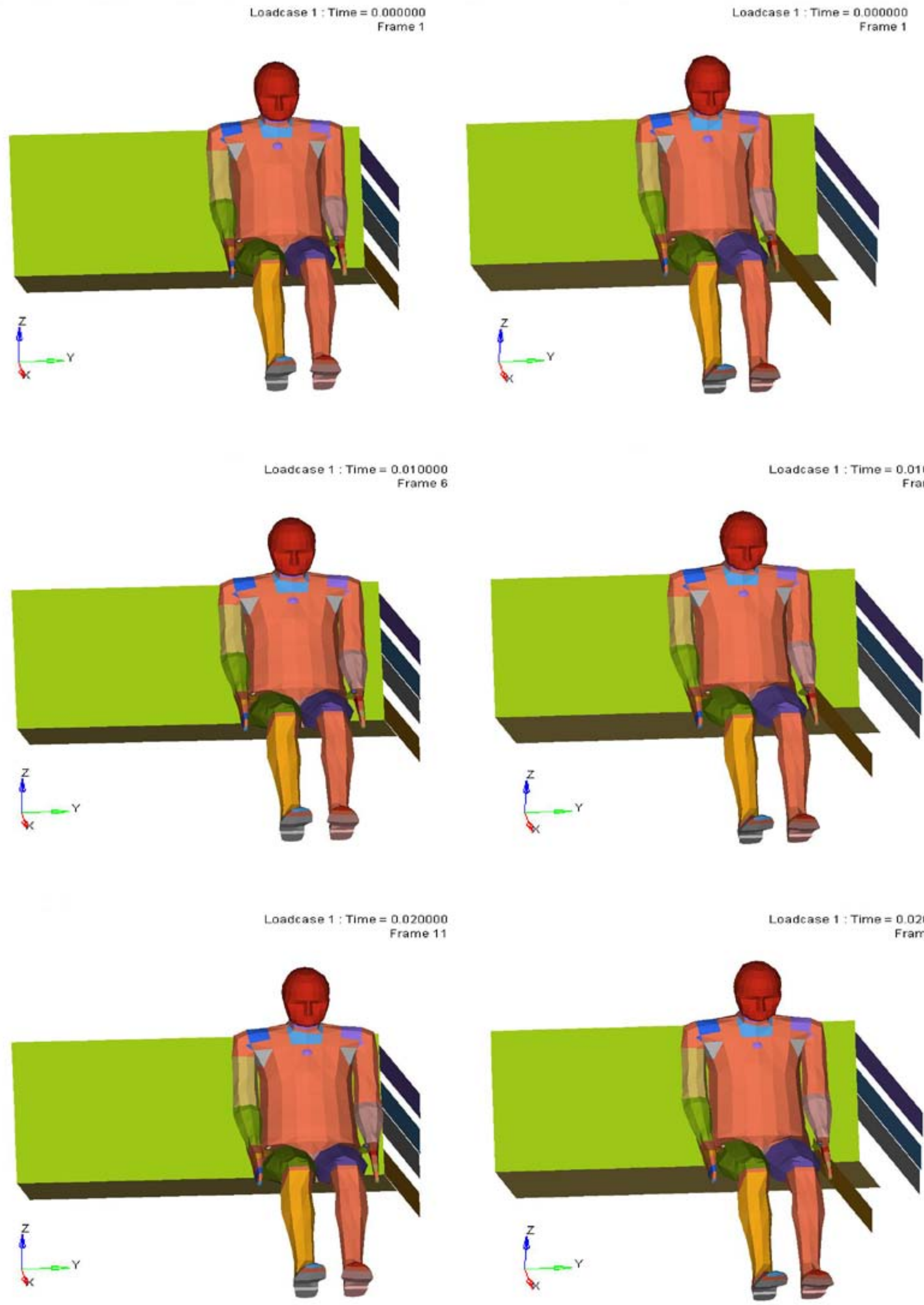

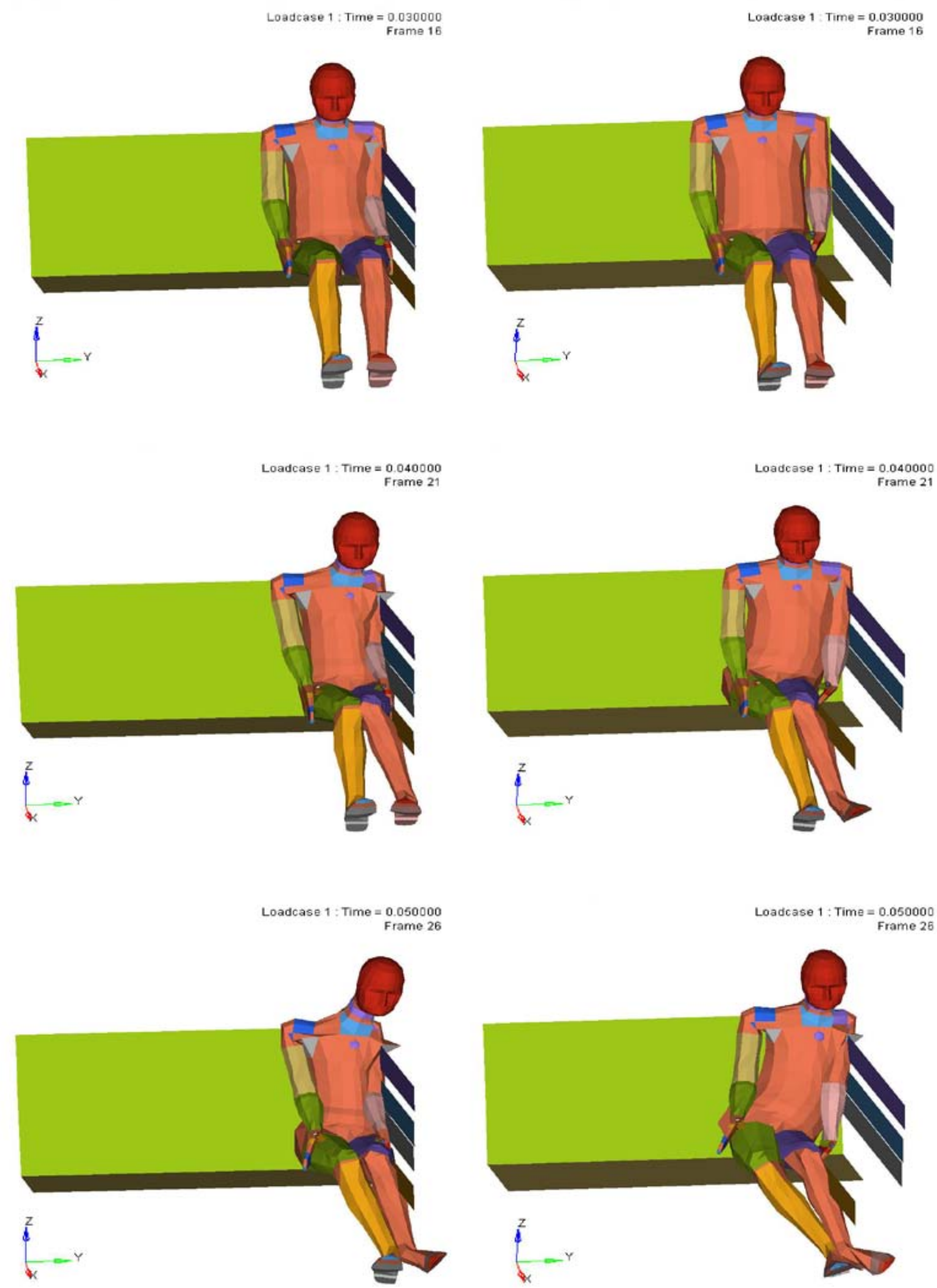
Loadcase 1 : Time = 0.030000
Frame 16
Z
Y
X
Loadcase 1 : Time = 0.030000
Frame 16
Z
Y
X
Loadcase 1 : Time = 0.040000
Frame 21
Z
Y
X
Loadcase 1 : Time = 0.040000
Frame 21
Z
Y
X
Loadcase 1 : Time = 0.050000
Frame 26
Z
Y
X
Loadcase 1 : Time = 0.050000
Frame 26
Z
Y
X

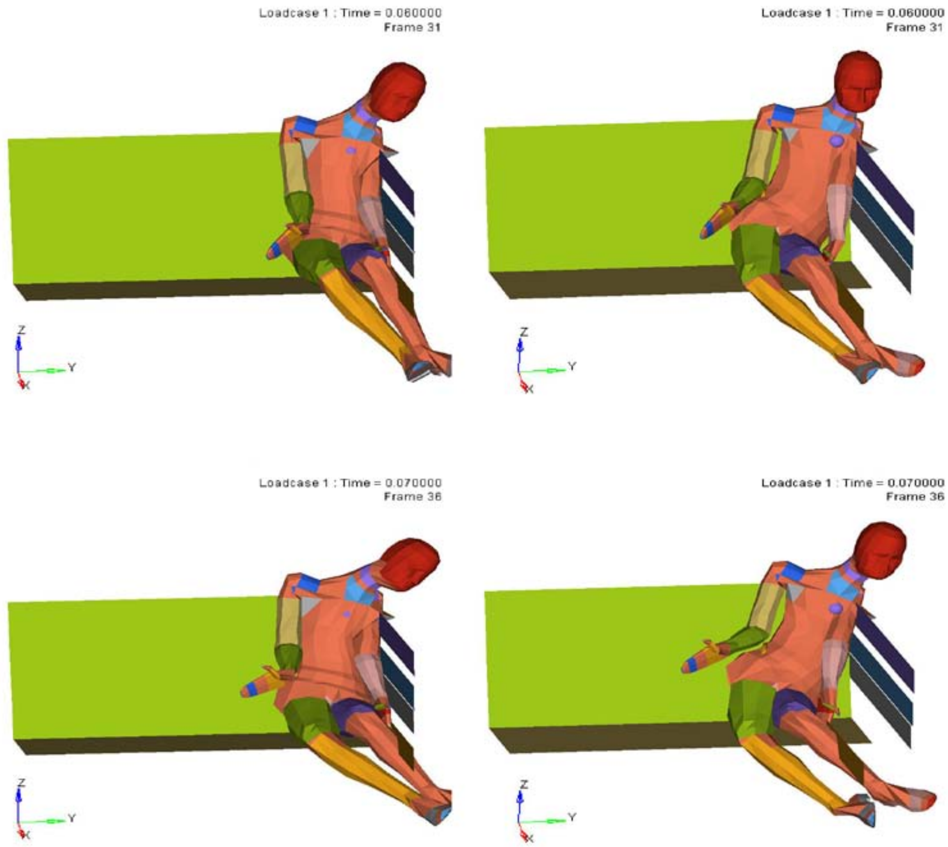

Figure 74 - Frontal view of sled test @ 12 m/s no offset (left) and sled test @ 9m/x with 6 inch offset (right).

11 Appendix D – Acceleration Graphics for NCAP, NCAP YDamage and IIHS tests without Side Airbag.

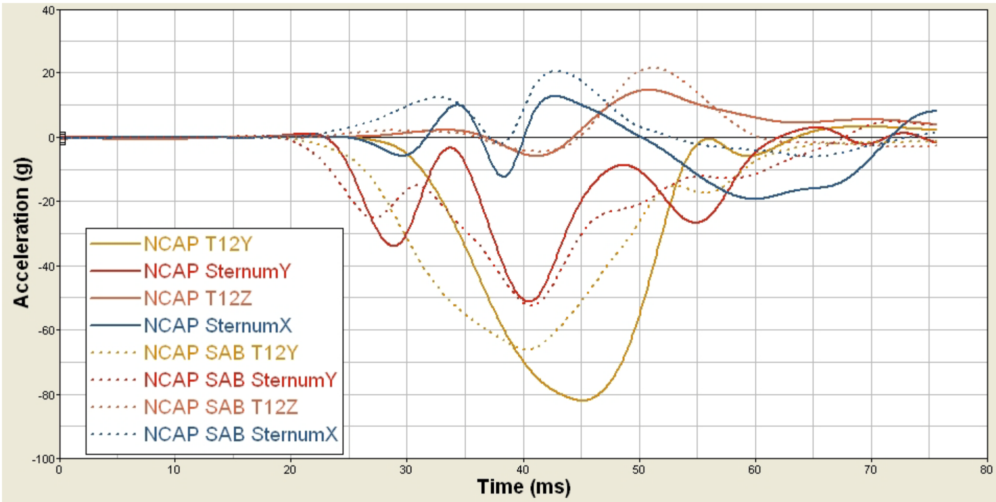

Figure 75 – NCAP T12 (Y&Z) and Sternum (X & Y) Accelerations (g)

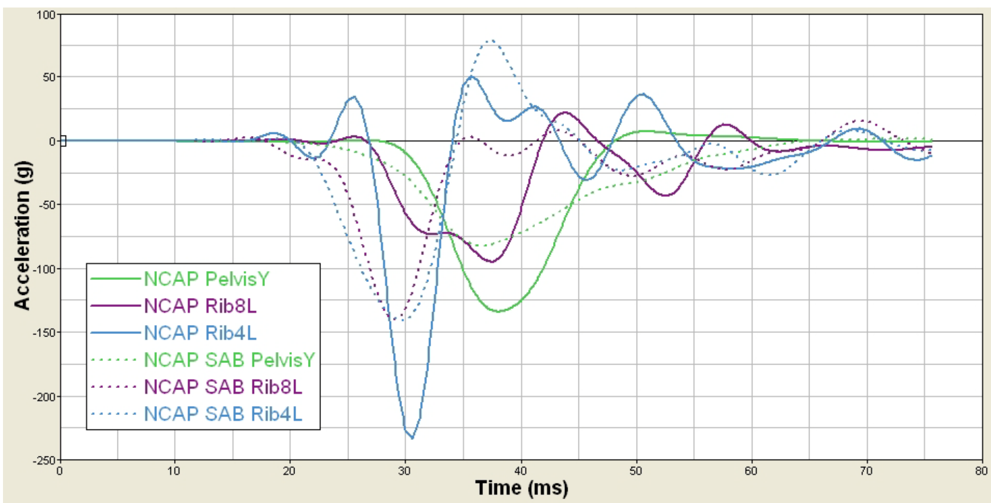

Figure 76 – NCAP Pelvis and Ribs (Y) Accelerations (g)

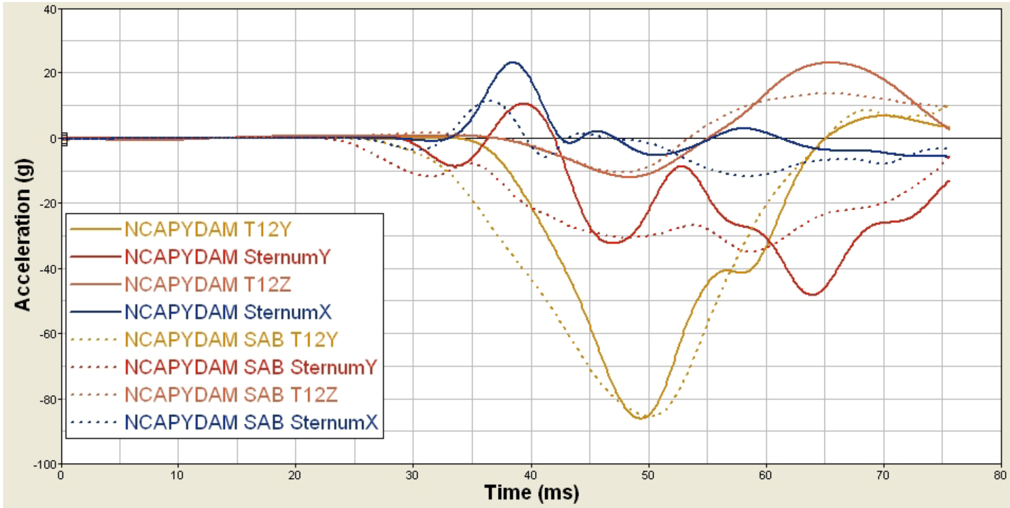

Figure 77 - NCAPYDam T12 (Y&Z) and Sternum (X & Y) Accelerations (g)

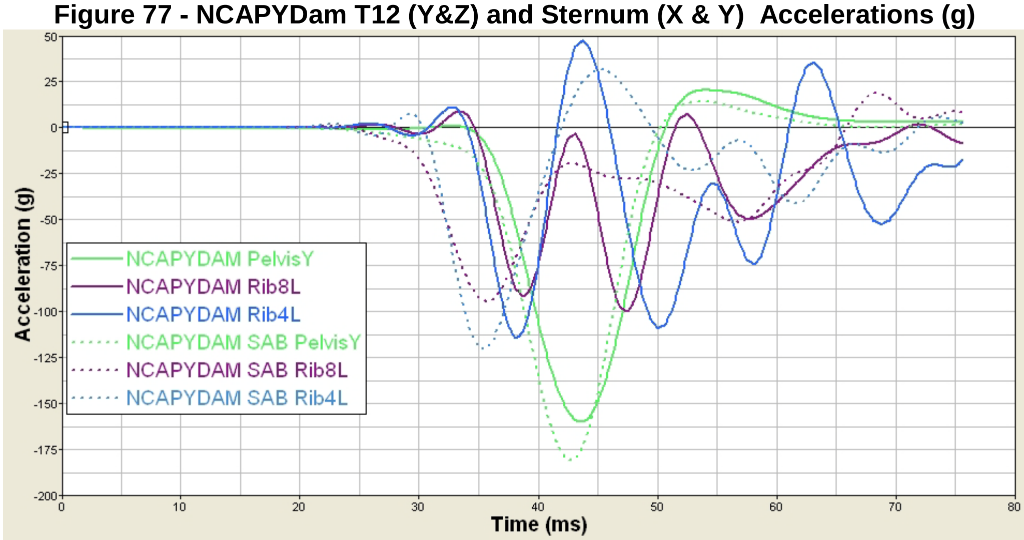

Figure 78 - NCAPYDam Pelvis and Ribs (Y) Accelerations (g)

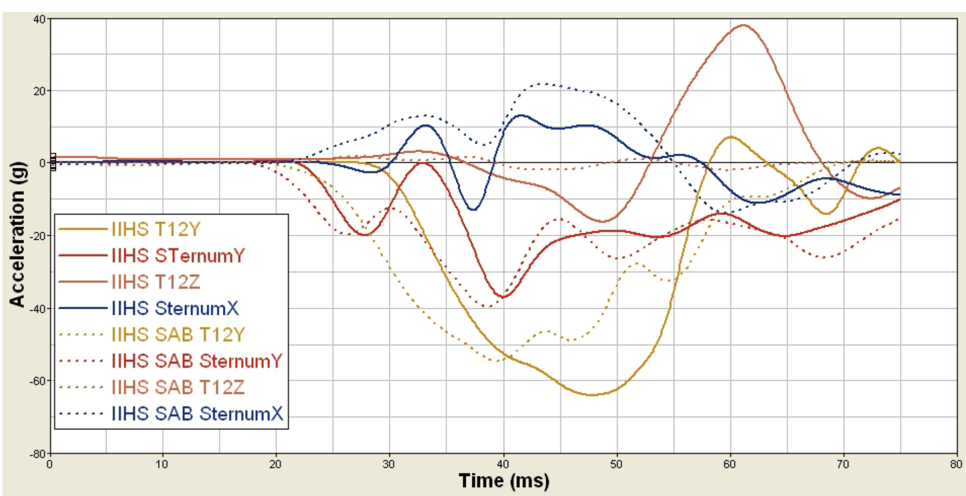

Figure 79 - IIHS T12 (Y&Z) and Sternum (X & Y) Accelerations (g)

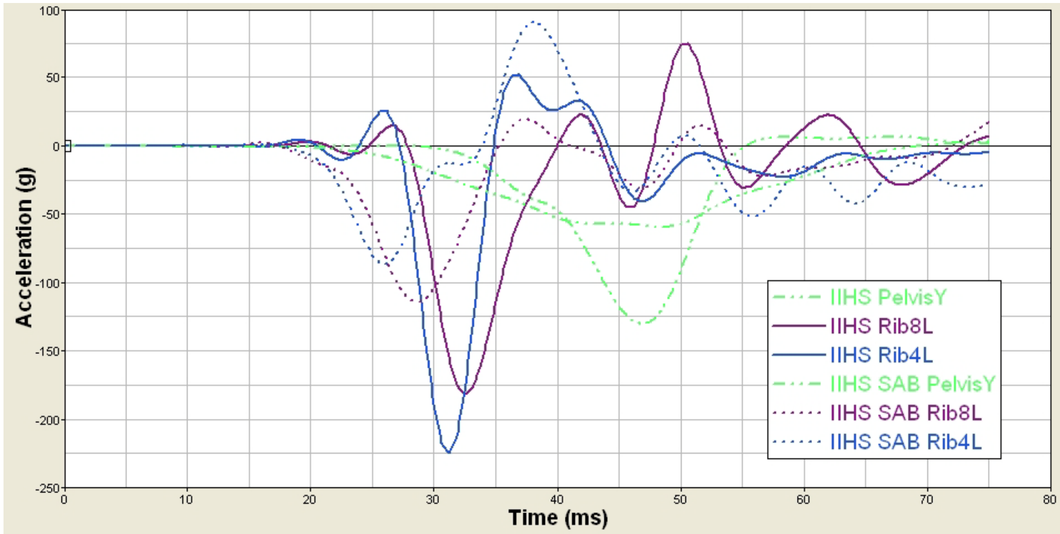

Figure 80 - IIHS Pelvis and Ribs (Y) Accelerations (g)

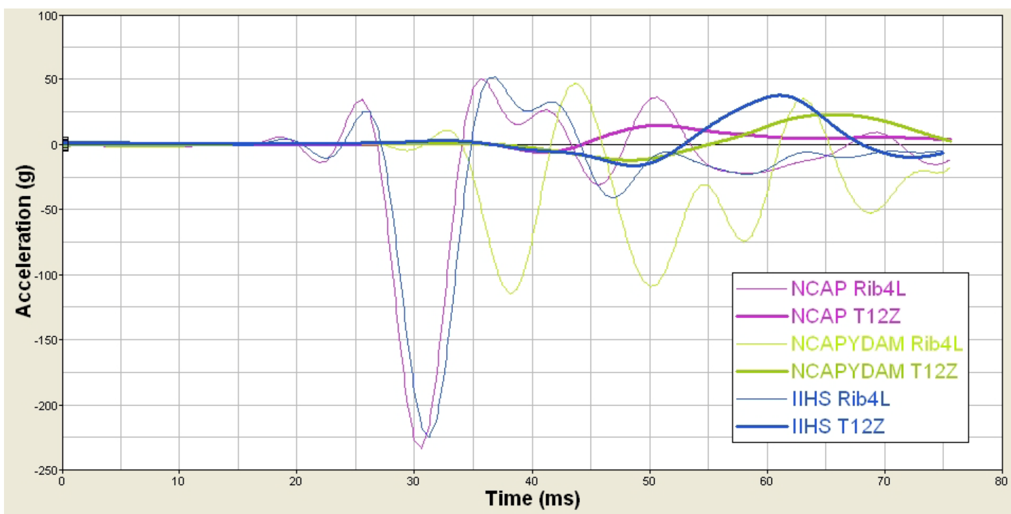

Figure 81. T12Z and Rib4L for NCAP, NCAPYDam and IIHS Accelerations (g)

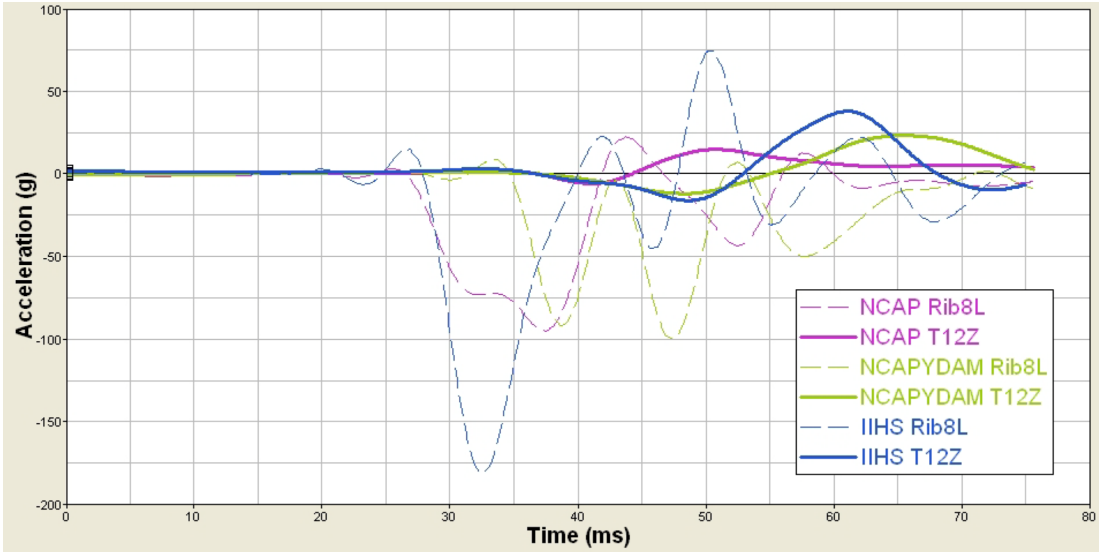

Figure 82. T12Z and Rib8L for NCAP, NCAPYDam and IIHS Accelerations (g)

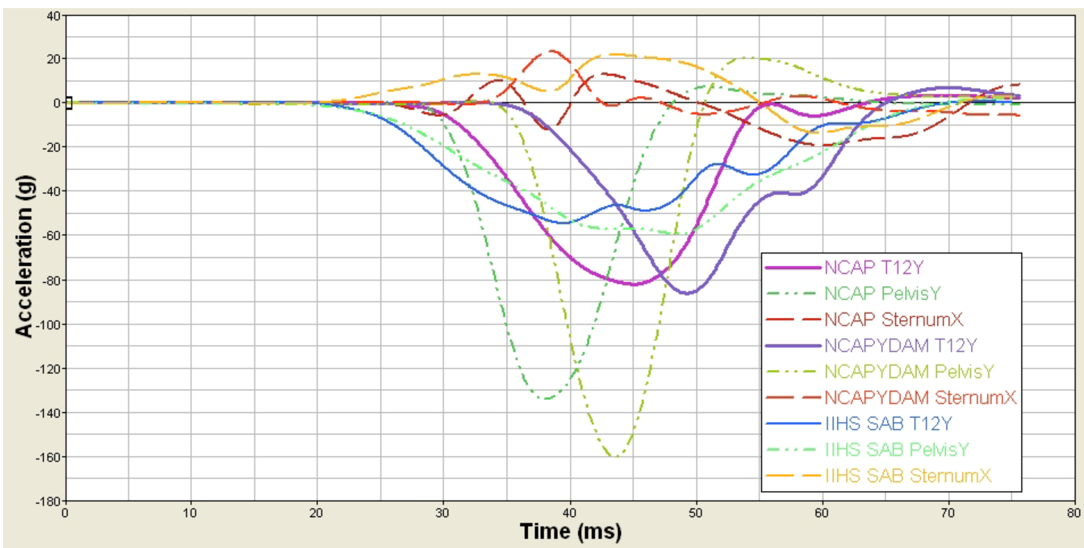

Figure 83. T12Y, PelvisY and SternumX NCAP, NCAPYDam and IIHS Accelerations (g)

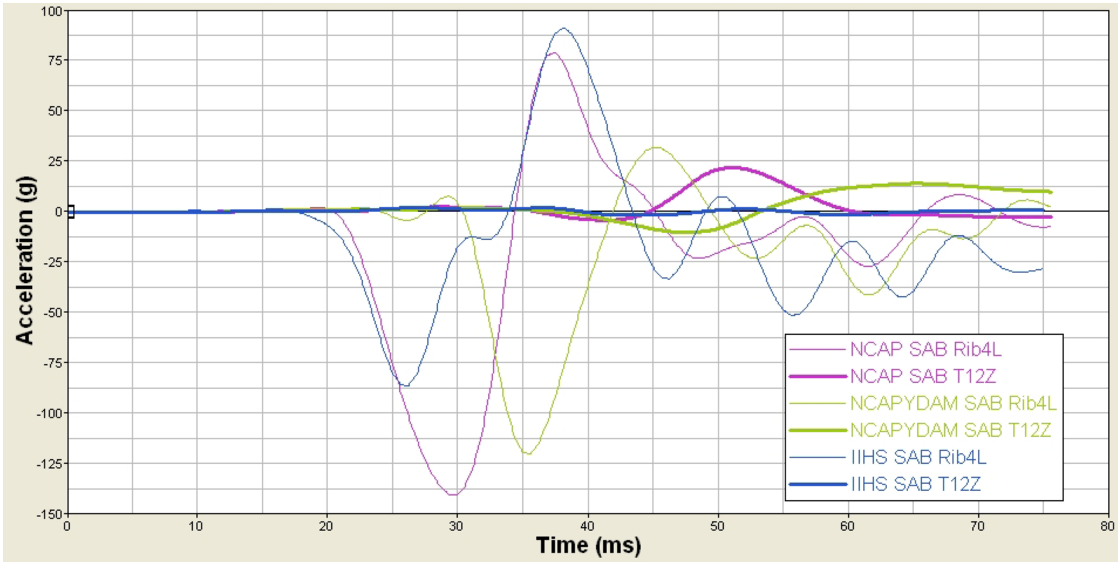

Figure 84 - T12Z and Rib4L for NCAP, NCAPYDam and IIHS with SAB Accelerations (g)

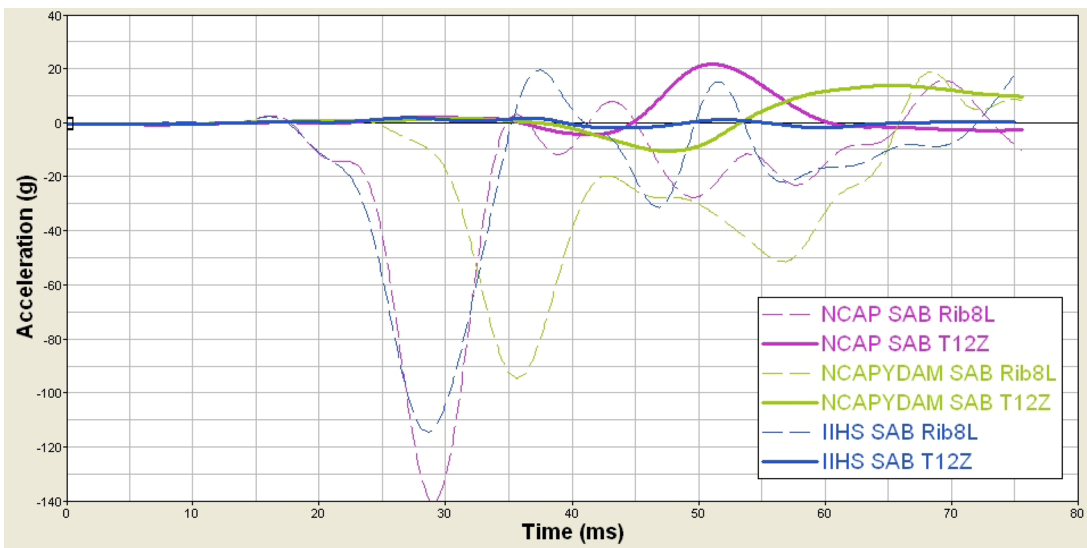

Figure 85 – T12Z and Rib8L for NCAP, NCAPYDam and with SAB IIHS Accelerations (g)

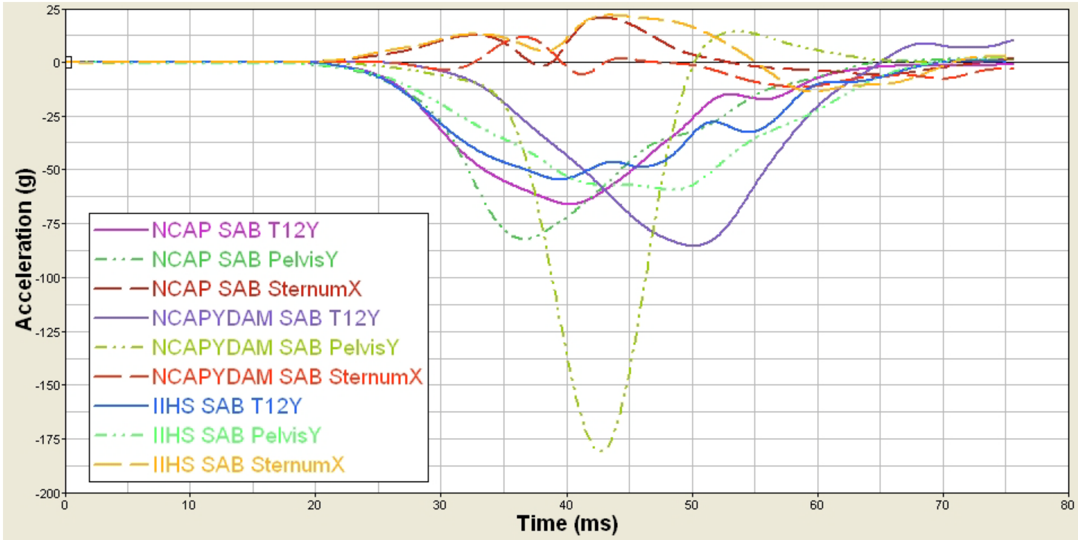

Figure 86 – T12Y, PelvisY and SternumX NCAP, NCAPYDam and IIHS with SAB Accelerations (g)

12 Appendix E – VC Max and CMax Graphics for Sled Tests with and without offset @ 12m/s

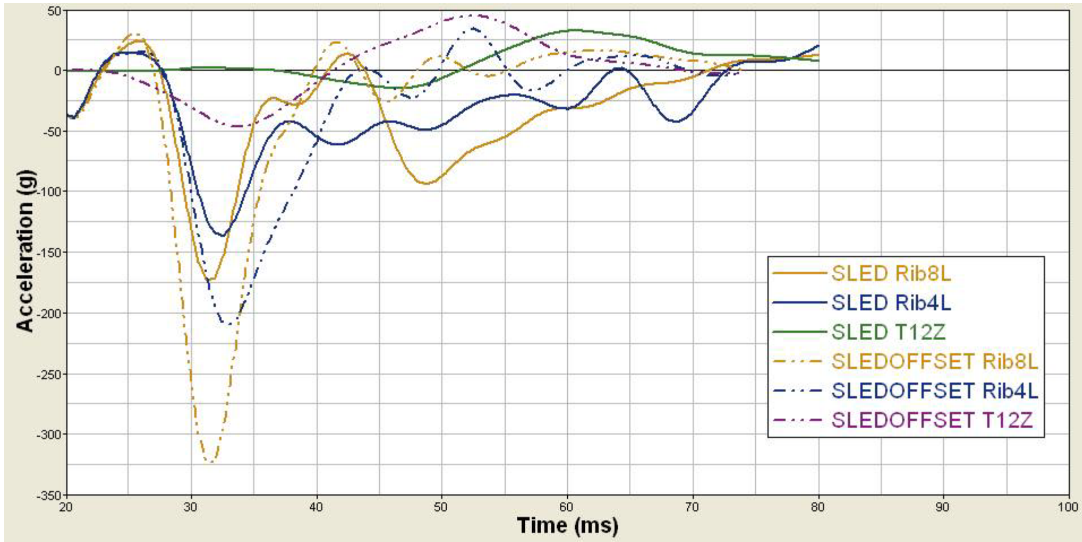

Figure 87 – T12Z and Left Ribs Accelerations for Sled Tests @ 12m/s

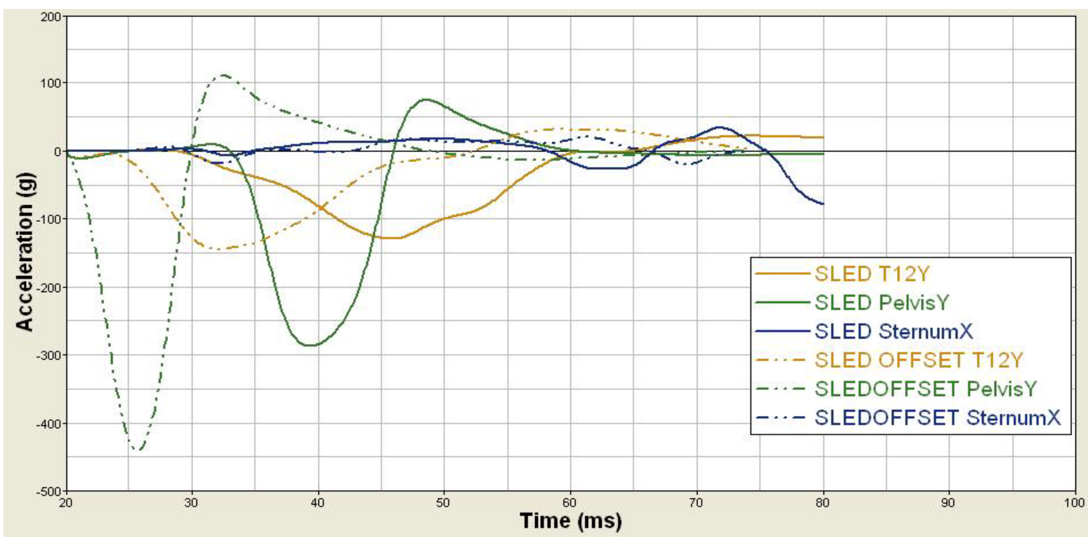

Figure 88 – T12Y, PelvisY and SternumX Accelerations for Sled Tests @ 12 m/s

13 Appendix F – NASS Cases Summary (NHTSA, 1997-2007)

13.1 Case 1994-8-27

Occupant: *1994-8-27-1-1*

NASS Weighting Factor

Weighting factor *148.319*

Crash Severity

Nr Quarter Turns *No rollover*
Impact Speed
Total, Long and Lateral DeltaV *30 -10 28*
CDC *10 L Y A W 3*
Damage (C1-C6) *0 24 32 22 9 0*
Crush (Land D) *278 64*
Object Contacted 1 *Vehicle No.2*
Object Contacted 2 *0*

Restraint Factors

Restrain *None used/avail*
AOPS *YES RES DET*
Airbag Deployment *Not Equip/Avail*

Pre-Crash Driver Data

Accident Type *89*
Pre-event Movement *Going Straight*
Critical Pre-crash Event *Cross Over Inter*

Vehicle Factors

Make Model *Chevrolet Cavalier*
Year *1991*
Body Type *4 Dr Sedan/HDTOP*
Weight *1110Kg*

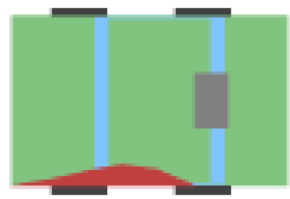

DRIVER Factors

Age *71*
Height *170*
Weight *64*
Gender *Female*
Ejection *Partial Ejection*
Ejection Area *Left Front*
Entrapment *Not Entrapped*

Injuries

Occupant *1994-8-27-1-1*
MAIS *5 Critical*
Seat Position *Front Left Side*

AIS Level	Injury Description	Contacts
1=Minor	Scalp avulsion, superficial (<100 cms2)	Left Window
1=Minor	Scalp laceration, minor	Left Window
1=Minor	Upper extremity skin abrasion	Left Interior
1=Minor	Facial skin laceration, minor	Left Window
1=Minor	Facial skin laceration, minor	Left Window
1=Minor	Thoracic skin abrasion	Left Interior
1=Minor	Thoracic skin contusion	Steering Column
1=Minor	Upper extremity skin contusion	Left Interior
1=Minor	Upper extremity skin laceration, minor	Left Interior
1=Minor	Leg skin abrasion	Left Window
1=Minor	Leg skin contusion (hematoma)	Left Interior
2=Moderate	Hepatic laceration, minor (<3cms deep)	Left Interior
5=Critical	>3 rib fxs on each side, stable chest & hemo-/pneumothorax	Left Interior
2=Moderate	Thoracic vertebral body fracture without cord injury NFS	Left Interior
2=Moderate	Arm, forearm, hand fracture NFS	Left Interior
4=Severe	Lung contusion, bilateral	Left Interior
5=Critical	Thoracic aortic laceration, major NFS	Left Interior
2=Moderate	Splenic laceration, minor (tear<3cms deep, no major vessel)	Left Interior

13.2 Case 1994 8 143

Occupant: *1994-8-143-2-1*

NASS Weighting Factor

Weighting factor *86.060*

Crash Severity

Nr Quarter Turns *No rollover*
Impact Speed
Total, Long and
Lateral DeltaV *30 -5 29*
CDC *9 L D A W 4*
Damage (C1-C6) *0 41 54 9 3 5*
Crush (Land D) *403 35*
Object Contacted 1 *Vehicle No.1*
Object Contacted 2 *0*

Restraint Factors

Restrain *None used/avail*
AOPS *Yes res DET*
Airbag Deployment *BAG Deploy-NOCOL*

Pre-Crash Driver Data
Accident Type *82*
Pre-event Movement *Turning Right*
Critical Pre-crash Event *Xing St-X-Path*

Vehicle Factors

Make Model *Chrysler Concorde*
Year *1993*
Body Type *4 Dr Sedan/HDT*op
Weight *1510Kg*

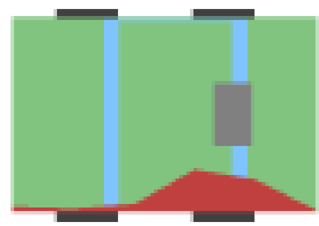

DRIVER Factors
Age *60*
Height *178*
Weight *141*
Gender *MALE*
Ejection *Partial Ejection*
Ejection Area *Left Front*
Entrapment *Not Entrapped*

Injuries

Occupant *1994-8-143-2-1*
MAIS *5=Critical*
Seat Position *Front Left Side*

AIS Level	Injury Description	Contacts
1=Minor	Facial skin abrasion	91
1=Minor	Facial skin laceration, minor	91
1=Minor	Scalp laceration, minor	91
1=Minor	690202	Left Interior
1=Minor	Upper extremity skin abrasion	91
1=Minor	Upper extremity skin laceration,minor	91
1=Minor	Upper extremity skin abrasion	Left Interior
1=Minor	Leg skin laceration, minor	Left interior
5=Critical	>3 fib fxs on each side, stable chest % hemo/pneumothorax	Steering column
3=Serious	Basiliar skull fracture, NFS	71
2=Moderate	Dislocation of atlantooccipital	71
3=Serious	Myocardial contusion NFS	Steering column
3=Serious	Lung contusion, unilateral	Left interior
4=Severe	Thoracic aortic laceration NFS	Steering Column
5=Critical	Brainstem contusion	71
3=Serious	Cerebellar subarachnoid hemorrhage	71
3=Serious	Cerebral subarachnoid hemorrhage	71

13.3 Case 2002-9-7

Occupant: *2002-9-7-2-1*




NASS Weighting Factor

Weighting factor *20.118*

Crash Severity

Nr Quarter Turns *No rollover*
Impact Speed
Total, Long and
Lateral DeltaV *26 -9 24*
CDC *10 L Y A W 4*
Damage (C1-C6) *0 37 49 37 26 7*
Crush (Land D) *245 14*
Object Contacted 1 *Vehicle No.1*
Object Contacted 2 *0*

Restraint Factors

Restrain *Lap and shldr*
AOPS *NO*
Airbag Deployment *Not EQUIP/Avail*

Pre-Crash Driver Data
Accident Type *82*
Pre-event Movement *Turning Left*
Critical Pre-crash Event *Turn Left Inters*

Vehicle Factors

Make Model *Chevrolet Caprice/Impala*
Year *1989*
Body Type *4 Dr Sedan/HDTop*
Weight *2200Kg*

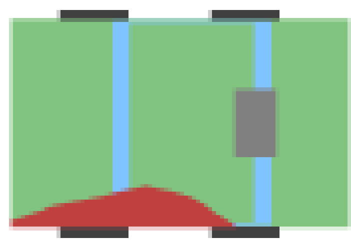

DRIVER Factors
Age *71*
Height *999*
Weight *999*
Gender *MALE*
Ejection *No Ejection*
Ejection Area *No Ejection*
Entrapment *Not Entrapped*

Injuries

Occupant *2002-9-7-2-1*
MAIS *5=Critical*
Seat Position *Front Left Side*

AIS Level	Injury Description	Contacts
1=Minor	Scalp contusion	Left B pillar
3=Serious	Cerebral subarachnoid hemorrhage	Left B pillar
3=Serious	Cerebral subarachnoid hemorrhage	Left B pillar
4=Severe	Basilar skull fracture, open with brain tissue loss	Left B pillar
5=Critical	Brainstem compression (includes herniation)	Left B pillar
3=Serious	>3 rib fractures one side & <3 other side, with stable chest	Left interior
4=Severe	Thoracic aortic laceration NFS	Left interior
3=Serious	Sacroilium fracture	Left Hardware
3=Serious	Symphysis pubis separation or fracture	Left Hardware
1=Minor	Upper extremity skin abrasion	Left interior

13.4 Case 2003-13-5

Occupant: *2003-13-5-1-1*

   

NASS Weighting Factor

Weighting factor *76.261*

Crash Severity

Nr Quarter Turns *No rollover*
Impact Speed
Total, Long and
Lateral DeltaV *32 -11 30*
CDC *10 L P E W 3*
Damage (C1-C6) *0 18 40 48 38 3*
Crush (Land D) *250 -50*
Object Contacted 1 *Vehicle No.2*
Object Contacted 2 *0*

Restraint Factors

Restrain *Lap and Sholdr*
AOPS *YES-RES DET*
Airbag Deployment *l NonDeployed*

Pre-Crash Driver Data
Accident Type *66*
Pre-event Movement *Going Straight*
Critical Pre-crash Event *poor road condition*

Vehicle Factors

Make Model *Pontiac Bonneville/Catalin*a
Year *1999*
Body Type *4DR SEDAN/HDTOP*
Weight *1560Kg*

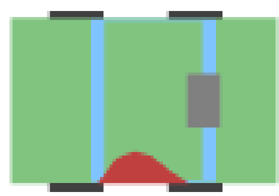

DRIVER Factors
Age *78*
Height *165*
Weight *77*
Gender *Female*
Ejection *NO Ejection*
Ejection Area *No Ejection*
Entrapment *Not Entrapped*

Injuries

Occupant *2003-13-5-1-1*
MAIS *6=Maximum*
Seat Position *Front left side*

AIS Level	Injury Description	Contacts
1=Minor	Thoracic skin contusion	Belt webb/buckle
1=Minor	Leg skin contusion (hematoma)	Belt webb/buckle
2=Moderate	Sternal fracture	Left interior
5=Critical	Flail chest, bilateral	Left interior
2=Moderate	Pericardial laceration (puncture)	Left interior
3=Serious	Myocardial laceration, without perforation or chamber injury	Left interior
6=Maximum	Thoracic aortic laceration, and extramediastinal bleeding	Left interior
4=Severe	440606	Left hardware

13.5 Case 1998-13-118

Occupant: *1998-13-118-1-2*


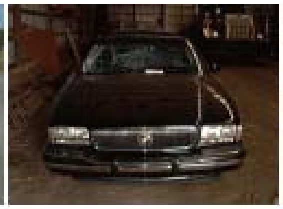

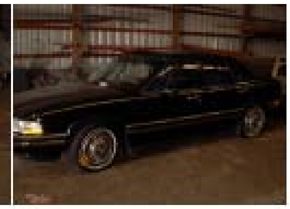

NASS Weighting Factor

Weighting factor *81.517*

Crash Severity

Nr Quarter Turns *No rollove*r
Impact Speed
Total, Long and
Lateral DeltaV *27 -23 -13*
CDC *1 R P E W 3*
Damage (C1-C6) *8 34 39 42 32* 1
Crush (Land D) *235 -47*
Object Contacted 1 *Vehicle No.2*
Object Contacted 2 *0*

Restraint Factors

Restrain *Lap and Sholdr*
AOPS *YESRES DET*
Airbag Deployment *NotEquip/Avail*

Pre-Crash Driver Data
Accident Type *87*
Pre-event Movement *Going Straight*
Critical Pre-crash Event *XING ST X Path*

Vehicle Factors

Make Model *Buick Lesabre-Wildcat-Centurion*
Year *1992*
Body Type *4DR SEDAN HDTO*P
Weight *1570Kg*

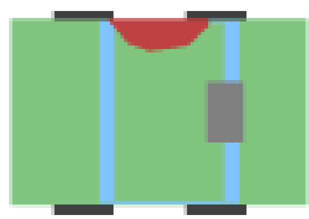

DRIVER Factors
Age *51*
Height *175*
Weight *999*
Gender *Female*
Ejection *No Ejection*
Ejection Area *No Ejection*
Entrapment *Jammed Door/Fire*

Injuries

Occupant *1998-13-118-1-2*
MAIS *6=Maximum*
Seat Position *Front right side*

AIS Level	Injury Description	Contacts
1=Minor	Facial skin laceration, minor	Flying glass
1=Minor	Neck skin laceration, minor	Flying glass
1=Minor	297402	Right wind frame
1=Minor	690402	Right interior
1=Minor	Leg skin contusion (hematoma)	Right hardware
4=Severe	>3 rib fxs on each side, stable chest	Right interior
3=Serious	Lung contusion, unilateral	Right interior
6=Maximum	Thoracic aortic laceration and extramediastinal bleeding	Right interior
2=Moderate	Hepatic laceration NFS	Right interior

13.6 Case 2005-13-144

Occupant: *2005-13-144-1-1*


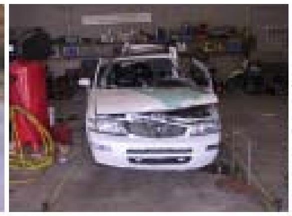
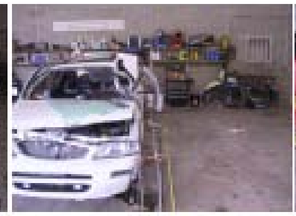
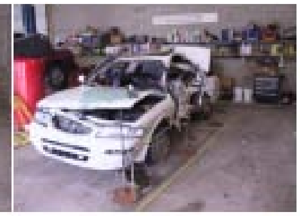

NASS Weighting Factor

Weighting factor *85.643*

Crash Severity

Nr Quarter Turns *No rollover*
Impact Speed
Total, Long and
Lateral DeltaV *27 -13 23*
CDC *10 L D A W 4*
Damage (C1-C6) *0 12 62 25 0 0*
Crush (Land D) *430 -207*
Object Contacted 1 *Vehicle No.2*
Object Contacted 2 *0*

Restraint Factors

Restrain *Lap and Shouldr*
AOPS *YES-RES DET*
Airbag Deployment *Nondeployed*

Pre-Crash Driver Data
Accident Type *89*
Pre-event Movement *Going Straight*
Critical Pre-crash Event *Cross Over inter*

Vehicle Factors

Make Model *Nissan 810/Maxima*
Year *1995*
Body Type *4-DR SEDAN HDTOP*
Weight *1360Kg*

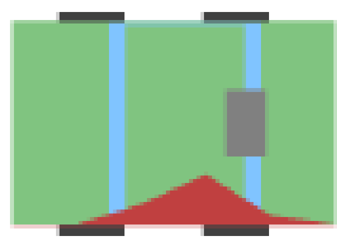

DRIVER Factors
Age *20*
Height *188*
Weight *113*
Gender *Male*
Ejection *No Ejection*
Ejection Area *No Ejection*
Entrapment *Entrapped*

Injuries

Occupant *2005-13-144-1-1*
MAIS *5=Critical*
Seat Position *Front left side*

AIS Level	Injury Description	Contacts
1=Minor	Facial skin abrasion	Belt B pillar
1=Minor	Neck skin abrasion	Belt web/buckle
1=Minor	Upper Extremity skin abrasion	Belt web/buckle
1=Minor	Abdominal skin abrasion	Belt web/buckle
1=Minor	Abdominal skin contusion	Belt web/buckle
5=Critical	Thoracic aortic laceration, major NFS	Left interior
2=Moderate	Rib cage fracture NFS	Left interior
3=Serious	Lung laceration, unilateral NFS	Left interioir
1=Minor	Facial skin abrasion	Belt B pillar
1=Minor	Upper extremity skin abrasion	Seat back
1=Minor	Leg skin abrasion	Knee bolster
1=Minor	Leg skin contusion (hematoma)	Belt web/buckle
1=Minor	Upper extremity skin abrasion	Left interior

13.7 Case 1997-41-123

Occupant: *1997-41-123-1-2*




NASS Weighting Factor

Weighting factor *30.504*

Crash Severity

Nr Quarter Turns No rollover
Impact Speed
Total, Long and
Lateral DeltaV *35 18 -30*
CDC *4 R D E W 4*
Damage (C1-C6) *10 23 49 37 27 12*
Crush (Land D) *187 14*
Object Contacted 1 *Vehicle No.2*
Object Contacted 2 *0*

Restraint Factors

Restrain *Noneused/avail*
AOPS *Yes-res Det*
Airbag Deployment *Not equip/avail*

Pre-Crash Driver Data
Accident Type *76*
Pre-event Movement *Turning left*
Critical Pre-crash Event *Turn left intersect*

Vehicle Factors

Make Model *Toyota Corolla*
Year *1990*
Body Type *4 Dr Sedan HD TOP*
Weight *1060Kg*

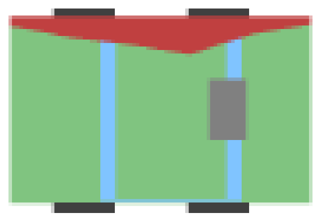

DRIVER Factors
Age *57*
Height *165*
Weight *98*
Gender *Female*
Ejection *No ejection*
Ejection Area *No ejection*
Entrapment *Not entrapped*

Injuries

Occupant 1997-41-123-1-2
MAIS *5=Critical*
Seat Position *Front right side*

AIS Level	Injury Description	Contacts
2=Moderate	Clavicle fracture	Right interior
2=Moderate	Sternal fracture	Right interior
5=Critical	Flail chest, bilateral	Right interior
4=Severe	Lung laceration, bilateral NFS	Right interior
5=Critical	Thoracic aortic laceration, major NFS	Right interior
2=Moderate	Hepatic laceration NFS	Right interior
2=Moderate	Kidney laceration, minor (<1cm, no urinary extravassation)	Right interior
3=Serious	Symphysis pubis separation or fracture	Right Hardware
1=Minor	Femoral shaft fracture	Right interior
1=Minor	Scalp laceration, minor	Flying glass
1=Minor	Facial skin abrasion	Roof right rail
1=Minor	Facial skin abrasion	Windshield
1=Minor	Facial skin abrasion	Windshield
1=Minor	Upper extremity skin abrasion	Windshield
2=Moderate	Leg skin laceration, major(>20cms & into Sub-Q)	Right panel
1=Minor	Leg skin contusion (hematoma)	Right panel
1=Minor	Leg skin abrasion	Right panel
1=Minor	Abdominal skin contusion	Right panel
1=Minor	Thoracic skin contusion	Right panel

13.8 Case 1998-49-148

Occupant: *1998-49-148-1-2*

NASS Weighting Factor

Weighting factor *19.768*

Crash Severity

Nr Quarter Turns *No rollover*
Impact Speed
Total, Long and
Lateral DeltaV *33 -17 -29*
CDC *2 R D A W* 4
Damage (C1-C6) *0 13 33 43 41 0*
Crush (Land D) *235 -26*
Object Contacted 1 *Vehicle No.2*
Object Contacted 2 *0*

Restraint Factors

Restrain *None used/avail*
AOPS *Yes-res Det*
Airbag Deployment *Bag Deployed*

Pre-Crash Driver Data
Accident Type *68*
Pre-event Movement *Turning left*
Critical Pre-crash Event *Turn left intersec*

Vehicle Factors

Make Model *Mitsubishi Galant*
Year *1995*
Body Type *4 DR Sedan/HD*TOP
Weight *1250 KG*

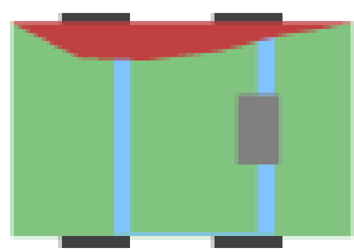

DRIVER Factors
Age *70*
Height *165*
Weight *76*
Gender *Male*
Ejection *No ejection*
Ejection Area *No ejection*
Entrapment *Jammed Door/Fire*

Injuries

Occupant *1998-49-148-1-2*
MAIS *5=Critical*
Seat Position *Front right side*

AIS Level	Injury Description	Contacts
5=Critical	Thoracic aortic laceration major NFS	Right Hardware
5=Critical	>3 rib fxs on each side, stable chest & hemo/pneumothorax	Right interior
3=Serious	Hepatic laceration, moderate (>3cms deep EBL>20)	Right hardware
2=Moderate	Pelvic Fracture NFS	Right Hardware
2=Moderate	Pelvic Fracture NFS	Right Hardware
1=Minor	Facial skin laceration, minor	OMV other front
1=Minor	Facial skin laceration, minor	OMV other front
1=Minor	Facial skin avulsion, superficial	OMV other front
1=Minor	Scalp laceration, minor	OMV other front other front
1=Minor	Scalp contusion	OMV other front
1=Minor	Upper extremity skin abrasion	Right interior
1=Minor	Thoracic skin contusion	Airbag PS Side
1=Minor	Leg skin contusion (hematoma)	Right interior
1=Minor	690402	Right interior
3=Serious	Lung contusion, unilateral	Right interior
1=Minor	Leg skin abrasion	Right interior
1=Minor	Leg skin abrasion	Seat, back
1=Minor	Leg skin contusion (hematoma)	Seat, back
1=Minor	Upper extremity skin contusion	Air bag ps side
1=Minor	Upper extremity skin laceration, minor	Right interior

13.9 Case 1995-49-209

Occupant: *1995-49-209-1-2*

NASS Weighting Factor

Weighting factor *10.884*

Crash Severity

Nr Quarter Turns *No rollover*
Impact Speed
Total, Long and
Lateral DeltaV *25 -22 -12*
CDC *1 R D A W 4*
Damage (C1-C6) *5 19 22 26 19 0*
Crush (Land D) *416 -43*
Object Contacted 1 *Vehicle No.2*
Object Contacted 2 *0*

Restraint Factors

Restrain *None used/avail*
AOPS *No*
Airbag Deployment *Not Equip/Avail*

Pre-Crash Driver Data
Accident Type *87*
Pre-event Movement *Going Straight*
Critical Pre-crash Event *Cross over inter*

Vehicle Factors

Make Model *Buick Regal 80*
Year *1980*
Body Type *2Dr SEDAN HD TOP*
Weight *1470Kg*

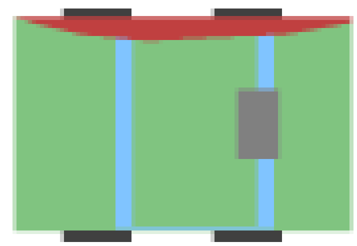

DRIVER Factors
Age *67*
Height *165*
Weight *68*
Gender *Male*
Ejection *No ejection*
Ejection Area *No ejection*
Entrapment *Not entrapped*

Injuries

Occupant *1995-49-209-1-2*
MAIS *6=Maximum*
Seat Position *Front right side*

AIS Level	Injury Description	Contacts
3=Serious	Dislocation of atlanto-axial joint (odontoid)	Right A pillar
6=Maximum	Brain stem laceration	Right A pillar
5=Critical	Brain stem hemorrhage	Right A pillar
4=Severe	Thoracic aortic laceration NFS	Right interior
5=Critical	Lung laceration, bilateral, with blood loss>20	Right interior
3=Serious	>3 rib fractures one side & <3 othe side, with stable chest	Right interior
4=Severe	Hepatic laceration, major (<50)	
2=Moderate	Splenic laceration NFS	Other occupants
2=Moderate	Humeral fracture NFS	Right interior
1=Minor	Leg skin abrasion	Right panel
1=Minor	Facial skin avulsion, superficial	Right A pillar
1=Minor	Facial skin laceration, minor	Right A pillar
1=Minor	Facial skin contusion	Right A pillar

13.10 Case 2004-73-8

Occupant: *2004-73-8-1-1*

   

NASS Weighting Factor

Weighting factor *14.284*

Crash Severity

Nr Quarter Turns *No rollover*
Impact Speed
Total, Long and
Lateral DeltaV *40 -38 14*
CDC *11 L D E W 3*
Damage (C1-C6) *0 23 38 28 18 0*
Crush (Land D) *293 -12*
Object Contacted 1 *Vehicle No.2*
Object Contacted 2 *0*

Restraint Factors

Restrain *None used/avail*
AOPS *No*
Airbag Deployment *Not Equip/avail*

Pre-Crash Driver Data
Accident Type *82*
Pre-event Movement *Turning left*
Critical Pre-crash Event *Xing St X Path*

Vehicle Factors

Make Model *Plymouth Horizon*
Year *1989*
Body Type *5DR/4DR Hatchbak*
Weight *1040Kg*

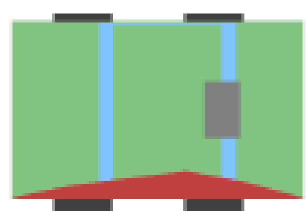

DRIVER Factors
Age *73*
Height *168*
Weight *91*
Gender *Male*
Ejection *Partial Ejection*
Ejection Area *Left Front*
Entrapment *Not Entrapped*

Injuries

Occupant *2004-73-8-1-1*
MAIS *5=Critical*
Seat Position *Front left Side*

AIS Level	Injury Description	Contacts
5=Critical	Brain stem hemorrhage	OMV hood edge
5=Critical	Cerebral epidural or extradural hematoma, bilateral, small	OMV hood edge
4=Severe	Thoracid aortic laceration NFS	Left interior
3=Serious	Basilar skull fracture, without CSF leak	OMV hood edge
4=Severe	Cerebellar hematoma, subdural, small (<30ccs)	OMV hood edge
4=Severe	Cerebral subdural hematoma, small (<50ccs)	OMV hood edge
3=Serious	Cerebral contusions, multiple, bilateral small	OMV hood edge
2=Moderate	Cervical vertebral body fracture, no cord injury NFS	OMV hood edge
4=Severe	Trachea and main stem bronchus fracture, NFS	OMV hood edge
2=Moderate	Maxilary fracture NFS	OMV hood edge
2=Moderate	Mandible fracture, open/displaced/comminuted, location NFS	OMV hood edge
1=Minor	Nose fracture, closed	OMV hood edge
2=Moderate	Zygoma fracture	OMV hood edge
2=Moderate	Orbit fracture, closed	OMV hood edge
3=Serious	>3 rib fractures one side & <3 other side, with stable chest	Left interior
4=Severe	Lung laceration, unilateral, with hemomediastinum	Left interior
3=Serious	Myocardial laceration NFS	Left interior
2=Moderate	Mesenteric laceration NFS	Left hardware
2=Moderate	Kidney laceration NFS	Left hardware
3=Serious	Pelvic fracture open displaced comminuted	Left hardware
1=Minor	Scalp contusion	OMV hood edge
1=Minor	Facial skin abrasion	OMV hood edge
1=Minor	Facial skin laceration, minor	OMV hood edge
1=Minor	Facial skin contusion	OMV hood edge
1=Minor	297402	OMV hood edge
1=Minor	297402	OMV hood edge
	Upper extremity skin laceration, minor	Left interior
	Leg skin abrasion	Left panel

13.11 Case 2007-9-136

Occupant: *2007-9-136-1-2*

   

NASS Weighting Factor

Weighting factor	*8.354*

Crash Severity

Nr Quarter Turns	*No rollover*
Impact Speed	998
Total, Long and Lateral DeltaV	*35 -18 30*
CDC	*2 R Z E W 4*
Damage (C1-C6)	*35 51 62 63 50 33*
Crush (Land D)	*161 -7*
Object Contacted 1	*Vehicle No.2*
Object Contacted 2	*0*

Restraint Factors

Restrain	Lap and Shoulder
AOPS	
Airbag Deployment	*Non deployed*

Pre-Crash Driver Data

Accident Type	*66*
Pre-event Movement	Negotiate Curve
Critical Pre-crash Event	Travel Too Fast

Vehicle Factors

Make Model	*Buick*
Year	*2000*
Body Type	*4DR SEDAN/HDTOP*
Weight	*1630 Kg*

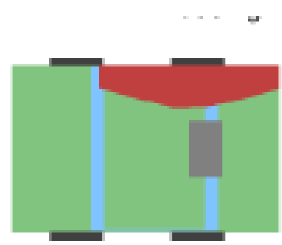

PASSENGER Factors

Age	16
Height	*163*
Weight	63
Gender	*Female*
Ejection	*No Ejection*
Ejection Area	*No Ejection*
Entrapment	*Entrapped*

Injuries

Occupant *2007-9-136-1-2*
MAIS *5=Critical*
Seat Position *Front right side*

AIS Level	Injury Description	Contacts
1=Minor	Scalp laceration, minor	Right B pillar
1=Minor	Scalp abrasion	Right B pillar
1=Minor	Thoracic skin abrasion	Transmiss lever
1=Minor	Abdominal skin abrasion	Transmiss lever
1=Minor	690202	Seat, back
1=Minor	Leg skin abrasion	Seat, back
1=Minor	Upper extremity skin abrasion	Right interior
1=Minor	Upper extremity skin contusion	Right interior
1=Minor	Upper extremity skin abrasion	Seat, back
1=Minor	Upper extremity skin laceration NFS	Transmiss lever
1=Minor	Upper extremity skin abrasion	Right B pillar
1=Minor	Leg skin abrasion	Right interior
1=Minor	Leg skin abrasion	Floor
2=Moderate	Cervical fracture with-out cord injury +/- dislocation NFS	Right B pillar
4=Severe	Thoracic aortic laceration, minor (incomplete, EBL<203=Serious	>3 rib fractures one side & <3 other side, with stable chest
2=Moderate	Kidney laceration NFS	Right Bpillar
2=Moderate	Hepatic laceration NFS	Right B pillar
2=Moderate	Splenic laceration NFS	Transmiss lever
2=Moderate	Bladder laceration NFS	Transmiss lever
3=Serious	Ovarian laceration, massive (avulsion, complex, rupture)	Transmiss lever
2=Moderate	Uterus contusion NFS	Transmiss lever
4=Severe	Lung contusion, bilateral	Right B Pillar
4=Severe	Lung laceration, bilateral NFS	Right B Pillar
2=Moderate	Wrist (carpus) joint dislocation (radio/inter/pericarpal)	Right interior
5=Critical	Cerebral diffuse axonal injury	Right B pillar
3=Serious	Cerebral contusions, multiple bilateral	Right B pillar
3=Serious	Cerebellar contusion or contusions, NFS	Right B Pillar

13.12 Case 2007-49-143

Occupant: *2007-49-143-1-1*

NASS Weighting Factor

Weighting factor *9.951*

Crash Severity

Nr Quarter Turns *No rollover*
Impact Speed 998
Total, Long and Lateral DeltaV *35 -30 18*
CDC *11 L Y E W 4*
Damage (C1-C6) 45 44 40 56 54 38
Crush (Land D) *107 149*
Object Contacted 1 *Vehicle No.2*
Object Contacted 2 *0*

Restraint Factors

Restrain *Lap and Shoulder*
AOPS
Airbag Deployment *Bag Deployed*

Pre-Crash Driver Data
Accident Type *89*
Pre-event Movement Going Straight
Critical Pre-crash Event XING ST X PATH

Vehicle Factors

Make Model *Chevrolet Malibu*
Year *1997*
Body Type *4DR SEDAN/HDTOP*
Weight *1410 Kg*

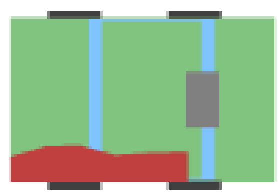

DRIVER Factors
Age *37*
Height *165*
Weight *128*
Gender *Male*
Ejection *No Ejection*
Ejection Area *No Ejection*
Entrapment *Entrapped*

Injuries

Occupant *2007-49-143-1-1*
MAIS *5=Critical*
Seat Position *Front left side*

AIS Level	Injury Description	Contacts
5=Critical	Abdominal Aorta laceration, major	440606
3=Serious	Rib fractures (>1 rib) open/displaced/comminuted	Left interior
3=Serious	Lung laceration, unilateral NFS	Left interior
7=Unk. sev	616099	Left hardware
3=Serious	Basilar skull fracture, without CSF leak	Left B pillar
3=Serious	Cerebral subarachnoid hemorrhage	Left B pillar
2=Moderate	Splenic laceration NFS	Left Hardware
2=Moderate	Kidney laceration NFS	Left Hardware
1=Minor	Adrenal gland laceration NFS	Left Hardware
2=Moderate	Pancreatic laceration NFS	Left Hardware
2=Moderate	Pancreatic contusion NFS	Left Hardware
2=Moderate	Duodenal contusion without obstruction	Left Hardware
2=Moderate	Bladder contusion (hematoma)	Left Hardware
2=Moderate	Mesenteric contusion NFS	Left Hardware
2=Moderate	Arm, forearem, hand fracture NFS	Sunvisor
3=Serious	Femoral shaft fracture	Other left pillar
3=Serious	Femoral shaft fracture	Other left pillar
3=Serious	Tibial shaft fracture, open/displaced/comminuted	Floor
1=Minor	Scalp contusion	Airbag DR side
1=Minor	Thoracic skin abrasion	Left interior
1=Minor	Thoracic skin contusion	Left interior
1=Minor	Abdominal skin abrasion	Left hardware
1=Minor	Abdominal skin contusion	Left hardware
1=Minor	Upper extremety skin abrasion	Left interior
1=Minor	Upper extremity skin contusion	Left interior
1=Minor	Leg skin abrasion	Other left pillar
1=Minor	Leg skin contusion (hematoma)	Other left pillar

13.13 Case 2007-49-153

Occupant: *2007-49-153-1-1*




NASS Weighting Factor

Weighting factor	*9.951*

Crash Severity

Nr Quarter Turns	*No rollover*
Impact Speed	998
Total, Long and Lateral DeltaV	*32 -11 30*
CDC	*10 L P A W 4*
Damage (C1-C6)	*5 25 51 25 28 9*
Crush (Land D)	*213 4*
Object Contacted 1	*Vehicle No.2*
Object Contacted 2	*0*

Restraint Factors

Restrain	*Lap and Shoulder*
AOPS	
Airbag Deployment	*None Deployed*

Pre-Crash Driver Data

Accident Type	*82*
Pre-event Movement	Turning left
Critical Pre-crash Event	Turn Left Inters

Vehicle Factors

Make Model	Oldsmobile Alero
Year	*2000*
Body Type	*4DR SEDAN/HDTOP*
Weight	*1370 Kg*

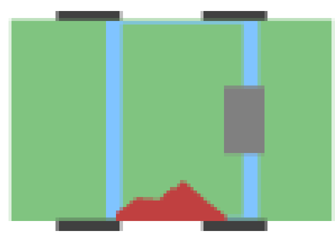

DRIVER Factors

Age	*76*
Height	*175*
Weight	*91*
Gender	*Female*
Ejection	*No Ejection*
Ejection Area	*No Ejection*
Entrapment	*Not Entrapped*

Injuries

Occupant *2007-49-153-1-1*
MAIS *5=Critical*
Seat Position *Front left side*

AIS Level	Injury Description	Contacts
5=Critical	>3 rib fxs on each side, stable chest & hemo/pneumothorax	Left interior
3=Serious	Cerebral subarachnoid hemorrhage	Left A Pillar
3=Serious	Cerebral subarachnoid hemorrhage	Left A Pillar
1=Minor	Myocardial contusion NFS	Left interior
4=Severe	Thoracic aortic injury NFS	Left interior
4=Severe	Abdominal aorta injury NFS	Left hardware
2=Moderate	Splenic laceration, minor (tear<3cms deep no major vessel)	Left hardware
2=Moderate	Hepatic laceration, minor (<3cms deep EBL)	
4=Severe	Lung contusion, bilateral	Left interior
2=Moderate	Bladder contusion (hematoma)	Left hardware
2=Moderate	Colonic contusion (hematoma)	Left hardware
2=Moderate	Sternal fracture	Left interior
2=Moderate	Pelvic fracture, closed	Left hardware
2=Moderate	Radial fracture NFS (+/- styloid process, including Colles)	Steering comb
1=Minor	Scalp contusion	Left A pillar
1=Minor	Facial skin abrasion	Left A pillar
1=Minor	Facial skin laceration, minor	Left A pillar
1=Minor	Upper extremity skin contusion	Belt webb/buckle
1=Minor	Thoracic skin contusion	Left interior
1=Minor	Leg skin contusion (hematoma)	Other left pillar
1=Minor	Leg skin contusion (hematoma)	Floor

13.14 Case 2007-74-25

NASS Weighting Factor

Weighting factor *8.309*

Crash Severity

Nr Quarter Turns	*No rollover*
Impact Speed	998
Total, Long and Lateral DeltaV	*39 -25 30*
CDC	*10 L D A W 3*
Damage (C1-C6)	*0 4040 40 19 0*
Crush (Land D)	*400 -22*
Object Contacted 1	*Vehicle No.2*
Object Contacted 2	*0*

Restraint Factors

Restrain AOPS	*None used/avail*
Airbag Deployment	*Not EQUIP/AVAIL*

Pre-Crash Driver Data

Accident Type	*89*
Pre-event Movement	Going Straight
Critical Pre-crash Event	Cross Over Inter

Vehicle Factors

Make Model	Chevrolet Lumina
Year	*1993*
Body Type	*4DR SEDAN/HDTOP*
Weight	*1480 Kg*

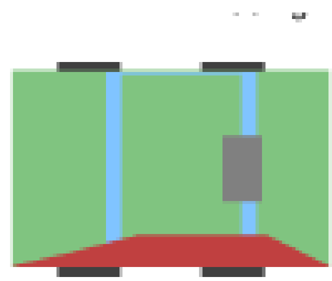

DRIVER Factors

Age	*24*
Height	*999*
Weight	*999*
Gender	*Male*
Ejection	*No Ejection*
Ejection Area	*No Ejection*
Entrapment	*Jammed Door/Fire*

Injuries

Occupant *2007-74-25-1-1*
MAIS *5=Critical*
Seat Position *Front left side*

AIS Level	Injury Description	Contacts
5=Critical	Thoracic aortic laceration, major NFS	Left interior
4=Severe	440606	Left Hardware
5=Critical	Brainstem compression (includes herniation)	Left A Pillar
5=Critical	Cerebral brain swelling, severe	Left A Pillar
2=Moderate	Pancreatic contusion NFS	Left Hardware
3=Serious	Celiac artery laceration NFS	Left interior
3=Serious	Other abdominal artery intimal laceration NFS	Left Hardware
2=Moderate	Splenic injury NFS	Left Hardware
2=Moderate	Hepatic laceration NFS	Left Hardware
4=Severe	>3 rib fxs on one side & <3 other side & hemo/pneumothorax	Left interior
3=Serious	Cerebral subarachnoid hemorrhage	Left A Pillar
4=Severe	Cerebral subdural hematoma, small (<50ccs)	Left A Pillar
1=Minor	Facial skin abrasion	Left A Pillar
1=Minor	Facial skin contusion	Left A Pillar

13.15 Case 1993-41-83

NASS Weighting Factor

Weighting factor	17.655

Crash Severity

Nr Quarter Turns	*No rollover*
Impact Speed	
Total, Long and Lateral DeltaV	
CDC	69 *L Z A W 3*
Damage (C1-C6)	*0 26 28 20 13 0*
Crush (Land D)	191 -124
Object Contacted 1	*Vehicle No.2*
Object Contacted 2	*0*

Restraint Factors

Restrain	*None used/avail*
AOPS	NO
Airbag Deployment	*Not EQUIP/AVAIL*

Pre-Crash Driver Data

Accident Type	*89*
Pre-event Movement	Going Straight
Critical Pre-crash Event	Cross Over Inter

Vehicle Factors

Make Model	Dodge Aries
Year	*1984*
Body Type	*4DR SEDAN/HDTOP*
Weight	*1080 Kg*

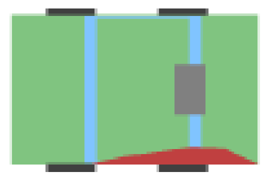

DRIVER Factors

Age	*85*
Height	160
Weight	*76*
Gender	*Female-NotPreg*
Ejection	*Ejection*
Ejection Area	Left Front
Entrapment	*Not Entrapped*

Injuries

Occupant 1993-41-83-1-1
MAIS *5=Critical*
Seat Position *Front left side*

AIS Level	Injury Description	Contacts
1=Minor	Scalp abrasion	84
1=Minor	Scalp avulsion, superficial (<100cm2)	84
1=Minor	Facial skin laceration NFS	84
1=Minor	Facial skin abrasion	84
1=Minor	Facial skin abrasion	84
2=Moderate	690804	84
1=Minor	690202	84
1=Minor	Upper extremity skin laceration, minor	84
1=Minor	Upper extremity skin contusion	84
1=Minor	Leg skin contusion (hematoma)	84
1=Minor	Leg skin laceration, minor	84
5=Critical	Flail chest, bilateral	84
2=Moderate	Thoracic spine fracture, no cord injury NFS	84
2=Moderate	Thoracic spine fracture, no cord injury, NFD	84
3=Serious	Diaphragm laceration or rupture	84
4=Severe	Thoracic aortic laceration, minor (incomplete EBL<20%)	84
4=Severe	Abdominal aorta laceration, minor (incomplete, EBL<20%)	84
2=Moderate	Splenic laceration NFS	84
2=Moderate	Gastric contusion (hematoma)	84
3=Serious	Inhalation injury minor (CO level<20 mg%)	92

13.16 Case 2006-48-64




NASS Weighting Factor

Weighting factor 163.242

Crash Severity

Nr Quarter Turns	*No rollover*
Impact Speed	999
Total, Long and Lateral DeltaV	
CDC	*1 R P A W 3*
Damage (C1-C6)	*0 6 20 33 4 0*
Crush (Land D)	*229 1*
Object Contacted 1	*Vehicle No.2*
Object Contacted 2	*0*

Restraint Factors

Restrain	*Lap and shoulder*
AOPS	NO
Airbag Deployment	BAG DEPLOYED

Pre-Crash Driver Data

Accident Type	*69*
Pre-event Movement	Turning left
Critical Pre-crash Event	Turn left inters

Vehicle Factors

Make Model	Chevrolet Malibu
Year	*2003*
Body Type	*4DR SEDAN/HDTOP*
Weight	*1410 Kg*

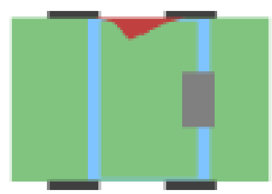

DRIVER Factors

Age	89
Height	157
Weight	*74*
Gender	*Female-NotPreg*
Ejection	*No Ejection*
Ejection Area	*No Ejection*
Entrapment	*Not Entrapped*

Injuries

Occupant *2006-48-64-1-2*
MAIS *5=Critical*
Seat Position *Front right side*

AIS Level	Injury Description	Contacts
5=Critical	Thoracic aortic laceration, major and mediastinal bleeding	Right interior
4=Severe	Cerebral subdural hematoma, small (<50ccs)	Right interior
3=Serious	540640	Right hardware
3=Serious	Lung contusion, unilateral	Right interior
4=Severe	>3 rib fxs on one side & <3 other side & hemo-/pneumothorax	Right interior
2=Moderate	Splenic laceration, minor (tear<3cm deep no major vessel)	Right Hardware
3=Serious	Pelvic fracture, open/displace/comminuted	Right hardware
2=Moderate	Arm, foreamrm, hand fracture NFS	Right interior
1=Minor	Thoracic skin contusion	Right interior
1=Minor	Facial skin abrasion	Flying glass
1=Minor	Facial skin laceration, minor	Flying glass

13.17 Case 1993-49-63

NASS Weighting Factor

Weighting factor	10.670

Crash Severity

Nr Quarter Turns	*No rollover*
Impact Speed	999
Total, Long and Lateral DeltaV	
CDC	*10 L Y A W 3*
Damage (C1-C6)	*0 10 17 22 20 0*
Crush (Land D)	*204 23*
Object Contacted 1	*Vehicle No.1*
Object Contacted 2	*0*

Restraint Factors

Restrain	*Lap and shoulder*
AOPS	NO
Airbag Deployment	Not EQUIP/AVAIL

Pre-Crash Driver Data

Accident Type	*89*
Pre-event Movement	Going Straight
Critical Pre-crash Event	XING ST X PATH

Vehicle Factors

Make Model	Buick Skylark (76-85)
Year	*1985*
Body Type	*4DR SEDAN/HDTOP*
Weight	*1170 Kg*

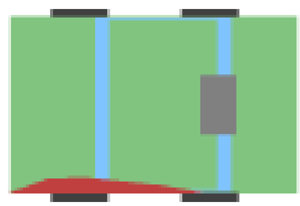

DRIVER Factors

Age	78
Height	160
Weight	*77*
Gender	*Female-NotPreg*
Ejection	*No Ejection*
Ejection Area	*No Ejection*
Entrapment	*Not Entrapped*

Injuries

Occupant 1993-49-63-2-1
MAIS *5=Critical*
Seat Position *Front left side*

AIS Level	Injury Description	Contacts
1=Minor	Facial skin laceration, minor	92
1=Minor	Neck skin abrasion	92
1=Minor	Leg skin contusion (hematoma)	Left interior
1=Minor	Leg skin contusion (hematoma)	Steering rim
1=Minor	Upper extremity skin contusion	92
1=Minor	Upper extremity skin abrasion	Left interior
1=Minor	Upper extremity skin laceration, minor	92
1=Minor	Upper extremity skin contusion	97
1=Minor	Mandible fracture NFS	97
4=Severe	>3 rib fxs on each side, stable chest	Left interior
2=Moderate	Dislocation of atlanooccipital	Left B Pillar
3=Serious	Cervical adontoid (dens) fracture, no cord injury	Left B Pillar
4=Severe	Lung contusion, bilateral	Left interior
4=Severe	Thoracic aortic laceration, minor (incomplete, EBL<20%	Left interior
3=Serious	Pulmorary artery laceration minor, (incomplete or EBL<20%	Left interior
5=Critical	Cerebral subdural hematoma, large (>50ccs)	Left B Pillar
3=Serious	Cerebral subpial hemorrhage	Left B Pillar

13.18 Case 1998-49-148

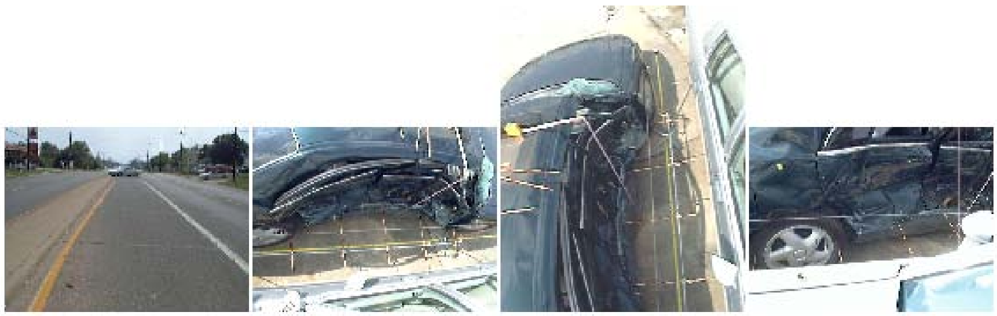

NASS Weighting Factor

Weighting factor	19.763

Crash Severity

Nr Quarter Turns	*No rollover*
Impact Speed	998
Total, Long and Lateral DeltaV	33 -17-29
CDC	2 R D A W 4
Damage (C1-C6)	*0 13 33 43 41 0*
Crush (Land D)	*235 -26*
Object Contacted 1	*Vehicle No.2*
Object Contacted 2	*0*

Restraint Factors

Restrain	Noneused/avail
AOPS	YES-RES DET
Airbag Deployment	BAG DEPLOYED

Pre-Crash Driver Data

Accident Type	*68*
Pre-event Movement	Turning left
Critical Pre-crash Event	Turn left inters

Vehicle Factors

Make Model	Mitsubishi Galant
Year	*1995*
Body Type	*4DR SEDAN/HDTOP*
Weight	*1250 Kg*

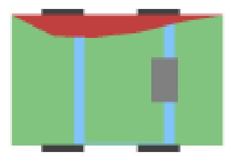

DRIVER Factors

Age	70
Height	165
Weight	*76*
Gender	*Male*
Ejection	*No Ejection*
Ejection Area	*No Ejection*
Entrapment	Jammed Door/Fire

Injuries

Occupant 1998-49-148-1-2
MAIS *5=Critical*
Seat Position *Front right side*

AIS Level	Injury Description	Contacts
5=Critical	Thoracic aortic laceration, major NFS	Right Hardware
5=Critical	>3 rib fxs on each side, stable chest & hemo/pneumothorax	Right interior
3=Serious	Hepatic laceration, moderate (>3cms deep, EBL>20%, ma duct)	Right Hardware
2=Moderate	Pelvic fracture NFS	Right Hardware
2=Moderate	Pelvic fracture NFS	Right Hardware
1=Minor	Facial skin laceration, minor	OMV other front
1=Minor	Facial skin laceration minor	OMV other front
1=Minor	Facial skin avulsion, superficial	OMV other front
1=Minor	Scalp laceration, minor	OMV other front
1=Minor	Scalp contusion	OMV other front
1=Minor	Upper extremity skin abrasion	Right interior
1=Minor	Thoracic skin contusion	Air bag PS side
1=Minor	Leg skin contusion (hematoma)	Right interior
1=Minor	690402	Right interior
3=Serious	Lung contusion, unilateral	Right interior
1=Minor	Leg skin abrasion	Right interior
1=Minor	Leg skin abrasion	Seat back
1=Minor	Leg skin contusion (hematoma)	Seat back
1=Minor	Upper extremity skin contusion	Air bag PS Side
1=Minor	Upper extremity skin laceration, minor	Right interior